DISSERTATION

CONTRIBUTIONS OF SPECIFIC TRPCS TO MYOMETRIAL CALCIUM ENTRY

Submitted by

Aida Erendira Ulloa

Graduate Degree Program in Cell and Molecular Biology

In partial fulfillment of the requirements

For the Degree of Doctor of Philosophy

Colorado State University

Fort Collins, Colorado

Fall 2010

COLORADO STATE UNIVERSITY

June 10th, 2010

WE HEREBY RECOMMEND THAT THE DISSERTATION PREPARED UNDER OUR SUPERVISION BY AIDA ERENDIRA ULLOA ENTITLED CONTRIBUTIONS OF SPECIFIC TRPCS TO MYOMETRIAL CALCIUM ENTRY BE ACCEPTED AS FULFILLING IN PART REQUIREMENTS FOR THE DEGREE OF DOCTOR OF PHILOSOPHY.

Committee on Graduate work

Colin Clay

Norman P. Curthoys

Sue C. Kinnamon

Deborah A. Roess

Advisor: Barbara M. Sanborn

Director: Paul J. Laybourn

ABSTRACT OF DISSERTATION

CONTRIBUTIONS OF SPECIFIC TRPCS TO MYOMETRIAL CALCIUM ENTRY

Understanding the mechanisms that regulate contractions in the myometrium during pregnancy may help avoid scenarios such as premature births. During labor, increases in intracellular calcium ($[Ca^{2+}]_i$) have been closely correlated with human myometrium contractions. Extracellular calcium enters the cell through voltage-operated and signal-regulated Ca^{2+}-entry (SRCE) mechanisms and is involved in actions such as stimulating the contractile apparatus and replenishing intracellular Ca^{2+} stores. In SRCE, activation of some receptors and/or depletion of agonist-sensitive $[Ca^{2+}]_i$-stores stimulates Ca^{2+}-uptake from the extracellular solution. This and other SRCE mechanisms are all important in providing regulation of calcium homeostasis. Ion channels potentially responsible for SRCE are the canonical transient receptor potential (TRPC) channels. The seven members (TRPC1-7) are postulated to form hetero- or homotetramers, thus allowing for the formation of a variety of channels possessing different physiological properties. Additional TRPC channel regulation is also provided by STIM1, an endoplasmic reticulum Ca^{2+} sensor. My studies show that human myometrium expresses higher concentrations of TRPC4 and TRPC1 mRNAs relative to other TRPCs as well as expressing STIM1 proteins. Furthermore, I have found that

specific TRPC proteins are involved in the SRCE pathways when studied in immortalized myometrial PHM1 cells.

The main objective of this work was to understand the functional role of TRPC1 and TRPC4 channels in relation to Ca^{2+} signaling in order to elucidate their relative significance in myometrium. The individual roles for TRPC1 and TRPC4 as well as the potential additive effects that a TRPC1 plus TRPC4 double knockdown exerted on SRCE were studied in PHM1 and primary human uterine smooth muscle (UtSMC) cells. This was achieved through RNAi mechanisms by expression of shRNAs targeting TRPC1, TRPC4, or TRPC1 plus TRPC4. The role of STIM1 in myometrial Ca^{2+} dynamics was also investigated by use of STIM1ΔERM, a dominant negative form of STIM1. The data presented here suggest that both TRPC1 and TRPC4 are activated by similar G protein-coupled receptor-stimulated Ca^{2+} entry mechanisms; however, no additive effects were observed by their combined knockdown. Additionally, thapsigargin- and OAG-stimulated Ca^{2+} entry were not affected by either the individual or combined knockdown of TRPC1 and TRPC4. In contrast, STIMΔERM appeared to induce an inhibitory effect on all three types of SRCE stimulation. These contributions, in addition to the important role in Ca^{2+} homeostasis played by voltage-operated channels and the influences of Ca^{2+} pumps, exchangers and potassium channels, provide the myometrium with the ability to respond in specific and precise ways to influences in its environment, both during pregnancy and at the time of parturition.

Aida Erendira Ulloa
Graduate Degree Program in Cell and Molecular Biology
Colorado State University
Fort Collins, Colorado
Fall 2010

ACKNOWLEDGEMENTS

I would like to thank all the people who have contributed near and far to the completion of this endeavor. First, I would like to thank my advisor, Dr. Barbara M. Sanborn. You are truly the greatest mentor I could have had and I am extremely honored for being your student. You ensured that I grew not only as scientist but also into a better person. The teachings that I take with me have forever changed me into, I hope, a better human being. I hope I have made you proud. Thank you for teaching me how to believe in myself.

Additionally, I would like to thank my Committee Members, as their patience, guidance and kind words helped me to bring this project to its completion.

I would also like to thank the following persons for provision of reagents: G. Hannon for the pSHAG vector, J.W. Putney Jr. for the TRPC4 cDNA clone, J. Cantlon and C. Clay for the pAdTrack-Rfa(f) vector, B. Singh for the TRPC1-overexpression adenovirus, P. Worley and S. Muallem for the original STIMΔERM original construct. I want to thank D. Murtazina for cloning STIM1ΔERM into the adenoviral vector, A. L. Gonzales and S. Earley for performing and analyzing the electrophysiological data, and K. J. Bois for creating CalciumComp. This work was supported in part by NIHF31-HD051037 (AU), NIHT32-(TN) NIH HD38970 and March of Dimes #6-FY05-77 (BMS), AHA 0535226N (SE), and NIHF31-HL09414 (ALG).

On a more personal note, I would like to thank my parents, my brother and sisters for their unconditional love and support. Having you away from me made me realize the absolute importance that you have on my life. I hope I have made you all proud. You have been and will always be my pillars. *No hay palabras suficientes para decirles cuanto los quiero y lo que les agradezco por todo lo que han hecho por mí. Los quiero mucho.*

I would like to thank my husband. You have taught me that to get anything one wants, one always has to give the best of oneself. I still wonder how you managed to stand what might have seemed like many years of a "woman on the edge". I thank you endlessly for your support, love, and friendship. *Merci, mon amour, car sans toi, je n'y serais pas arriver.*

I would need to thank my two hairy boys, without whom I could not have survived this long through this journey. My Huber, you were such an inspiration and wonderful teacher. I will have you in my heart forever, always remembering what true love and strength in life are all about. And to you my Nico, your kind heart will always be a reminder of what great hope this world can have to become a beautiful place.

Most importantly, I have to thank you my son, Liam Caleb Bois, for you have taught me so much about happiness and unconditional love. You are my greatest achievement. I will love you with all my heart forever. You are my proof that miracles do indeed exist and can actually happen. I love you my amazing little miracle.

TABLE OF CONTENTS

LIST OF TABLES

LIST OF FIGURES

LIST OF ABBREVIATIONS

ΔNP_o	open probability of a channel
AKAP	A-kinase anchoring protein
Ca^{2+}	calcium
$[Ca^{2+}]_i$	intracellular calcium concentration
CaM	calmodulin
CaCaM	Ca^{2+}/calmodulin
CaMK	Ca^{2+}/calmodulin-dependent protein kinase
DAG	diacylglycerol
ER	endoplasmic reticulum
GFP	green fluorescent protein
GPCR	G protein-coupled receptor
GSK-3β	glycogen synthase kinase-3 beta
IP_3	inositol 1,4,5-triphosphate
IP_3R	inositol 1,4,5-triphosphate receptor
LC	light chain of myosin
MLCK	myosin light chain kinase
OAG	1-oleoyl-2-acetyl-*sn*-glycerol; cell-permeable diacylglycerol
OT	oxytocin
PGF2α	prostaglandin F2α

PIP_2	phosphatidylinositol 4,5-bisphosphate
PKA	protein kinase A
PLC	phospholipase C
PMCA	plasma membrane Ca^{2+}-ATPase
RNAi	RNA interference
RT	reverse transcriptase
qPCR	quantitative/ real time PCR
SERCA	sarcoplasmic/endoplasmic reticulum Ca^{2+}-ATPase
shRNA	short hairpin RNA
SOCs	store-operated channels
SRCE	signal-regulated calcium entry
TC4OE	TRPC4 overexpression
TG	thapsigargin
TRP	transient receptor potential channel
TRPC	Canonical type of transient receptor potential channel
VOC	voltage-operated channels

CHAPTER 1

Introduction

Ion channels, important in controlling processes such as intracellular permeability, can provide regulated calcium (Ca^{2+})-entry pathways [1]. These Ca^{2+} ions can act as signals that control a variety of processes such as protein secretion, cell death, cell proliferation, and muscle contraction.

The Ca^{2+} signal involves an increase in intracellular Ca^{2+}-concentration ($[Ca^{2+}]_i$) [2;3]. This rise in $[Ca^{2+}]_i$ is of great importance in controlling the contractile activity in the myometrium [4]. The myometrium is the distinct smooth muscle layer of the uterine wall that expands during pregnancy and is involved in contraction during labor [5].

In the myometrium, increases in $[Ca^{2+}]_i$ induce contractile activity through activation of G protein-coupled receptors which can be achieved by stimulation with uterine contractants such as oxytocin. Additionally, intracellular Ca^{2+} store refilling has proven vital for continued contractile activity [6]. Activation of receptors and/or depletion of agonist-sensitive intracellular Ca^{2+} stores as well as activation of second messengers can stimulate the rate of Ca^{2+}- uptake from the

extracellular solution. Receptor-operated Ca^{2+} entry from the extracellular environment can be achieved by mechanisms that are dependent or independent of intracellular Ca^{2+} store depletion [7]. Store depletion can also induce extracellular Ca^{2+} entry through several mechanisms (reviewed in [7-9]). For simplicity, receptor- and store-operated Ca^{2+} entry mechanisms, as well as those activated by other second messengers, measured as stimulus- and extracellular Ca^{2+}-dependent increases in $[Ca^{2+}]_i$, are operationally termed signal-regulated Ca^{2+} entry (SRCE) in this study. Increases in $[Ca^{2+}]_i$ play important roles in the contraction of the myometrium. These increases in $[Ca^{2+}]_i$, obtained either from receptor activation or store depletion, are necessary for the production of the Ca^{2+}-calmodulin complex (CaCaM). The CaCaM complex activates myosin-light chain kinase which in turn phosphorylates the 20 kDa regulatory light chain of myosin, allowing for an actin-myosin interaction. Finally, the actin-activated myosin ATPase results in contraction (reviewed on [10]) (Fig. 1.1). Relaxation, on the other hand, is facilitated by decreases in $[Ca^{2+}]_i$ and by covalent modification of components of the contractile apparatus. The process for increases in $[Ca^{2+}]_i$ is mediated through cation channels [11]; however, the molecules that constitute these channels have not been identified with certainty. Potential candidates for the cation channels mediating SRCE are the canonical type of transient receptor potential (TRPC) proteins [11].

TRP channels constitute a superfamily of cation permeable channels. The TRP proteins were originally identified in *Drosophila*. The TRP proteins described here are light-sensitive cation influx channels that are Ca^{2+}-permeable and play a central role in phototransduction pathways [12]. Since then, several different homologues have been identified in flies, worms, fish, tunicates and mammals. In humans alone, the TRP family

Fig. 1.1. Hormones such as oxytocin (OT) activate GPCRs leading to the production of diacylglycerol (DAG) and inositol-1,4,5-triphosphate (IP3) through the activity of phospholipase C (PLC). IP3 in turn, releases Ca^{2+} from the endoplasmic reticulum (ER). Ca^{2+} binds calmodulin (CaM) and activates myosin light chain kinase (MLCK), which induces the phosphorylation of myosin light chain (LC), leading to ATP-dependent contractions. Store-operated depletion, as well as IP3, and DAG, activate signal-regulated Ca^{2+} entry (SRCE) to allow Ca^{2+} back into the cell. The canonical transient receptor potential (TRPC) channels are potential candidates involved in SRCE. Similarly to $[Ca^{2+}]_i$, smooth muscle contractions can be modulated via changes in $[Na^+]_i$. Increases in $[Na^+]_i$ can activate transporters and exchangers, potentially allowing Na^+ influx through Na^+/Ca^{2+} exchanger working in reverse mode. Also, increases in intracellular $[Na^+]$ can induce membrane depolarization leading to the activation of voltage-operated calcium channels and thus Ca^{2+} entry. Ca^{2+} entry via L-type voltage-dependent Ca^{2+} channels (VOC) is also highly important for the regulation of myometrial contractions.

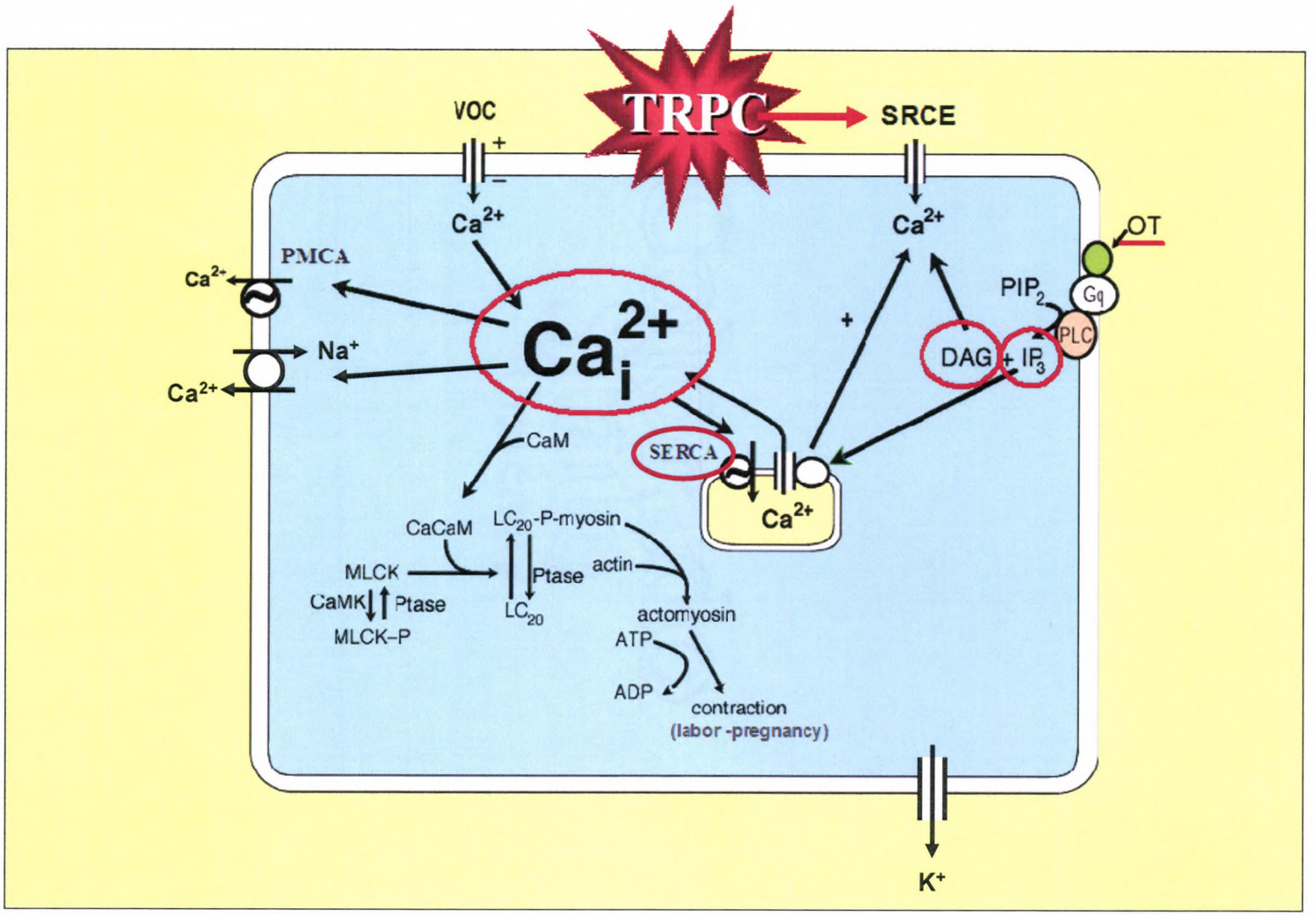
TRPC
VOC
SRCE
+
−
Ca2+
Ca2+
OT
PMCA
Ca2+
PIP2
Gq
Na+
Ca2+
Cai2+
+
PLC
DAG
+ IP3
CaM
SERCA
Ca2+
CaCaM
LC20-P-myosin
MLCK
Ptase
actin
CaMK
Ptase
LC20
actomyosin
MLCK–P
ATP
ADP
contraction
(labor -pregnancy)
K+

is comprised of more than twenty different cation channels [13]. The TRP family is subdivided into seven subfamilies [14]. The vanilloid TRPs (TRPV), which hold similarities to the vanilloid receptor, are activated by temperature as well as being involved in pain-sensing, osmolarity changes and mechanical stimuli. Two members of the melastatin TRPM family that are highly homologous to the tumor suppressor melastatin, TRPM6 and TRPM7, contain a protein kinase on their C-terminal end as part of the protein. The ankyrin TRP (TRPA) subfamily formed by its single member TRPA1 is activated by noxious stimuli such as cold temperature, mechanical stimuli and environment irritants as well as by compounds found in garlic, horseradish and wasabi. It is suggested to have a role in inflammatory and mechanical pain [15]. The TRPN (NOMP-C homologues) subfamily consists of only one member found in worms, flies and zebrafish with a role involved in mechanotransduction. The polycystin (TRPP) subfamily is formed by the polycystic kidney disease (PKD) proteins. Potential roles in fertility, retinal development and testis have been identified. The mucolipin (TRPML) subfamily has been detected in intracellular vesicles and endosomes [16].

The classical or canonical TRPs (TRPC) hold the highest homology to *Drosophila* TRP and they present a large number of different activation modes. The phototransduction process in *Drosophila* is suggested to be analogous to the phosphoinositide-mediated Ca^{2+} influx process in other cells [17]. Characteristics of TRPC channels range from cation nonselectivity, where both mono- and divalent ions can carry inward currents, to channels exhibiting high Ca^{2+} selectivity [7]. Some TRPCs are thought to be $G_{q/11}$ receptor-operated channels while others are activated by store depletion and stretch. Additional activation mechanisms involve diacylglycerol (DAG)

production [7;8] and the redox process [18]. These characteristics placed TRPC proteins as good candidates for the study intracellular Ca^{2+} dynamics in the human myometrium.

1.1 Topology of TRP channels

TRP proteins consist of six transmembrane (TM) spanning helices, cytoplasmic amino- and carboxy-terminal ends, and a potential pore-forming region between TM5 and TM6 [19] (Fig. 1.2). A conserved TRP box/domain, found at the C-terminal end of the TM6, is hypothesized to aid formation of TRPs into homo-/heterotetramer channels [20], PIP_2 binding [21] as well as a possible negative allosteric modulator of the channel [22]. Each TRP channel-forming subunit can form a signalplex, a macromolecular complex formed by interaction of TRP domains with other proteins (i.e., scaffold proteins and kinases) to bring them into close proximity and facilitate the transmembrane signaling process [23;24]. For instance, in *Drosophila* the signalplex is brought together by INAD (NHERF homologue in mammals), a protein containing five PDZ domains. INAD is able to tether to the TRP channel, phospholipase C (PLC), protein kinase C (PKC), and calmodulin (CaM) among others. Coexpression experiments with TRP and INAD suggest that binding of TRP to the signalplex may abolish the apparent store-dependent regulation of TRP [23;24].

The TRPC subfamily is composed of seven members (TRPC1-7) divided into TRPC4/5, TRPC3/6/7, and TRPC1 subgroups based on their amino acid homology. TRPC2 has been found to be a pseudogene in humans but encodes channels in rat and mouse systems. It has been suggested that TRPC3/6/7 group members cannot associate with members of the TRPC1/4/5 group [25-28], but others indicate association between

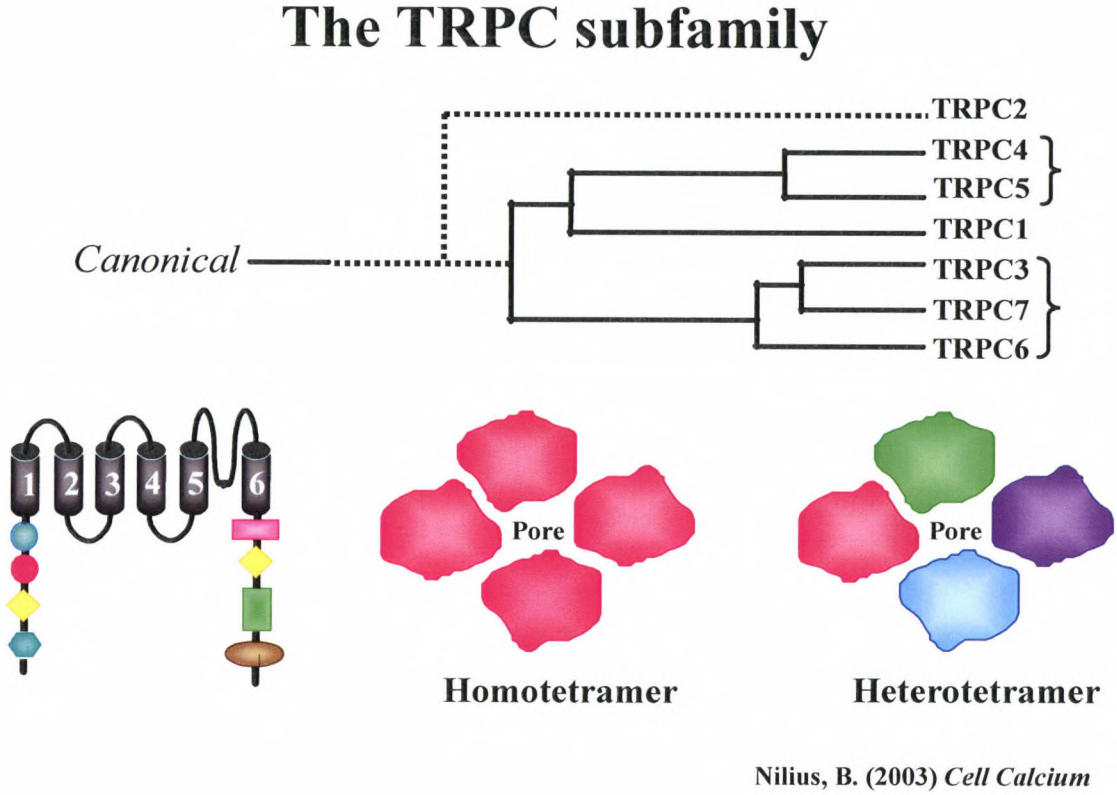

Fig. 1.2. The TRPC subfamily is composed of seven members (TRPC1-7) divided into TRPC4/5, TRPC3/6/7, and TRPC1 subgroups based on their amino acid homology. TRPC proteins consist of six transmembrane (TM) spanning helices, cytoplasmic amino- and carboxy-terminal ends, and a potential pore-forming region between TM5 and TM6. A conserved TRP box/domain is hypothesized to aid formation of TRPCs into homo- or heterotetramer channels.

members of both groups (reviewed on [14;29;30]. Domains aiding in the tetramerization of TRPC channels may include N-terminal interactions through ankyrin-coiled coil domains along with other C-terminal interactions [31]. The TRPC1-7 isoform expression

profile can vary dramatically from one cell type to another as well as among the same cell types in different organisms. The tetrameric nature of the channel and the differential expression of specific TRPCs create the possibility of cell-specific homo- or heterotetrameric channels with unique functional properties [25]. As a result of interaction domains in both N- and C-termini, each TRPC subunit forming the channel can potentially contribute to the formation of macromolecular complexes unique to specific cell types [7]. The functional and regulatory properties of these potentially unique endogenous TRPC homo- and/or heterotetramer channels are still unknown.

1.2 Activation of TRPC channels

TRPC proteins can be activated by hormones and neurotransmitters via agonist receptors such as G-protein coupled receptors (GPCRs) and receptor tyrosine kinases (RTKs). Activation of receptors and/or depletion of agonist-sensitive intracellular Ca^{2+} stores stimulate Ca^{2+}-uptake from the extracellular environment. These receptors can activate phospholipase Cs (PLC) which can induce hydrolysis of phosphatidylinositol bisphosphate to produce inositol-(1,4,5) triphosphate (IP_3) and 1,2-diacylglycerol (DAG). IP_3 binds to and activates the IP_3 receptors (IP_3-R) in the endoplasmic reticulum (ER), resulting in Ca^{2+} release from these intracellular stores. In addition to the PLC-dependent Ca^{2+} release from these intracellular stores, inhibition of ER/SR Ca^{2+}-ATPase (SERCA) pumps resulting in Ca^{2+} release and DAG itself are suggested to induce TRPC activation directly or indirectly [7;8] (Fig. 1.1).

1.3 Characteristics of the TRPC subfamily

1.3.1 TRPC4, and TRPC5

TRPC4/5 channels are suggested receptor-operated cation (ROC) channels activated in a PLC-dependent manner [32-35], since their activation can be abolished by PLC inhibitors [36]. Some studies define these channels as Ca^{2+}-permeable, nonselective cation channels, activated independently of IP3-R activation or Ca^{2+}-store depletion [32-34;37-40] while others define them as activated by store depletion [34;40-43]. TRPC4 knockout studies ($TRPC4^{-/-}$) in mouse implicate TRPC4 proteins in agonist-induced Ca^{2+} entry [37;44-47]. These studies suggest that $TRPC4^{-/-}$ mice show impaired agonist-dependent vasorelaxation. Also, DAG exhibits a negative regulatory effect on TRPC4 and TRPC5 activation, through protein kinase C (PKC) [38;48].

Activation of TRPC4/5 may also involve signalplex formation. TRPC4/5 contain PDZ-binding motifs absent in other TRPC isoforms, allowing TRPC4/5 interaction with scaffolding protein NHERF/EBP50 and PLCβ [35;49;50]. In addition, TRPC4/5 contain C-terminal CaM-binding sites, enabling them to interact with CaM in a Ca^{2+}-dependent manner [51]; these sites may be involved in feedback inhibition of channel activity by Ca^{2+}. Interestingly, two of the three CaM binding sites are also IP3-R-binding domains [52;53], consistent with regulation by IP3-mediated Ca^{2+}-store depletion [37].

Most TRPC4 studies have focused on the functional properties of exogenously overexpressed TRPC4 channels. Some studies indicate that TRPC4, and the closely related TRPC5 channels, are receptor-operated cation channels activated in a phospholipase C-dependent manner. Other studies define these channels as Ca^{2+}-permeable, nonselective cation channels, activated independent of IP_3-R activation or

Ca^{2+}-store depletion, whereas still others suggest activation by store depletion, with or without a potential interaction with TRPC1 [41;42;54]. Interactions of TRPC4 with TRPC1 have been recorded both with endogenously and exogenously expressed proteins [25;55;56]. Interestingly, overexpression of TRPC4 renders a current-voltage relationship (I-V) that strongly differs from that obtained in cells overexpressing both TRPC1 and TRPC4 [32]. Studies conducted by Greka et. al. [57] show that TRPC5 and TRPC1 proteins are capable of forming both homotetrameric as well as heterotetrameric channels in the same cell. However, it is thought that overexpression systems may render the majority of the channels as homotetramers of the subunit being overexpressed [58]. Thus, endogenous and exogenously expressed channels may display significantly different properties depending on the TRPCs already expressed in the system of study [58]. Because of the putative heterotetrameric nature of the TRPC channels, overexpression may not replicate the endogenous configuration of channels containing TRPC4 in a particular tissue and may promote interactions with other proteins that do not normally occur when TRPC4 is present at endogenous concentrations.

1.3.2 TRPC1

TRPC1 is widely expressed throughout the body; it is unclear if TRPC1 has a common or tissue-specific roles [59]. It can be localized at intracellular sites such as the endoplasmic reticulum (ER) and the Golgi apparatus as well as at the plasma membrane [60]. Interestingly, some studies show that ectopically expressed TRPC1 requires expression of TRPC4/5 for its translocation to the plasma membrane [25;61]. In smooth muscle cells and astrocytes, TRPC1 is suggested to localize in regions adjacent to the underlying ER when TRPC1 is present in the plasma membrane [62;63].

TRPC1 may act within cholesterol-rich lipid raft domains [64-66] where it can interact with molecules such as IP_3-Rs, $G_{\alpha q/11}$, plasma membrane Ca^{2+}-ATPase (PMCA), and the scaffolding protein INAD [55;64;67-70]. Localization of TRPC1 within lipid rafts as well as its interaction with cholesterol are required for smooth muscle contraction [71] and for Ca^{2+} influx in submandibular gland cells [64]. Similarly to TRPC4, TRPC1 contains binding sites for calmodulin that can also bind IP_3-Rs [60]. Furthermore, identification of PKCα- dependent phosphorylation of TRPC1 as a necessary step for store-operated Ca^{2+} entry [59] emphasizes the differential regulatory mechanisms governing independent TRPC proteins.

TRPC1 contains putative coiled-coil domains, important for its ability to induce oligomerization of TRPC subunits [72;73]. It can form homotetramers [27;59;74], heterotetramers with TRPC4/5 [25;27;32], and heterotetramers with TRPC3/6/7 [27;59;75;76], all of which exhibit different physiological characteristics. Moreover, TRPC1 may act as the key factor for heterotetramer formation, bringing members of TRPC4/5 together with members of TRPC3/6/7 as part of the same channel [56]. Since the subunit composition of a TRPC channel may modify its biophysical properties, combinations of TRPC subunits could form different channels, possibly affecting different responses when compared to its homotetrameric counterparts [73;77].

Studies of overexpressed TRPC1 report either no channel activity [32], basal channel activity unresponsive to store-depletion [72;78] or enhanced store-operated Ca^{2+} entry [67;79-82]. Such incongruities stress the disadvantage of overexpression studies that may induce formation of nonendogenous channels, while also helping to identify the functions of potential homotetramer channels. Conversely, attenuation of TRPC1

expression/activity results in reduction of store-operated Ca^{2+} entry [71;77;83-87]. Thus, expression or attenuation of each TRPC may impact the type of channels formed and thus elicit concomitant differential effects in their biophysical properties.

Based mostly on TRPC1 overexpression studies, TRPC1 is suggested to be a non-selective cation channel that facilitates entry of Na^+ and Ca^{2+} across the plasma membrane. TRPC1-mediated increases in $[Na^+]_i$ and $[Ca^{2+}]_i$ can help regulate smooth muscle contractions [88]. Studies using skeletal fibers from adult $TRPC1^{-/-}$ mice suggest that TRPC1 may be involved in Ca^{2+} entry regulation during repeated contractions as well as maintenance of force during sustained repeated contractions. These $TRPC1^{-/-}$ mice display a decrease of endurance of physical activity [89].

1.3.3 TRPC3, TRPC6 and TRPC7

TRPC3/6/7 share biophysical characteristics such as their sensitivity towards diacylglycerols analogs [90] whose effects are not mediated by protein kinase C (PKC). PKC induces negative feedback regulation of these channel proteins [53;91-93]. For instance, TRPC6 is phosphorylated by PKC, inducing an inhibition of TRPC6 activation after carbachol-stimulation [94]. In contrast, Fyn, a member of the Src family of protein tyrosine kinases, induces increases in TRPC6 channel activity. Response to other SRCE mechanisms such as store depletion is dependent on the TRPC isotype expressed [95].

Some studies define TRPC3 as an agonist-operated cation channel not activated by store-depletion [96-102], summarized in [95]). However, TRPC3 shows two different modes of activation depending on its expression levels [103]. At high expression levels, TRPC3 is regulated via receptor-coupling to PLC, independent of Ca^{2+}-store-depletion, while at low levels, TRPC3 displays activation through depletion of Ca^{2+} stores. This

suggests that TRPC3 expression levels may impact the properties of the channels that it forms [90;95;104]. In contrast, store-depletion is unable to induce TRPC6 and TRPC7 activation.

Additionally, TRPC3 and 7 share their ability to be regulated by Ca^{2+}/CaM, which causes increased activation of these proteins [53;92]. In contrast, TRPC6 exhibits an inhibitory control induced by Ca^{2+}/CaM [105]. An interesting finding however, is that both TRPC6 and TRPC3 contain similar CaM-IP3-R binding (CIRB) domains [52;53]. Therefore, controversy as to the regulation of this domain remains to be solved.

1.4 Other channels

Interplay among different channels allow the coordinated regulation of intracellular calcium dynamics in the cell. For instance, smooth muscle contractions can be modulated via changes in $[Na^+]_i$ and $[Ca^{2+}]_i$. Na^+ is linked to an array of cation transporters such as (Na^++K^+) ATPase, Na^+-anion cotransporter, and plasma membrane Na^+/Ca^{2+} exchanger. Increases in intracellular $[Na^+]$ can activate these transporters and exchangers, having the possibility of allowing Na^+ influx through Na^+/Ca^{2+} exchanger working in reverse mode [88]. Also, increases in intracellular $[Na^+]$ can induce membrane depolarization leading to the activation of voltage-operated calcium channels and thus Ca^{2+} entry. Ca^{2+} entry via L-type voltage-dependent Ca^{2+} channels regulates myometrial contractions. T-type voltage-dependent Ca^{2+} channels induce Ca^{2+} oscillations, pacemaker activity and contractility in smooth muscle. These increases in Ca^{2+} entry can in turn, activate the sarcoplasmic/endoplasmic reticulum Ca^{2+} ATPase (SERCA) and plasma membrane Ca^{2+} ATPase (PMCA) pumps. Other channels which

can be expressed in the myometrium are also important in regulation calcium dynamics such as the ATP-dependent, BK_{Ca}, small conductance (SK), voltage-gated (K_v) and 2-pore K^+ channels by promoting membrane repolarization. These channels in turn can be regulated by kinases stimulated via $G_{\alpha s}$, $G_{\alpha q}$ and $G_{\beta\gamma}$ signaling pathways [106]. Exploration of the relationships between these and other proteins regulating intracellular calcium dynamics in the myometrium is of the outmost importance to achieve an understanding of the control of myometrial contractions (reviewed on [107]).

1.5 STIM and Orai

Regulation of intracellular calcium dynamics involves increases in $[Ca^{2+}]_i$ which can be evoked by signals such as depletion of intracellular Ca^{2+}stores. In order to sustain the physiological response of Ca^{2+} oscillations, store-operated Ca^{2+} channels (SOCs) allow influx and refill of intracellular Ca^{2+} stores such as the ER. STIM1, an ER Ca^{2+}-binding protein, has been identified as a major player in the regulation and activation of SOCs [108]. It acts as an ER Ca^{2+} sensor which can interact with Orai1, a plasma membrane protein implicated in Ca^{2+} entry [109]. STIM1 is suggested to regulate TRPC channel opening and Orai1 is thought to be co-functional with TRPCs. STIM1 binds some TRPCs via the SOAR (STIM Orai activating region) within the STIM1 ERM domain [110]. STIM1 binds to and activates TRPC1, TRPC4 and TRPC5 directly [29]. However, channel activation of TRPC3 and TRPC6 by STIM1 requires the heteromultimerization of TRPC1-TRPC3 and TRPC4-TRPC6 to allow TRPC1 and TRPC4 presentation of STIM1 to TRPC3 and TRPC6, respectively [29]. Interestingly, knockdown of either TRPC1 or TRPC4 was unable to inhibit TRPC3 or TRPC6 channel

activity as STIM1-independent channel activities remained instead [29]. The authors suggest that these TRPCs can act in a STIM1-dependent and a STIM1-independent mode, regulating their functions as SOCs or non-SOCs (reviewed in [108]).

1.6 TRPCs in the myometrium

There has been limited study of the mechanisms governing SRCE in the myometrium. In rat myometrial cells increases in $[Ca^{2+}]_i$ stimulated by oxytocin, norepinephrine, and carbachol were partially dependent on extracellular Ca^{2+} and were not inhibited by L-type voltage-operated Ca^{2+}-channel (VOC) blockers [111]. Even though voltage-operated Ca^{2+} entry plays an important role in regulating myometrial contractions [107;112], PHM1-41 cells exhibit minimal response to depolarization with KCl [113], and oxytocin- and thapsigargin-mediated SRCE is nifedipine-independent [111;114]. Thus, PHM1 cells exhibit SRCE activated by GPCRs and more directly by the depletion of $[Ca^{2+}]_i$ stores [115].

1.6.1 Endogenous expression of TRPC channel proteins in myometrial cells

Since the profile of endogenous TRPC channels influences their properties, it is important to determine what channels are likely to be most abundant in myometrium. While it is difficult to quantitate TRPC isoform protein expression, it is possible to quantitate mRNA expression. Although there is not always a direct correlation between relative mRNA and protein expression, the mRNA is a reasonable starting point. Accordingly, endogenous expression profiles of TRPC isoform mRNAs were determined in pregnant human myometrium, primary human myometrial cells (UTSMC), and in 2

human myometrial cell lines (PHM1 and PHM2) by quantitative real-time PCR (RT-qPCR) [113;116]. TRPC1, TRPC4 and TRPC6 mRNAs were the most abundant mRNAs followed by TRPC3. Western blot experiments detected TRPC1, 3 and 4 proteins in both PHM1 cells and in human pregnant myometrium, while TRPC6 protein was only detected in human pregnant myometrium [113;115-117].

In contrast, I have determined that human embryonic kidney HEK293 cells, human mammary gland MCF-7 cells, and human placental Bewo cells have strikingly different TRPC mRNA profiles compared to PHM1 cells (Fig. 1.3). These data emphasize the importance of knowing the TRPC profile in the cells of interest. The presence of different TRPCs offers the possibility for channels to be in homo- or heterotetramer conformations holding unique properties in myometrium.

1.6.2 Functions of TRPC channels in signal-regulated Ca^{2+} entry in the human myometrium

PHM1 myometrial cells [51] exhibit SRCE in response to different stimuli such as oxytocin to activate a GPCR-response, thapsigargin to activate a store-depletion response, and 1-oleoyl-2-acetyl-*sn*-glycerol (OAG), a cell permeable analog of DAG. [113;114;116;118;119]. These modes of Ca^{2+} entry were inhibited by SKF96365, a selective inhibitor of receptor-mediated Ca^{2+} entry, and gadolinium, a stretch-activated ion channel blocker, at concentrations relatively specific for SRCE. On the other hand, nifedipine, a dihydropyridine L-type calcium channel blocker, did not affect these SRCE mechanisms. These type of responses are also observed in primary human myometrial cells. Additionally, infection of PHM1 cells with an adenovirus containing TRPC3

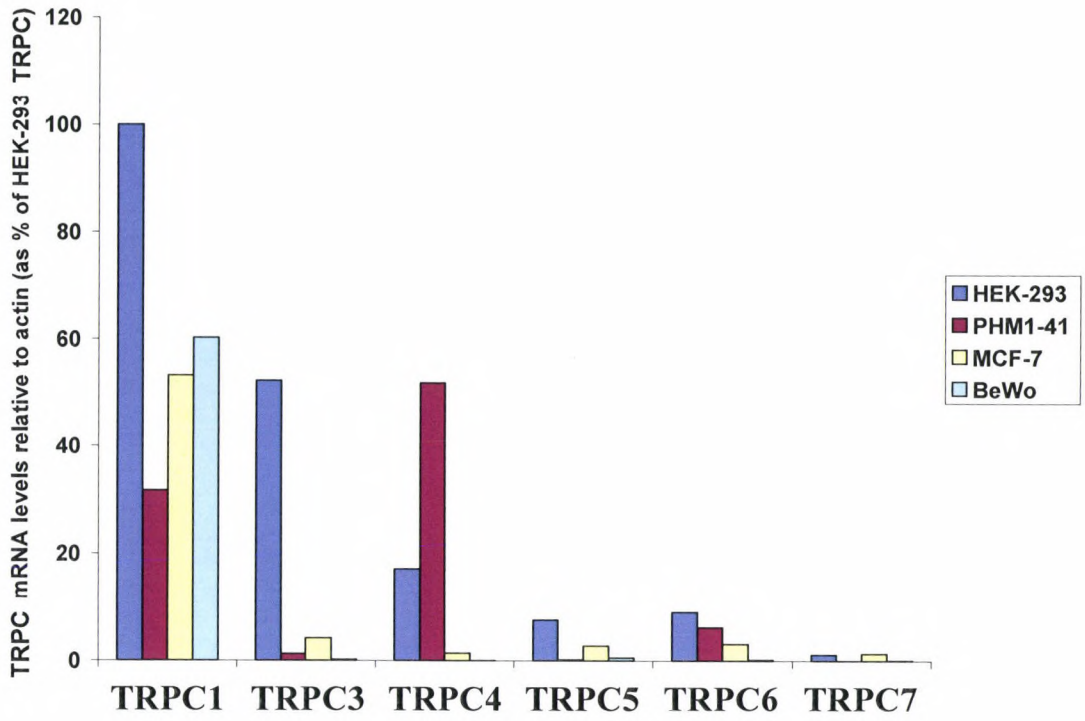

Fig. 1.3. TRPC profile in different human cell lines. Isolated RNA from these cells types were subjected to RT-qPCR using primers specific for each TRPC. mRNA levels are relative to β-actin. HEK293 (blue), PHM1(red), MCF-7(yellow), and Bewo (green), respectively (left to right) (n=1).

mRNA sequence resulted in a significant TRPC3 overexpression [114]. TRPC3 overexpression enhanced the oxytocin-, thapsigargin- and OAG-stimulated $[Ca^{2+}]_i$ response [115]. These data demonstrate the action of TRPC3 channels in SRCE via agonist-mediated activation, store-depletion, and DAG in myometrial cells. Even though Ca^{2+} entry by means of voltage-operated channels (VOC) plays important roles in myometrium in vivo and in freshly isolated tissue, the cultured cells do not respond

strongly to depolarization [51]. Thus, the Ca^{2+} entry measured in these experiments is unlikely to be VOC-mediated.

1.7 Summary and rationale for the present study

Increases in $[Ca^{2+}]_i$ correlate with increases in myometrial contractile activity. Uterine contractants such as oxytocin can induce these increases in $[Ca^{2+}]_i$ through G protein-coupled receptor and further PLC activation, similarly to the TRP-mediated phototransduction process in *Drosophila*. Previous studies in our laboratory have shown that myometrial cells present SRCE mechanisms which are not inhibited by L-type channel blockers, thus placing TRPC proteins as good candidates for the study intracellular Ca^{2+} dynamics in the human myometrium. TRPC3 overexpression in PHM1 cells displayed increases in SRCE after stimulation with oxytocin, thapsigargin and OAG. Additionally, TRPC3 mRNA and protein expression levels were found to be up-regulated in response to stretch in human myometrium [117]. As shown in Fig. 1.3, endogenous levels of TRPCs differ strongly from one system to another, potentially dictating the functional properties of the TRPC channels due to their relative abundance in the system of study. TRPC1, TRPC4 and TRPC6 are the most abundant TRPCs in the human myometrium. The aim of the present study was to attenuate the expression of TRPC1 and TRPC4 in order to determine the contributions of these TRPCs to SRCE mechanisms in human myometrial cells.

References

1. Nilius B, Droogmans G. Ion channels and their functional role in vascular endothelium. *Physiol Rev* **2001**; 81: 1415-1459.

2. Nowycky MC, Thomas AP. Intracellular calcium signaling. *J Cell Sci* **2002**; 115: 3715-3716.

3. Putney JW, Jr. Cell biology. Channelling calcium. *Nature* **2001**; 410: 648-649.

4. Sanborn BM. Relationship of ion channel activity to control of myometrial calcium. *J Soc Gynecol Investig* **2000**; 7: 4-11.

5. Rehman KS, Yin S, Mayhew BA, Word RA, Rainey WE. Human myometrial adaptation to pregnancy: cDNA microarray gene expression profiling of myometrium from non-pregnant and pregnant women. *Mol Hum Reprod* **2003**; 9: 681-700.

6. Mironneau J. Ion channels and excitation-contraction coupling in myometrium. In: Garfield RE (Ed.). 100 Longwater Circle, Norwell, Massachusetts 02061, Serono, 1990: pp. 9-19.

7. Ramsey IS, Delling M, Clapham DE. An introduction to TRP channels. *Annu Rev Physiol* **2006**; 68: 619-647.

8. Parekh AB, Putney JW, Jr. Store-operated calcium channels. *Physiol Rev* **2005**; 85: 757-810.

9. Putney JW, Jr. Recent breakthroughs in the molecular mechanism of capacitative calcium entry (with thoughts on how we got here). *Cell Calcium* **2007**; 42**:** 103-110.

10. Sanborn BM. Hormones and calcium: mechanisms controlling uterine smooth muscle contractile activity. The Litchfield Lecture. *Exp Physiol* **2001**; 86**:** 223-237.

11. Nilius B. From TRPs to SOCs, CCEs, and CRACs: consensus and controversies. *Cell Calcium* **2003**; 33**:** 293-298.

12. Hardie RC. TRP channels in Drosophila photoreceptors: the lipid connection. *Cell Calcium* **2003**; 33**:** 385-393.

13. Montell C, Birnbaumer L, Flockerzi V et al. A unified nomenclature for the superfamily of TRP cation channels. *Mol Cell* **2002**; 9**:** 229-231.

14. Latorre R, Zaelzer C, Brauchi S. Structure-functional intimacies of transient receptor potential channels. *Q Rev Biophys* **2009**; 42**:** 201-246.

15. Clapham DE. Clapham, D.E. Clapham Lab Webpage . 2007. Ref Type: Electronic Citation

16. Nilius B, Owsianik G. Transient receptor potential channelopathies. *Pflugers Arch* **2010**.

17. Hardie RC. Regulation of TRP channels via lipid second messengers. *Annu Rev Physiol* **2003**; 65**:** 735-759.

18. Groschner K, Rosker C, Lukas M. Role of TRP channels in oxidative stress. *Novartis Found Symp* **2004**; 258**:** 222-230.

19. Voets T, Nilius B. The pore of TRP channels: trivial or neglected? *Cell Calcium* **2003**; 33**:** 299-302.

20. Garcia-Sanz N, Fernandez-Carvajal A, Morenilla-Palao C et al. Identification of a tetramerization domain in the C terminus of the vanilloid receptor. *J Neurosci* **2004**; 24**:** 5307-5314.

21. Rohacs T. Regulation of TRP channels by PIP(2). *Pflugers Arch* **2007**; 453**:** 753-762.

22. Garcia-Sanz N, Valente P, Gomis A et al. A role of the transient receptor potential domain of vanilloid receptor I in channel gating. *J Neurosci* **2007**; 27**:** 11641-11650.

23. Harteneck C. Proteins modulating TRP channel function. *Cell Calcium* **2003**; 33**:** 303-310.

24. Montell C. Molecular genetics of Drosophila TRP channels. *Novartis Found Symp* **2004**; 258**:** 3-12.

25. Hofmann T, Schaefer M, Schultz G, Gudermann T. Subunit composition of mammalian transient receptor potential channels in living cells. *Proc Natl Acad Sci U S A* **2002**; 99**:** 7461-7466.

26. Amiri H, Schultz G, Schaefer M. FRET-based analysis of TRPC subunit stoichiometry. *Cell Calcium* **2003**; 33**:** 463-470.

27. Schilling WP, Goel M. Mammalian TRPC channel subunit assembly. *Novartis Found Symp* **2004**; 258**:** 18-30.

28. Ambudkar IS, Bandyopadhyay BC, Liu X, Lockwich TP, Paria B, Ong HL. Functional organization of TRPC-Ca2+ channels and regulation of calcium microdomains. *Cell Calcium* **2006**; 40**:** 495-504.

29. Yuan JP, Zeng W, Huang GN, Worley PF, Muallem S. STIM1 heteromultimerizes TRPC channels to determine their function as store-operated channels. *Nat Cell Biol* **2007**; 9**:** 636-645.

30. Saleh SN, Albert AP, Large WA. Diverse properties of store-operated TRPC channels activated by protein kinase C in vascular myocytes. *J Physiol* **2008**.

31. Lepage PK, Lussier MP, Barajas-Martinez H et al. Identification of two domains involved in the assembly of transient receptor potential canonical channels. *J Biol Chem* **2006**; 281**:** 30356-30364.

32. Strubing C, Krapivinsky G, Krapivinsky L, Clapham DE. TRPC1 and TRPC5 form a novel cation channel in mammalian brain. *Neuron* **2001**; 29**:** 645-655.

33. Lee YM, Kim BJ, Kim HJ et al. TRPC5 as a candidate for the nonselective cation channel activated by muscarinic stimulation in murine stomach. *Am J Physiol Gastrointest Liver Physiol* **2003**; 284**:** G604-G616.

34. Zeng F, Xu SZ, Jackson PK et al. Human TRPC5 channel activated by a multiplicity of signals in a single cell. *J Physiol* **2004**; 559**:** 739-750.

35. Suh PG, Hwang JI, Ryu SH, Donowitz M, Kim JH. The roles of PDZ-containing proteins in PLC-beta-mediated signaling. *Biochem Biophys Res Commun* **2001**; 288**:** 1-7.

36. Plant TD, Schaefer M. TRPC4 and TRPC5: receptor-operated Ca2+-permeable nonselective cation channels. *Cell Calcium* **2003**; 33**:** 441-450.

37. Freichel M, Philipp S, Cavalie A, Flockerzi V. TRPC4 and TRPC4-deficient mice. *Novartis Found Symp* **2004**; 258**:** 189-199.

38. Venkatachalam K, Zheng F, Gill DL. Regulation of canonical transient receptor potential (TRPC) channel function by diacylglycerol and protein kinase C. *J Biol Chem* **2003**; 278**:** 29031-29040.

39. So I, Kim KW. Nonselective cation channels activated by the stimulation of muscarinic receptors in mammalian gastric smooth muscle. *J Smooth Muscle Res* **2003**; 39**:** 231-247.

40. Beech DJ, Muraki K, Flemming R. Non-selective cationic channels of smooth muscle and the mammalian homologues of Drosophila TRP. *J Physiol* **2004**; 559**:** 685-706.

41. Plant TD, Schaefer M. Receptor-operated cation channels formed by TRPC4 and TRPC5. *Naunyn Schmiedebergs Arch Pharmacol* **2005**; 371**:** 266-276.

42. Vanden AF, Lemonnier L, Thebault S et al. Two types of store-operated Ca2+ channels with different activation modes and molecular origin in LNCaP human prostate cancer epithelial cells. *J Biol Chem* **2004**; 279**:** 30326-30337.

43. Wang X, Pluznick JL, Wei P, Padanilam BJ, Sansom SC. TRPC4 forms store-operated Ca2+ channels in mouse mesangial cells. *Am J Physiol Cell Physiol* **2004**; 287**:** C357-C364.

44. Freichel M, Suh SH, Pfeifer A et al. Lack of an endothelial store-operated Ca2+ current impairs agonist-dependent vasorelaxation in TRP4-/- mice. *Nat Cell Biol* **2001**; 3**:** 121-127.

45. Tiruppathi C, Freichel M, Vogel SM et al. Impairment of store-operated Ca2+ entry in TRPC4(-/-) mice interferes with increase in lung microvascular permeability. *Circ Res* **2002**; 91**:** 70-76.

46. Freichel M, Vennekens R, Olausson J et al. Functional role of TRPC proteins in vivo: lessons from TRPC-deficient mouse models. *Biochem Biophys Res Commun* **2004**; 322**:** 1352-1358.

47. Freichel M, Vennekens R, Olausson J et al. Functional role of TRPC proteins in native systems: implications from knockout and knock-down studies. *J Physiol* **2005**; 567**:** 59-66.

48. Venkatachalam K, Zheng F, Gill DL. Control of TRPC and store-operated channels by protein kinase C. *Novartis Found Symp* **2004**; 258**:** 172-185.

49. Mery L, Strauss B, Dufour JF, Krause KH, Hoth M. The PDZ-interacting domain of TRPC4 controls its localization and surface expression in HEK293 cells. *J Cell Sci* **2002**; 115**:** 3497-3508.

50. Tang Y, Tang J, Chen Z et al. Association of mammalian trp4 and phospholipase C isozymes with a PDZ domain-containing protein, NHERF. *J Biol Chem* **2000**; 275**:** 37559-37564.

51. Monga M, Ku CY, Dodge K, Sanborn BM. Oxytocin-stimulated responses in a pregnant human immortalized myometrial cell line. *Biol Reprod* **1996**; 55**:** 427-432.

52. Tang J, Lin Y, Zhang Z, Tikunova S, Birnbaumer L, Zhu MX. Identification of common binding sites for calmodulin and inositol 1,4,5-trisphosphate receptors on the carboxyl termini of trp channels. *J Biol Chem* **2001**; 276**:** 21303-21310.

53. Zhang Z, Tang J, Tikunova S et al. Activation of Trp3 by inositol 1,4,5-trisphosphate receptors through displacement of inhibitory calmodulin from a common binding domain. *Proc Natl Acad Sci U S A* **2001**; 98**:** 3168-3173.

54. Abad E, Lorente G, Gavara N, Morales M, Gual A, Gasull X. Activation of store-operated Ca(2+) channels in trabecular meshwork cells. *Invest Ophthalmol Vis Sci* **2008**; 49**:** 677-686.

55. Goel M, Sinkins WG, Schilling WP. Selective association of TRPC channel subunits in rat brain synaptosomes. *J Biol Chem* **2002**; 277**:** 48303-48310.

56. Strubing C, Krapivinsky G, Krapivinsky L, Clapham DE. Formation of novel TRPC channels by complex subunit interactions in embryonic brain. *J Biol Chem* **2003**; 278**:** 39014-39019.

57. Greka A, Navarro B, Oancea E, Duggan A, Clapham DE. TRPC5 is a regulator of hippocampal neurite length and growth cone morphology. *Nat Neurosci* **2003**; 6**:** 837-845.

58. Cavalie A. Ionic channels formed by TRPC4. *Handb Exp Pharmacol* **2007**; 93-108.

59. Ahmmed GU, Mehta D, Vogel S et al. Protein kinase Calpha phosphorylates the TRPC1 channel and regulates store-operated Ca2+ entry in endothelial cells. *J Biol Chem* **2004**; 279**:** 20941-20949.

60. Rychkov G, Barritt GJ. TRPC1 Ca(2+)-permeable channels in animal cells. *Handb Exp Pharmacol* **2007**; 23-52.

61. Yuan JP, Kiselyov K, Shin DM et al. Homer binds TRPC family channels and is required for gating of TRPC1 by IP3 receptors. *Cell* **2003**; 114**:** 777-789.

62. Dalrymple A, Slater DM, Beech D, Poston L, Tribe RM. Molecular identification and localization of Trp homologues, putative calcium channels, in pregnant human uterus. *Mol Hum Reprod* **2002**; 8**:** 946-951.

63. Golovina VA. Visualization of localized store-operated calcium entry in mouse astrocytes. Close proximity to the endoplasmic reticulum. *J Physiol* **2005**; 564**:** 737-749.

64. Lockwich TP, Liu X, Singh BB, Jadlowiec J, Weiland S, Ambudkar IS. Assembly of Trp1 in a signaling complex associated with caveolin-scaffolding lipid raft domains. *J Biol Chem* **2000**; 275**:** 11934-11942.

65. Ambudkar IS, Brazer SC, Liu X, Lockwich T, Singh B. Plasma membrane localization of TRPC channels: role of caveolar lipid rafts. *Novartis Found Symp* **2004**; 258**:** 63-70.

66. Brownlow SL, Harper AG, Harper MT, Sage SO. A role for hTRPC1 and lipid raft domains in store-mediated calcium entry in human platelets. *Cell Calcium* **2004**; 35**:** 107-113.

67. Singh BB, Zheng C, Liu X et al. Trp1-dependent enhancement of salivary gland fluid secretion: role of store-operated calcium entry. *FASEB J* **2001**; 15**:** 1652-1654.

68. Singh BB, Liu X, Tang J, Zhu MX, Ambudkar IS. Calmodulin regulates Ca(2+)-dependent feedback inhibition of store-operated Ca(2+) influx by interaction with a site in the C terminus of TrpC1. *Mol Cell* **2002**; 9**:** 739-750.

69. Rosado JA, Sage SO. Activation of store-mediated calcium entry by secretion-like coupling between the inositol 1,4,5-trisphosphate receptor type II and human

transient receptor potential (hTrp1) channels in human platelets. *Biochem J* **2001**; 356**:** 191-198.

70. Tsiokas L, Arnould T, Zhu C, Kim E, Walz G, Sukhatme VP. Specific association of the gene product of PKD2 with the TRPC1 channel. *Proc Natl Acad Sci U S A* **1999**; 96**:** 3934-3939.

71. Bergdahl A, Gomez MF, Dreja K et al. Cholesterol depletion impairs vascular reactivity to endothelin-1 by reducing store-operated Ca2+ entry dependent on TRPC1. *Circ Res* **2003**; 93**:** 839-847.

72. Engelke M, Friedrich O, Budde P et al. Structural domains required for channel function of the mouse transient receptor potential protein homologue TRP1beta. *FEBS Lett* **2002**; 523**:** 193-199.

73. Burkhard P, Stetefeld J, Strelkov SV. Coiled coils: a highly versatile protein folding motif. *Trends Cell Biol* **2001**; 11**:** 82-88.

74. Liu X, Singh BB, Ambudkar IS. TRPC1 is required for functional store-operated Ca2+ channels. Role of acidic amino acid residues in the S5-S6 region. *J Biol Chem* **2003**; 278**:** 11337-11343.

75. Lintschinger B, Balzer-Geldsetzer M, Baskaran T et al. Coassembly of Trp1 and Trp3 proteins generates diacylglycerol- and Ca2+-sensitive cation channels. *J Biol Chem* **2000**; 275**:** 27799-27805.

76. Zagranichnaya TK, Wu X, Villereal ML. Endogenous TRPC1, TRPC3, and TRPC7 proteins combine to form native store-operated channels in HEK-293 cells. *J Biol Chem* **2005**; 280**:** 29559-29569.

77. Beech DJ, Xu SZ, McHugh D, Flemming R. TRPC1 store-operated cationic channel subunit. *Cell Calcium* **2003**; 33**:** 433-440.

78. Sinkins WG, Estacion M, Schilling WP. Functional expression of TrpC1: a human homologue of the Drosophila Trp channel. *Biochem J* **1998**; 331 (Pt 1)**:** 331-339.

79. Delmas P, Wanaverbecq N, Abogadie FC, Mistry M, Brown DA. Signaling microdomains define the specificity of receptor-mediated InsP(3) pathways in neurons. *Neuron* **2002**; 34**:** 209-220.

80. Liu X, Wang W, Singh BB et al. Trp1, a candidate protein for the store-operated Ca(2+) influx mechanism in salivary gland cells. *J Biol Chem* **2000**; 275**:** 3403-3411.

81. Zhu X, Jiang M, Peyton M et al. trp, a novel mammalian gene family essential for agonist-activated capacitative Ca2+ entry. *Cell* **1996**; 85**:** 661-671.

82. Kunichika N, Yu Y, Remillard CV, Platoshyn O, Zhang S, Yuan JX. Overexpression of TRPC1 enhances pulmonary vasoconstriction induced by capacitative Ca2+ entry. *Am J Physiol Lung Cell Mol Physiol* **2004**; 287**:** L962-L969.

83. Vandebrouck C, Martin D, Colson-Van SM, Debaix H, Gailly P. Involvement of TRPC in the abnormal calcium influx observed in dystrophic (mdx) mouse skeletal muscle fibers. *J Cell Biol* **2002**; 158**:** 1089-1096.

84. Vaca L, Sampieri A. Calmodulin modulates the delay period between release of calcium from internal stores and activation of calcium influx via endogenous TRP1 channels. *J Biol Chem* **2002**; 277**:** 42178-42187.

85. Mori Y, Wakamori M, Miyakawa T et al. Transient receptor potential 1 regulates capacitative Ca(2+) entry and Ca(2+) release from endoplasmic reticulum in B lymphocytes. *J Exp Med* **2002**; 195**:** 673-681.

86. Xu SZ, Beech DJ. TrpC1 is a membrane-spanning subunit of store-operated Ca(2+) channels in native vascular smooth muscle cells. *Circ Res* **2001**; 88**:** 84-87.

87. Sweeney M, Yu Y, Platoshyn O, Zhang S, McDaniel SS, Yuan JX. Inhibition of endogenous TRP1 decreases capacitative Ca2+ entry and attenuates pulmonary artery smooth muscle cell proliferation. *Am J Physiol Lung Cell Mol Physiol* **2002**; 283**:** L144-L155.

88. Eder P, Poteser M, Romanin C, Groschner K. Na(+) entry and modulation of Na(+)/Ca(2+) exchange as a key mechanism of TRPC signaling. *Pflugers Arch* **2005**; 451**:** 99-104.

89. Zanou N, Shapovalov G, Louis M et al. Role of TRPC1 channel in skeletal muscle function. *Am J Physiol Cell Physiol* **2010**; 298**:** C149-C162.

90. Trebak M, Vazquez G, Bird GS, Putney JW, Jr. The TRPC3/6/7 subfamily of cation channels. *Cell Calcium* **2003**; 33**:** 451-461.

91. Inoue R, Okada T, Onoue H et al. The transient receptor potential protein homologue TRP6 is the essential component of vascular alpha(1)-adrenoceptor-activated Ca(2+)-permeable cation channel. *Circ Res* **2001**; 88**:** 325-332.

92. Okada T, Inoue R, Yamazaki K et al. Molecular and functional characterization of a novel mouse transient receptor potential protein homologue TRP7. Ca(2+)-permeable cation channel that is constitutively activated and enhanced by stimulation of G protein-coupled receptor. *J Biol Chem* **1999**; 274**:** 27359-27370.

93. Trebak M, Hempel N, Wedel BJ, Smyth JT, Bird GS, Putney JW, Jr. Negative regulation of TRPC3 channels by protein kinase C-mediated phosphorylation of serine 712. *Mol Pharmacol* **2005**; 67**:** 558-563.

94. Estacion M, Li S, Sinkins WG et al. Activation of human TRPC6 channels by receptor stimulation. *J Biol Chem* **2004**; 279**:** 22047-22056.

95. Gudermann T, Hofmann T, Schnitzler M, Dietrich A. Activation, subunit composition and physiological relevance of DAG-sensitive TRPC proteins. *Novartis Found Symp* **2004**; 258**:** 103-118.

96. Zitt C, Obukhov AG, Strubing C et al. Expression of TRPC3 in Chinese hamster ovary cells results in calcium-activated cation currents not related to store depletion. *J Cell Biol* **1997**; 138**:** 1333-1341.

97. Kamouchi M, Philipp S, Flockerzi V et al. Properties of heterologously expressed hTRP3 channels in bovine pulmonary artery endothelial cells. *J Physiol* **1999**; 518 Pt 2: 345-358.

98. Zhu X, Jiang M, Birnbaumer L. Receptor-activated Ca2+ influx via human Trp3 stably expressed in human embryonic kidney (HEK)293 cells. Evidence for a non-capacitative Ca2+ entry. *J Biol Chem* **1998**; 273: 133-142.

99. McKay RR, Szymeczek-Seay CL, Lievremont JP et al. Cloning and expression of the human transient receptor potential 4 (TRP4) gene: localization and functional expression of human TRP4 and TRP3. *Biochem J* **2000**; 351 Pt 3: 735-746.

100. Ma HT, Patterson RL, van Rossum DB, Birnbaumer L, Mikoshiba K, Gill DL. Requirement of the inositol trisphosphate receptor for activation of store-operated Ca2+ channels. *Science* **2000**; 287: 1647-1651.

101. Trebak M, Bird GS, McKay RR, Putney JW, Jr. Comparison of human TRPC3 channels in receptor-activated and store-operated modes. Differential sensitivity to channel blockers suggests fundamental differences in channel composition. *J Biol Chem* **2002**; 277: 21617-21623.

102. Groschner K, Hingel S, Lintschinger B et al. Trp proteins form store-operated cation channels in human vascular endothelial cells. *FEBS Lett* **1998**; 437: 101-106.

103. Vazquez G, Wedel BJ, Trebak M, St JB, Putney JW, Jr. Expression level of the canonical transient receptor potential 3 (TRPC3) channel determines its mechanism of activation. *J Biol Chem* **2003**; 278**:** 21649-21654.

104. Putney JW, Jr., Trebak M, Vazquez G, Wedel B, Bird GS. Signalling mechanisms for TRPC3 channels. *Novartis Found Symp* **2004**; 258**:** 123-133.

105. Boulay G. Ca(2+)-calmodulin regulates receptor-operated Ca(2+) entry activity of TRPC6 in HEK-293 cells. *Cell Calcium* **2002**; 32**:** 201-207.

106. Brainard AM, Korovkina VP, England SK. Potassium channels and uterine function. *Semin Cell Dev Biol* **2007**; 18**:** 332-339.

107. Sanborn BM. Hormonal signaling and signal pathway crosstalk in the control of myometrial calcium dynamics. *Semin Cell Dev Biol* **2007**; 18**:** 305-314.

108. Lee KP, Yuan JP, Hong JH, So I, Worley PF, Muallem S. An endoplasmic reticulum/plasma membrane junction: STIM1/Orai1/TRPCs. *FEBS Lett* **2009**.

109. Deng X, Wang Y, Zhou Y, Soboloff J, Gill DL. STIM and Orai: dynamic intermembrane coupling to control cellular calcium signals. *J Biol Chem* **2009**; 284**:** 22501-22505.

110. Huang GN, Zeng W, Kim JY et al. STIM1 carboxyl-terminus activates native SOC, I(crac) and TRPC1 channels. *Nat Cell Biol* **2006**; 8**:** 1003-1010.

111. Anwer K, Sanborn BM. Changes in intracellular free calcium in isolated myometrial cells: role of extracellular and intracellular calcium and possible

involvement of guanine nucleotide-sensitive proteins. *Endocrinology* **1989**; 124**:** 17-23.

112. Wray S, Jones K, Kupittayanant S et al. Calcium signaling and uterine contractility. *J Soc Gynecol Investig* **2003**; 10**:** 252-264.

113. Yang M, Gupta A, Shlykov SG, Corrigan R, Tsujimoto S, Sanborn BM. Multiple Trp isoforms implicated in capacitative calcium entry are expressed in human pregnant myometrium and myometrial cells. *Biol Reprod* **2002**; 67**:** 988-994.

114. Shlykov SG, Yang M, Alcorn JL, Sanborn BM. Capacitative cation entry in human myometrial cells and augmentation by hTrpC3 overexpression. *Biol Reprod* **2003**; 69**:** 647-655.

115. Dalrymple A, Slater DM, Poston L, Tribe RM. Physiological induction of transient receptor potential canonical proteins, calcium entry channels, in human myometrium: influence of pregnancy, labor, and interleukin-1 beta. *J Clin Endocrinol Metab* **2004**; 89**:** 1291-1300.

116. Ku CY, Babich L, Word RA et al. Expression of transient receptor channel proteins in human fundal myometrium in pregnancy. *J Soc Gynecol Investig* **2006**; 13**:** 217-225.

117. Dalrymple A, Mahn K, Poston L, Songu-Mize E, Tribe RM. Mechanical stretch regulates TRPC expression and calcium entry in human myometrial smooth muscle cells. *Mol Hum Reprod* **2007**; 13**:** 171-179.

118. Monga M, Campbell DF, Sanborn BM. Oxytocin-stimulated capacitative calcium entry in human myometrial cells. *Am J Obstet Gynecol* **1999**; 181: 424-429.

119. Shlykov SG, Sanborn BM. Stimulation of intracellular Ca2+ oscillations by diacylglycerol in human myometrial cells. *Cell Calcium* **2004**; 36: 157-164.

CHAPTER 2

Materials and Methods

2.1 Reagents and solutions

Primers were purchased from Integrated DNA Technologies, Inc (Coralville, IA). SYBR Green I nucleic acid gel stain was purchased from Lonza (Rockland, ME). Restriction enzymes were obtained from New England Biolabs Inc. (Beverly, MA) or Promega (Madison, WI). Fura-2/acetoxymethylester (Fura 2-AM) and Pluronic F127 were obtained from Molecular Probes (Invitrogen, Carlsbad, CA). Oxytocin, thapsigargin, ATP, prostaglandin F (PGF)2α, collagen solution and protease inhibitor cocktail were purchased from Sigma-Aldrich (St. Louis, MO). 1-oleoyl-2-acetyl-*sn*-glycerol (OAG) was obtained from Calbiochem (San Diego, CA). Cell culture media and other reagents were obtained from Gibco BRL Invitrogen (Carlsbad, CA). TRPC1 rabbit monoclonal antibody and its corresponding blocking peptide were obtained from Epitomics (Burlingame, CA). TRPC4 polyclonal antibody and its corresponding blocking peptide were purchased from Alomone Labs (Jerusalem, Israel). Anti-HA

peroxidase mouse monoclonal antibody was purchased from Roche (Indianapolis, IN). Primary polyclonal human PLCB3 antibody and horseradish peroxidase (HRP) conjugated donkey anti-rabbit secondary antibodies were purchased from Santa Cruz Biotechnology Inc. (Santa Cruz, CA)

2.2 Cell Culture

UtSMC (Uterine Smooth Muscle Cells) cells derived from nonpregnant human myometrium (Catalog #: CC-2562 Lot # 17590) were purchased from Lonza (Walkersville, MD). AD293 cells were obtained from Stratagene (La Jolla, CA). UtSMC and AD293 cells were cultured in Dulbecco's Modified Eagle Medium (DMEM) containing 10% fetal calf serum, 2 mM L-glutamine, 50 units/ml penicillin, and 50 μg/ml streptomycin. Immortalized PHM1-41 cells were derived from late-term pregnant human myometrial tissue and retain many morphological and biological characteristics of myometrial smooth muscle cells [1-5]. PHM1-41 cells were cultured in the media described above including 0.1 mg/ml of G418 sulfate (Gibco BRL Invitrogen, Carlsbad, CA). PHM1-41 cells were used at passages 20-25 and UtSMC were used at passages 6-10. Myometrial cells were trypsinized and plated in 35 mm glass-bottomed dishes (MatTek, Ashland, MA) or into 12 mm coverglass slides precoated with collagen solution at 10 $\mu g/cm^2$ for Ca^{2+}-imaging experiments or into 100-mm dishes for RT-qPCR and immunoblot studies.

2.3 Cloning, adenovirus construction and adenoviral infection

2.3.1 Cloning

Full-length human TRPC4 alpha cDNA in pcDNA3 was obtained from Dr. J.W. Putney, Jr. (NIEHS, Raleigh NC). The TRPC4 luciferase reporter (psiTC4) vector was constructed by introducing a NotI restriction site by polymerase chain reaction (PCR) at each end of the TRPC4 cDNA sequence using the Expand High Fidelity PLUS PCR System (Roche Applied Science, Indianapolis, IN); the resulting product was cloned into the NotI site of the psiCHECK-2 vector (Promega, Madison, WI).

Addition of a CMV enhancer was placed upstream of the U6 promoter in the pSHAG vector (pSHIE). The enhancer region of the CMV promoter (CMV-IE) in the pEGFP-C1 vector (GenBank Accession #U55763; BD Biosciences Clonetech, Mountain View, CA) was excised and cloned into the pSHAG vector through Not I restriction sites, giving rise to pSHAG-IE.

Full-length human TRPC1 cDNA derived by PCR from PHM1-41 myometrial cell mRNA [6] and cloned into pcDNA6-B was subcloned into pcDNA6-V5 through use of Kpn I and Not I restriction sites. TRPC1 cDNA was then excised and cloned into the psiCHECK-2 vector via Pme I and Not I restriction site to obtain the TRPC1 luciferase reporter (psiTC1) vector.

STIMΔERM cDNA in pRK5/myc vector was obtained from Dr. P.W. Worley (The Johns Hopkins University School of Medicine, Baltimore, MD). STIMΔERM cDNA was excised and cloned into pAdTrack-CMV vector through EcoR I and Not I restriction sites.

TRPC4 and TRPC1 shRNAs were designed using the Dharmacon siDesign Center (Lafayette, CO). Sequences were examined for features indicating siRNA functionality [7]. Candidate sequences homologous to other TRPCs, other ion channels and common interaction domains, as judged by NCBI BLAST analysis, were rejected. Selected siRNA duplex sequences were constructed to contain a human pre-microRNA stem sequence (miR-30) which allows efficient processing of the shRNA [8]. A scrambled control sequence was designed by entering the TRPC4-shRNA#4 sequence into the siRNA Sequence Scrambler software (GenScript, Piscataway, NJ). Oligonucleotides containing TRPC1-shRNA or TRPC4-shRNA sequences (four sequences for each) were synthesized (Integrated DNA Technologies, Coralville, IA) and cloned into the BseRI and BamHI sites downstream of a U6 promoter in the pSHAG vector (provided by G. Hannon, Cold Spring Harbor Laboratory, NY), producing the pSH-TC1sh1 to pSH-TC1sh4 and pSH-TC4sh1 to pSH-TC4sh4 vectors (Table 1).

In addition, oligonucleotides containing TC1sh2, TC4sh1, and TC6sh1 sequences, as well as a Renilla luciferase-shRNA sequence (Table 2), were synthesized (Integrated DNA Technologies, Coralville, IA) and cloned into the pAdT-CMR vector in different combinations. The Rnllash construct expresses three copies of the Renilla-shRNA sequence in tandem cloned into the Fse I, Stu I, Mlu I and Cla I restriction sites in the multiple cloning region. TC1sh and TC4sh were created in a similar fashion. TC1+4sh as well as other combinations were created by introducing a single copy of the desired shRNA (i.e., TC1sh2 plus TC4sh1 plus Renilla-shRNA for TC1+4sh) using the same restriction sites specified above. Cloning efficiency for creation of these constructs was about 50-70%. Integrity of sequences were checked by DNA sequencing. A maximum

Table 1. Short-hairpin RNA (shRNA) sequences for targeting TRPC4 mRNA and PCR primers. shRNA target sequences for TRPC4 (in bold) were incorporated into the human miR-30 pre-micro RNA (pre-miRNA) backbone. Bases in italics were used for cloning of shRNA construct into the pSHAG vector. PMCA1, PMCA4 and SERCA2 primers detect both a and b isoforms.

Target	Orientation	oligonucleotide sequence (5'-3')	Target Location
TC4sh1 shRNA	Forward	5'GCG**CATGTTGGAGATGCTCTATTAC**CTGTGAAGCC ACAGATGGG**GTAATAGAGCATCTCCAACATA**TGCTT TTTT3'	516-538 NM_016179
	Reverse	5'*GATC*AAAAAAGCA**TATGTTGGAGATGCTCTATTAC** CCCATCTGTGGCTTCACAG**GTAATAGAGCATCTCCAA CATG**CGC*CG3*'	
TC4sh2 shRNA	Forward	5'GCG**AAGGTGCCTCCTATACTCCTTG**CTGTGAAGCC ACAGATGGG**CAAGGAGTATAGGAGGCACCTG**TGCTT TTTT3'	609-631 NM_016179
	Reverse	5'*GATC*AAAAAAGCA**CAGGTGCCTCCTATACTCCTTG** CCCATCTGTGGCTTCACAG**CAAGGAGTATAGGAGGC ACCTT**CGC*CG3*'	
TC4sh3 shRNA	Forward	5'GCG**AAGACGAGAAGTTCCAGAGAAC**CTGTGAAGCC ACAGATGGG**GTTCTCTGGAACTTCTCGTCTG**TGCTTT TTT3'	1005-1027 NM_016179
	Reverse	5'*GATC*AAAAAAGCA**CAGACGAGAAGTTCCAGAGAA CCCCATCTGTGGCTTCACAG GTTCTCTGGAACTTCTC GTCTT**CGC*CG3*'	
TC4sh4 shRNA	Forward	5'GCG**AAACTGATTGCTGACCATGCAG**CTGTGAAGCC ACAGATGGG**CTGCATGGTCAGCAATCAGTTGT**GCTT TTTT3'	2106-2128 NM_016179
	Reverse	5'*GATC*AAAAAAGCA**CAACTGATTGCTGACCATGCAG** CCCATCTGTGGCTTCACAG**CTGCATGGTCAGCAATCA GTTT**CGC*CG3*'	
shx1 shRNA	Forward	5'GCG**CGTAGTAATGACAATCCGCGCT**CTGTGAAGCC ACAGATGGG**AGCGCGGATTGTCATTACTACT**TGCTT TTTT3'	N/A
	Reverse	5'*GATC*AAAAAAGCA**AGTAGTAATGACAATCCGCGCT** CCCATCTGTGGCTTCACAG**AGCGCGGATTGTCATTAC TACG**CGC*CG3*'	
TRPC4 PCR	Forward	5'-TCAGACTTGAACAGGCAAGGTCCA-3'	1399
	Reverse	5'-AGTCCGCCATCCCACATCTGTTTA-3'	1508 NM_016179
GUS PCR	Forward	5'-GGCTTCGAGGAGCAGTGGTAC-3'	248
	Reverse	5'-TGTCATTGAAGCTGGAGGGAAC-3'	332 NM_000181
PMCA1 PCR	Forward	5'-GGGTGGGAGAAATGAACTGA-3'	4194
	Reverse	5'-CTCTCTCCCATCCAGGACTG-3'	4328 NM_001001323

PMCA4 PCR	Forward Reverse	5'-CAATGCGGTGGATTGCAAAGT-3' 5'-AACACAGCAGCTGACGTGACAATG-3'	4605 4786 NM_001001396
SERCA2 PCR	Forward Reverse	5'-TGCTGTTGGTGACAAAGTTCCTGC-3' 5'-TATCTTGGTTGACAGCTCGTGGGT-3'	622 773 NM_170665

of six shRNAs can be read in a given construct and no constructs were used that contained more than three shRNAs per construct, except for the experiment described in Fig. 5.2 (Chapter 5).

2.3.2 Adenovirus Construction

A modified pAdTrack-RfA(f) plasmid was constructed (by J. Cantlon and C. Clay) by introduction of the Reading Frame Cassette A (RfA) from the Gateway Vector Conversion System (Invitrogen, Carlsbad, CA) into the XbaI/XhoI restriction sites in pAdTrack (ATCC, Manassas, VA). This vector is used for introducing the shRNAs from the pSHAG vector into the adenoviral vector. This approach was used to produce the shRNA TRPC4 constructs used in Chapter 4. TRPC4 shRNA adenoviral vector assembly was performed by recombination between the *attR* sites of pSH-TC4sh1 and the *attL* sites of pAdTrack-RfA(f) using LR clonase. The pAdT-TC4shRNA clones were checked by restriction enzyme digestion and sequence integrity was confirmed by direct sequencing.

pAdT-MCS was modified from the pAdTrack-CMV vector by introduction of a new multiple cloning site (MCS) between the CMV promoter and the sequence for the GFP protein through use of the Age I restriction site. The MCS sequence is specified in Table 2 and unique restriction sites within the new MCS of pAdT-MCS shown (Fig. 2.1). Cloning of this sequence into the pAdTrack-CMV vector in the correct orientation was

Table 2. Short-hairpin RNA (shRNA) sequences for targeting TRPC1 mRNA. shRNA target sequences for TRPC1, TRPC4 and Renilla-luciferase (in bold) were incorporated into the human miR-30 pre-micro RNA (pre-miRNA) backbone. Bases in italics were used for cloning of shRNA construct into either the pSHAG vector (pSH-TC1sh2 and pSH-TC4sh1) or the pAdT-CMR vector (Rnllash, TC1sh2 and TC4sh1). pAdT-MCS was cloned into pAdTrack-CMV vector as a new cloning site for introduction of tandem shRNAs resulting in the pAdT-CMR vector. Forward and reverse primer sets 1-3 were used to clone the tandem shRNAs into the pAdT-CMR vector.

Target	Orientation	oligonucleotide sequence (5'-3')	Target Location
pSH-TC1sh1 shRNA	Forward	5'GCG**GCCAGGTTTCGTCTTGATATAT**CTGTGAAGCCA CAGATGGG**ATATATCAAGACGAAACCTGGA**TGCTTTTT T3'	663-684 NM_003304
	Reverse	5'*GATC*AAAAAAGCA**TCCAGGTTTCGTCTTGATATAT**CC CATCTGTGGCTTCACAG**ATATATCAAGACGAAACCTGG** CCG*CCG*3'	
pSH-TC1sh2 shRNA	Forward	5'GCG**CTTCTCGTGAATTGGAAGTTAT**CTGTGAAGCCA CAGATGGG**ATAACTTCCAATTCACGAGAAT**TGCTTTTT T3'	868-889 NM_003304
	Reverse	5'*GATC*AAAAAAGCA**ATTCTCGTGAATTGGAAGTTAT**C CCATCTGTGGCTTCACAG**ATAACTTCCAATTCACGAGA AG**CG*CCG*3'	
pSH-TC1sh3 shRNA	Forward	5'GCG**ACTGCTCATCGTAACAACTATG**CTGTGAAGCCA CAGATGGG**CATAGTTGTTACGATGAGCAGC**TGCTTTTT T3'	531-552 NM_003304
	Reverse	5'*GATC*AAAAAAGCA**GCTGCTCATCGTAACAACTATG**C CCATCTGTGGCTTCACAG**CATAGTTGTTACGATGAGCA GTC**G*CCG*3'	
pSH-TC1sh4 shRNA	Forward	5'GCG**CAGGGTGACTATTATATGGTTA**CTGTGAAGCCA CAGATGGG**TAACCATATAATAGTCACCCTT**TGCTTTTT T3'	306-327 NM_003304
	Reverse	5'*GATC*AAAAAAGCA**AATTTACTGAGTTTGTTGGTGC**C CCATCTGTGGCTTCACAG**GCACCAACAAACTCAGTAAA TGC**G*CCG*3'	
pSH-TC4sh1 shRNA	Forward	5'GCG**CGTAGTAATGACAATCCGCGCT**CTGTGAAGCCA CAGATGGG**AGCGCGGATTGTCATTACTACT**TGCTTTTT T3'	516-538 NM_016179
	Reverse	5'*GATC*AAAAAAGCA**AGTAGTAATGACAATCCGCGCT**C CCATCTGTGGCTTCACAG**AGCGCGGATTGTCATTACTA CG**CGC*CCG*3'	
Rnllash	Forward	5'TGCTGTTGACAGTGAGCG**CAACTTCTTCGTCGAGACC ATG**CTGTGAAGCCACAGATGGG**CATGGTCTCGACGAA**	1227-1248 psiCHECK-2

	Reverse	**GAAGTTA**TGCCTACTGCCTCGGA3' 5'TCCGAGGCAGTAGGCA**TAACTTCTTCGTCGAGACCAT GCCCATCTGTGGCTTCACAG<u>CATGGTCTCGACGAAGAA GTTG</u>**CGCTCACTGTCAACAGCA3'	vector
TC1sh	Forward	5'TGCTGTTGACAGTGAGCG**CTTCTCGTGAATTGGAAGT TAT**CTGTGAAGCCACAGATGGG**ATAACTTCCAATTCAC GAGAAT**TGCCTACTGCCTCGGA3'	868-889 NM_003304
	Reverse	5'TCCGAGGCAGTAGGCA**ATTCTCGTGAATTGGAAGTTA TCCCATCTGTGGCTTCACAG<u>ATAACTTCCAATTCACGA GAAG</u>**CGCTCACTGTCAACAGCA3'	
TC4sh	Forward	5'*TGCTGTTGACAGTGAGCG***CGTAGTAATGACAATCCGC GCT**CTGTGAAGCCACAGATGGG**AGCGCGGATTGTCAT TACTACT**TGCCTACTGCCTCGGA3'	516-538 NM_016179
	Reverse	5'*TCCGAGGCAGTAGGCA***AGTAGTAATGACAATCCGCGC** TCCCATCTGTGGCTTCACAG**AGCGCGGATTGTCATTAC TACG**CGCTCACTGTCAACAGCA3'	
CMR Primer 1	Forward	5'CCTGCA<u>GGCCGGCC</u>ATGGCTGGACCTGAGATCCAAGA AGGTATAT*TGCTGTTGACAGTGAGCG*3'	Fse I restriction site
	Reverse	5'TTC<u>AGGCCT</u>ATCGTAGCCCTTGAAGAC*TCCGAGGCAGT AGGCA*3'	Stu I restriction site
CMR Primer 2	Forward	5'CGAT<u>AGGCCT</u>GAAGATCCAAGAAGGTATAT*TGCTGTTG ACAGTGAGCG*3'	Stu I restriction site
	Reverse	5'TTC<u>ACGCGT</u>ATCGTAGCCCTTGAAGAC*TCCGAGGCAGT AGGCA*3'	Mlu I restriction site
CMR Primer 3	Forward	5'CGAT<u>ACGCGT</u>GAAGATCCAAGAAGGTATAT*TGCTGTTG ACAGTGAGCG*3'	Mlu I restriction site
	Reverse	5'ACCGGT<u>ATCGAT</u>ATCGTAGCCCTTGAAGAC*TCCGAGGC AGTAGGCA*3"	Cla I restriction site
pAdT-MCS	Forward	5'*CCGGT*AGTACTCGATCGAAGTCATTCACGTGGCGCGCC TGCAGGCCGGCCAGGCCTACGCGTATCGAT*A*3'	
	Reverse	5'*CCGG*TATCGATACGCGTAGGCCTGGCCGGCCTGCAGGC GCGCCACGTGAATGACTTCGATCGAGTACT*A*3'	

checked through sequencing. The Renilla-luciferase cDNA sequence was excised from the psiCHECK-2 vector and cloned into the newly obtained pAdT-MCS through use of Nhe I and Xho I restriction sites, giving rise to pAdT-<u>CMR</u> (pAdTrack-<u>C</u>MV, <u>M</u>CS, <u>R</u>enilla-luc).

Once shRNA constructs were either in the pAdTrack-RfA(f) (Chapter 4) or in the pAdT-CMR (Chapter 5), clones were linearized with PmeI and subsequently

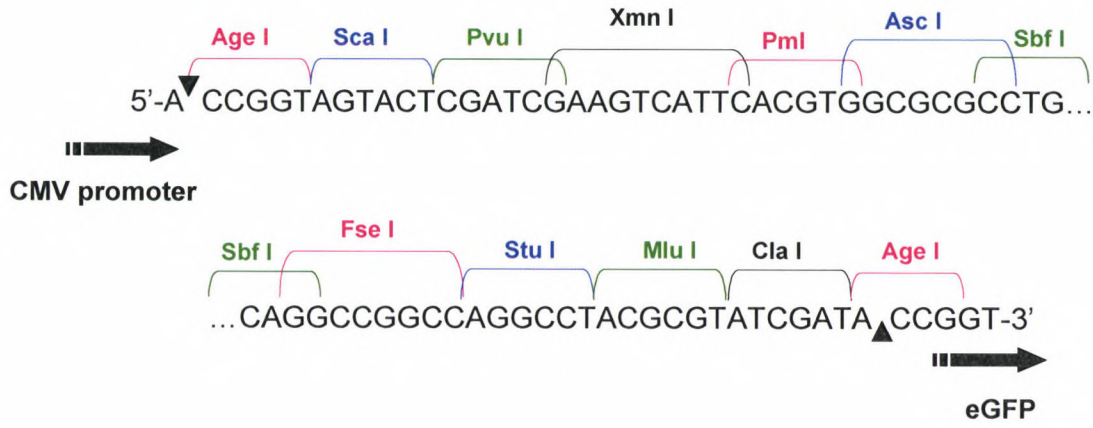

Fig. 2.1. Diagram of the Multiple Cloning Site (MCS) cloned into pAdTrack-CMV. The sequence shown was cloned into the pAdTrack-CMV vector through use of the Age I restriction site found between the CMV promoter and GFP transcription start site, giving rise to the pAdT-MCS vector. Unique restriction sites present in the pAdT-MCS vector are specified.

electroporated into *Escherichia coli* BJ5183 cells according to the manufacturer's instructions to achieve recombination of the shRNAs in the pAdTrack-RfA(f) or pAdT-CMR with the adenoviral backbone plasmid pAdEasy-1 (Stratagene, La Jolla, CA). The obtained recombined plasmids were linearized with PacI and transfected into AD-293 cells to allow viral synthesis and packaging (Fig. 2.2). The adenoviruses were amplified, purified and titered by viral particle titration and end-point dilution. Adenoviruses used for Chapter 4 were purified using the BD Adeno-X Maxi Purification kit (Clontech, Mountain View, CA). Due to the higher costs involved in purifying adenoviruses through use of this kit, adenoviruses used for Chapter 5 were crudely purified by passing the adenovirus-containing cell lysates through a 0.45 μm PVDF filter after three rounds

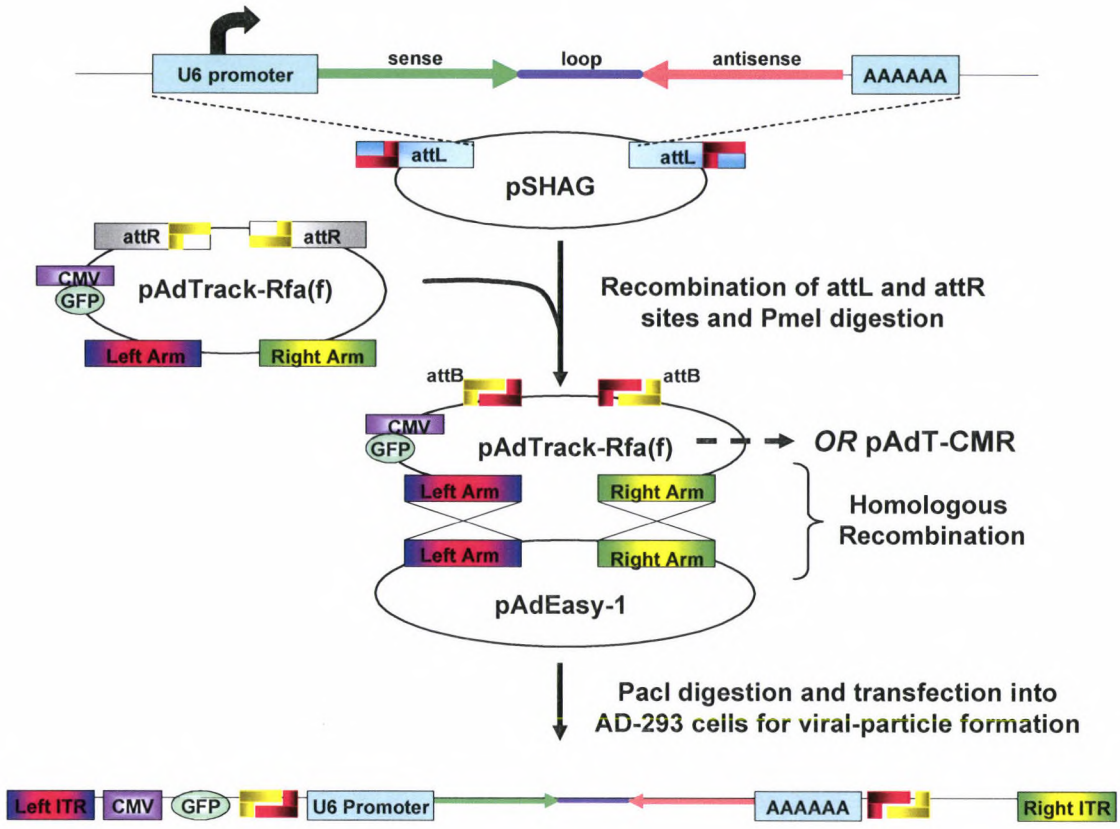

Fig. 2.2. Homologous recombination to introduce the pSHAG-shRNA constructs into the pAdTrack-Rfa vector. A second homologous recombination between the pAdTrack-Rfa(f) or pAdT-CMR constructs and pAdEasy-1 was carried out to produce the adenoviral particle.

of freezing in a methanol-dry ice bath for five minutes and thawing at 37°C for five minutes. No apparent differences were observed between adenoviruses purified using the BD Adeno-X Maxi Purification kit and those crudely purified through use of the PVDF membrane.

2.3.3 Adenoviral infections

Produced adenoviruses were used to infect UtSMC and PHM1-41 cells, using the enhanced green fluorescent protein (eGFP) marker to identify infected cells. Multiplicity of infection (MOI) of 1000 and 500 were used in PHM1-41 and UtSMC cells respectively, resulting in 90-95% infection efficiency as determined by eGFP expression. Cells were plated on minimal media and spun at 800 x g for five minutes at room temperature to allow maximum contact between cells and adenovirus. Cells were used within 72-96 h post-infection and exhibited morphology similar to that of noninfected cells, as determined by visual inspection.

2.4 Transfection and electroporation

AD293 cells were plated at 1 x 10^5 cells/well in 12-well plates. Transient transfections were performed 24 h after plating using the GenePORTER2 transfection reagent according to the manufacturer's instructions (Genlantis, San Diego, CA). Cells were cotransfected with either the psiTC4 reporter plus constructs pSH-TC4sh1 to pSH-TC4sh4 or with the psiTC1 reporter and constructs pSH-TC1sh1 to pSH-TC1sh4, at 1:3 molar ratios. In the case where effects of pooled TRPC4-shRNAs were analyzed versus those of a single TRPC4-shRNA, equal molar ratios were added of each shRNA (i.e., a 1:1:1 molar ratio for TC4sh1+2+3). Samples were analyzed 48-72 hours post-transfection using the Dual-luciferase Reporter Assay (Promega, Madison, WI).

COSM6 cells were plated at 1 x 10^5 cells/well in 6-well plates. Transient transfections were performed 24 h after plating using the FuGENE 6 transfection reagent

(Roche, Indianapolis, IN) according to manufacturer's instructions. Cells were cotransfected with the TRPC4 overexpression plasmid and the pSH-TC4sh1 construct at a 1:3 molar ratio. Samples were analyzed 72 hours post-transfection.

PHM1-41 and UtSMC cells were trypsinized and washed with PBS (137 mM NaCl, 27 mM KCl, 100 mM Na_2HPO_4, 2 mM K_2HPO_4, pH 7.4). Electroporation was performed using the Basic Smooth Muscle Cell kit (Amaxa Inc., Gaithersburg, MD). 2 x 10^6 cells were pelleted and resuspended in 100 µl Basic Nucleofector solution together with 2 µg psiTC4 reporter, 1.5 µg pSH-TC4sh1-4 and 0.5 µg maxGFP vectors and transferred to the provided 2 mm cuvette. Cells were electroporated for 140 V, 35 ms in the time constant mode, using the Gene Pulser Xcell system (Bio-Rad, Hercules, CA), and were immediately diluted into 500 µl of pre-warmed culture media. Cells were dispensed (80 µl into 3 x 35-mm glass bottomed dishes for Ca^{2+} imaging experiments and 350 µl into a 100 mm dish for RNA analyses), and incubated for 24 h before media was replaced. Samples were analyzed 72-96 h after electroporation. A transfection efficiency of 60% was achieved.

2.5 mRNA isolation and quantitative real-time RT-PCR

Myometrial cell mRNA was isolated 72-96 h post-infection using the RNeasy kit (Qiagen, Valencia, CA). An on-column DNase digestion was performed using the RNase-free DNase set according to the manufacturer's instructions (Qiagen, Valencia, CA). Quantitative real-time PCR (RT-qPCR) was performed using 100 ng mRNA and the iScript one-step RT-PCR kit with SYBR Green (Bio-Rad, Hercules, CA) in an

iCycler Thermal Cycler (Bio-Rad, Hercules, CA). Previously designed PCR primers for TRPC1,3,5,6, and 7 [9] and newly designed primers for TRPC4, beta-glucuronidase (GUS), plasma membrane Ca^{2+}-ATPase isoform 1 (PMCA 1), PMCA 4, and sarcoplasmic endoplasmic reticulum Ca^{2+} ATPase isoform 2 (SERCA 2) (Table 1) were used at 500 nM. The PCR conditions were as follows: cDNA synthesis at 50°C for 30 min, iScript Reverse-transcriptase inactivation at 95°C for 5 min, PCR cycling where cDNA was denatured at 95°C for 15 sec, annealed at 60°C for 30 sec, and extended at 72°C for 1 min. Sequence integrity of RT-qPCR products was verified by direct sequencing. Melting curves for all products showed single peaks. Calculations were performed using the ΔΔCt method [10] where a given RNA was first normalized to GUS in each sample and then expressed relative to the corresponding value in cells infected with empty adenovirus.

RT-qPCR products for TRPCs and GUS, using 100 ng of RNA for TRPC1, TRPC4, TRPC6 and GUS and 1 μg of RNA for TRPC3, TRPC5 and TRPC7, were run in 3% agarose gels in 1X Tris-acetate-EDTA (TAE) electrophoresis buffer (40 mM Tris-acetate, 1mM EDTA, pH 8.0). Gels were then incubated in 1X TAE buffer with SYBR Green I nucleic acid gel stain (1:1000 dilution) for 30 min at room temperature with gentle rocking. Bands were visualized by using a Storm imager (Amersham Biosciences).

2.6 Immunoblotting

PHM1-41 cells (6 x 10^5) were plated in 100-mm dishes in culture medium and infected with adenovirus at an MOI of 1000. Cells were harvested after 72-96 h and whole cell extracts and plasma membrane extracts were prepared. For whole cell extract preparation, cells were lysed in modified RIPA buffer (50 mM Tris-HCl pH 7.4, 150 mM NaCl, 1% NP-40 (v/v), 1 mM EDTA, 0.25% Na-deoxycholate (v/v), 0.1% SDS (w/v)) plus protease inhibitor cocktail containing 1.04 mM 4-(2-Aminoethyl)benzenesulfonyl fluoride hydrochloride (AEBSF), 0.8 μM aprotonin, 21 μM leupeptin, 36 μM bestatin, 15 μM pepstatin A, 14 μM *trans*-Epoxysuccinyl-L-leucylamido(4-guanidino)butane (E-64). Lysates were incubated on ice for 10 min and sonicated on ice for 3 cycles at 10 sec/cycle, output setting 3, using a Micro Tip in a Branson Sonifier 250 (Danbury, CT). Mixtures were then centrifuged at 14,000 x g for 15 min at 4°C. The protein concentrations in the supernatants were measured by BCA Protein Assay (Pierce, Rockford, IL).

For plasma membrane preparation, a previously validated method [11] was adapted for use with small amounts of material. Cells were lysed in 200 μl homogenization buffer (100 mM KCl, 5 mM $MgCl_2$, 50 mM Tris-HCl, 1 mM EGTA, pH 7.2) plus protease inhibitor cocktail as above and sonicated on ice. Mixtures were centrifuged at 10,000 x g for 15 min at 4°C, and the resulting supernatants were centrifuged at 100,000 x g for 1 h at 4°C in a TLA100.3 rotor. The resulting pellets were dissolved in 10% ice-cold sucrose in homogenization buffer and layered over a layer of 28% sucrose in homogenization buffer. Samples were centrifuged at 57,000 x g for 30 min at 4°C in a TLS55 swinging bucket rotor. The plasma membrane fractions at the 10-28% sucrose

interface were withdrawn and centrifuged at 100,000 x g for 30 min at 4°C. The resulting pellets were resuspended in modified RIPA buffer and stored at -80°C. The protein concentration was determined by BCA protein assay (Pierce Biotechnology, Rockford, IL).

Cell and membrane extracts were subjected to sodium dodecylsulfate-polyacrylamide electrophoresis in 8% gels and transferred to Millipore Immobilon-P transfer membrane (Billerica, MA). Immunoblots were probed with primary antibodies against TRPC1 (1:500) and TRPC4 (1:200). Primary polyclonal human PLCB3 (loading control) antibody and HRP-conjugated secondary antibodies were used at 1:2000 dilution. Where indicated, antibodies against TRPC4 and TRPC1 were preabsorbed prior to use with the corresponding antigenic peptides overnight at 4°C at mass ratios of 1:1 and 25:1 antigenic peptide:antibody, respectively, as recommended by the manufacturers. Bands were visualized by enhanced chemiluminescence (ECL) reagent (Amersham Biosciences, GE Healthcare, Pittsburgh, PA). ECL signals were detected using a Storm imager and quantitation was accomplished by ImageQuant TL software (Amersham Biosciences).

2.7 Measurement of Intracellular Calcium

PHM1-41 and UtSMC cells were plated at 1 x 10^5 and 0.4 x 10^5 cells/ 0.8 ml, respectively, in 35-mm glass-bottomed dishes. Alternatively, PHM1-41 and UtSMC cells were plated at 0.25 x 10^5 and 0.1 x 10^5 cells/ 0.4 ml, respectively cells onto 12 mm glass slides that were precoated with collagen solution at 10 μg/cm^2. Cells were loaded 72-96 h after infection at room temperature for 30 min with 5 μM Fura-2-AM and 0.1%

Pluronic F-127 in fluorescence buffer (145 mM NaCl, 5 mM KCl, 1 mM Na_2HPO_4, 0.5 mM $MgCl_2$, 1 mM $CaCl_2$, 10 mM HEPES, 5 mM glucose, pH 7.4). Cells were then washed twice in the same buffer and incubated an additional 45 min at room temperature to allow for Fura-2 ester hydrolysis. Immediately prior to assay, cells were placed in Ca^{2+}-free fluorescence buffer (buffer containing 100 μM EGTA but no $CaCl_2$) and changes in fluorescence were measured at 340 and 380 nm excitation and 510 nm emission wavelengths in an ImCyt2 imaging system (Intracellular Imaging, Inc., Cincinnati, OH). Cells co-expressing eGFP were identified using an eGFP/fluorescein excitation filter (485 nm). Electroporated or virally infected cells did not display nonspecific membrane leaks, as evidenced by the fact that no significant increases in $[Ca^{2+}]_i$ were observed following addition of 1 mM $CaCl_2$ if cells were not exposed to stimuli eliciting SRCE. Changes in Ca^{2+} were observed in 20-45 cells/dish.

2.8 Electrophysiological Recordings

PHM1-41 cells exposed to adenoviral constructs expressing empty vector or TC4sh1 sequences were cultured on glass coverslips for >72 h prior to patch clamp experiments. Cultured cells were placed into a recording chamber (SA-OLY, Warner Instruments) at room temperature. Cell-attached recordings were performed using an AxoPatch 200B amplifier equipped with an Axon CV 203BU headstage (Axon Instruments). Recording electrodes (resistance, 3–5 MΩ) were pulled, polished, and coated with wax to reduce capacitance. Currents were filtered at 1 kHz, digitized at 40 kHz, and stored for subsequent analysis. Clampex and Clampfit versions 10.2 (Axon Instruments) were used for data acquisition and analysis, respectively. Pipette potential

was clamped at -40 mV and all recordings were performed at room temperature (22°C). The bath solution was 125.4 mM NaCl, 20 mM tetraethylammonium chloride (TEA), 0.1 mM $MgCl_2$ 5 mM HEPES, 11 mM glucose, 1 μM $CaCl_2$, and 100 nM nifedipine. The pipette solution contained 135 mM CsCl, 2.5 mM $MgCl_2$, 10 mM HEPES, 10 mM glucose, 10 mM EGTA, and 10 μM paxilline (pH7.2). Cell-attached channel activity was recorded before and after addition of oxytocin (100 nM).

2.9 Data Analyses

Data are presented as mean ± S.E.M. and were analyzed by t-test or one-way ANOVA and Tukey's test, as appropriate, using Prism software (GraphPad Software, La Jolla CA) software. Changes in intracellular Ca^{2+} were analyzed using numerical analyses software (CalciumComp) developed by an engineer consultant (K. J. Bois, Fort Collins, CO). CalciumComp aligns the initial $[Ca^{2+}]_i$ peaks, removes noise, and calculates the extent of the increase $[Ca^{2+}]_i$ (peak height) and integrated area under the $[Ca^{2+}]_i$ transient curve. Data obtained using this method agreed within 95% with that analyzed by manual methods.

References

1. Monga M, Ku CY, Dodge K, Sanborn BM. Oxytocin-stimulated responses in a pregnant human immortalized myometrial cell line. *Biol Reprod* **1996**; 55**:** 427-432.

2. Burghardt RC, Barhoumi R, Sanborn BM, Andersen J. Oxytocin-induced Ca2+ responses in human myometrial cells. *Biol Reprod* **1999**; 60: 777-782.

3. Shlykov SG, Yang M, Alcorn JL, Sanborn BM. Capacitative cation entry in human myometrial cells and augmentation by hTrpC3 overexpression. *Biol Reprod* **2003**; 69: 647-655.

4. Pollard AJ, Krainer AR, Robson SC, Europe-Finner GN. Alternative splicing of the adenylyl cyclase stimulatory G-protein G alpha(s) is regulated by SF2/ASF and heterogeneous nuclear ribonucleoprotein A1 (hnRNPA1) and involves the use of an unusual TG 3'-splice Site. *J Biol Chem* **2002**; 277: 15241-15251.

5. Ciarmela P, Wiater E, Vale W. Activin-A in myometrium: characterization of the actions on myometrial cells. *Endocrinology* **2008**; 149: 2506-2516.

6. Yang M, Gupta A, Shlykov SG, Corrigan R, Tsujimoto S, Sanborn BM. Multiple Trp isoforms implicated in capacitative calcium entry are expressed in human pregnant myometrium and myometrial cells. *Biol Reprod* **2002**; 67: 988-994.

7. Reynolds A, Leake D, Boese Q, Scaringe S, Marshall WS, Khvorova A. Rational siRNA design for RNA interference. *Nat Biotechnol* **2004**; 22: 326-330.

8. Boden D, Pusch O, Silbermann R, Lee F, Tucker L, Ramratnam B. Enhanced gene silencing of HIV-1 specific siRNA using microRNA designed hairpins. *Nucleic Acids Res* **2004**; 32: 1154-1158.

9. Ku CY, Babich L, Word RA et al. Expression of transient receptor channel proteins in human fundal myometrium in pregnancy. *J Soc Gynecol Investig* **2006**; 13**:** 217-225.

10. Pfaffl MW. A new mathematical model for relative quantification in real-time RT-PCR. *Nucleic Acids Res* **2001**; 29**:** e45.

11. Wen Y, Anwer K, Singh SP, Sanborn BM. Protein kinase-A inhibits phospholipase-C activity and alters protein phosphorylation in rat myometrial plasma membranes. *Endocrinology* **1992**; 131**:** 1377-1382.

CHAPTER 3

Logistics for short hairpin RNA (shRNA) selection and adenoviral construction

To assess the roles of individual TRPC channels in SRCE, gene silencing experiments were performed by using small interference RNA (siRNA) techniques (Fig. 3.1) [1-3]. The use of siRNA oligodeoxynucleotides is a poor option since myometrial cells are difficult to transfect and are not easily selectable because they grow slowly when plated at low density. Thus, a viral vector-mediated RNAi method was chosen to express both sense and antisense strands of the siRNA linked by a hairpin loop (termed short hairpin or shRNA) from a single promoter.

3.1 Short hairpin RNA (shRNA) criteria and selection

Ten mRNA target sequences were initially selected for siRNA applications based on TRPC4 mRNA regions targeted previously for gene silencing through siRNA and

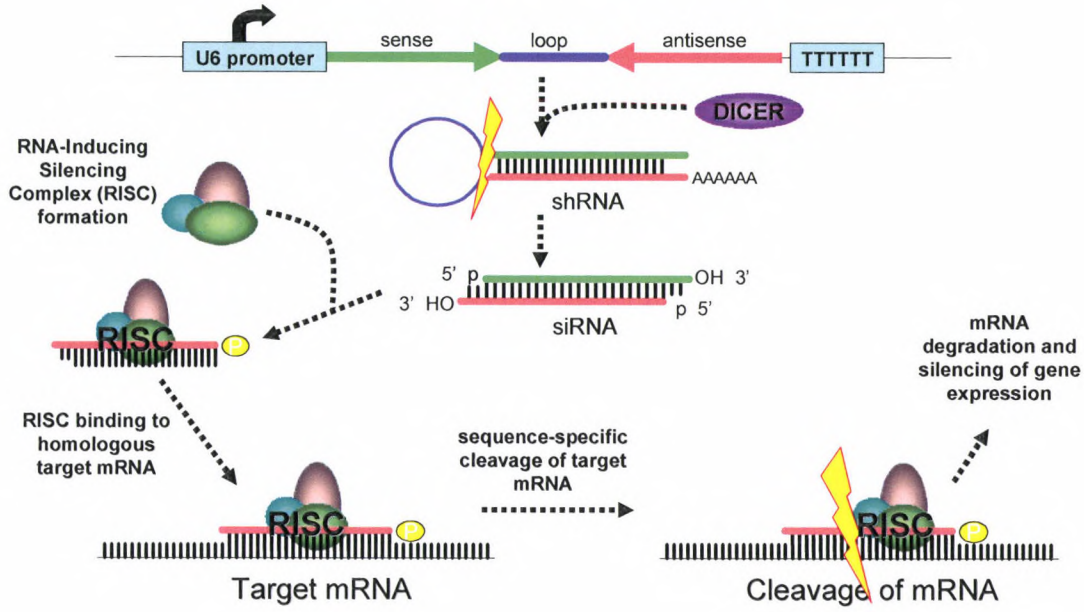

Fig. 3.1. Schematic representation of targeted degradation of TRPC mRNAs through RNA interference (RNAi) mechanism by using short hairpin RNAs (shRNAs).

antisense methods [4-8]. Additionally, different loop sequences were selected in an attempt to find the most effective constructs able to knockdown TRPC4 mRNA and protein expression [9;10]. However, these constructs were found to be inefficient in silencing TRPC4 mRNA expression when tested in HEK-293 cells.

Four more shRNA constructs were designed, as more information about efficient shRNA design became available in the literature. Selection of these sequences made use of the Dharmacon siDesign center for analysis of TRPC1 and TRPC4 mRNA (accession # NM_003304 and NM_016179, respectively). Sequences were examined for features indicating siRNA functionality (summarized in [9-12]). A 36-52% G/C content avoids a very high and very low internal stability of the siRNA. High internal stability may

prevent efficient unwinding of the siRNA, while low stability could attenuate the target binding affinity of the siRNA. Also, three or more A/U bases at positions 15-19 of the sense strand (SS) may aid unwinding and proper loading of the siRNA into the RISC complex. The presence of A/T at position 19 of the SS may mimic dynamics used by naturally occurring microRNA (mRNA) precursors. Furthermore, occurrence of a U at position 10 of the SS may enhance the RISC complex ability to cleave complementary target mRNA.

Step-by-step design of shRNA constructs

1. Go to Dharmacon website (http://www.dharmacon.com) and select siRNA→ siDesign Center
2. Select organism of interest and place accession number for mRNA of gene of interest (GOI); alternatively copy-paste your mRNA sequence of interest
3. Obtain siRNA sequences and select sequences holding most important set of criteria [9-12]
    a. BLAST sequences in PubMed (NCBI)
    b. Try to avoid sequences with high homology to other proteins
4. Place siRNA sequence (19nt) into miRNA backbone (miR30) [13;14]
    a. Take 19nt siRNA sequence (from Dharmacon) and find its position in mRNA sequence of GOI
    b. Identify the 5' and 3' nucleotide (nt) sequences flanking siRNA sequence in mRNA-GOI

c. From the mRNA-GOI, add 2nt at 5' end and 1nt at 3' end of siRNA sequence (siRNA+flanking)

d. Place this sequence into miRNA backbone of miR-30

    i. Notice that miR-30 backbone will produce 2 base pairs between G & U after it is transcribed; base pairing is allowed AND necessary in backbone

    ii. Place siRNA+flanking sequence –sense strand- (siRNA-SS) between the "5'-GCG" and loop sequences of the miR-30 backbone

    iii. Place the complementary siRNA+flanking sequence –antisense strand- (siRNA-AS) between the loop and the "TGC-3'" of the miR-30 backbone

e. Create a base pair mismatch between the 1st nt of the siRNA-SS and the last nt of the siRNA-AS

    i. Keep last nt of siRNA-AS intact

    ii. To create mismatch simply change the 1st nt of siRNA-SS; if 1st nt in siRNA-SS is

        1. T→C
        2. C→A / A→C
        3. G→T / G→A
        4. DO NOT create a C→T mutation as this will create a G:U base pair, and the mismatch will not be created

-$(N)_{19}$- →siRNA sequence (19nt long)

5'-NNNNNNNNNNN$(N)_{19}$NNNNNNNNNNNNN-3' → mRNA-GOI

5'-NN$(N)_{19}$N-3' →siRNA seq + flanking seq

-miR-30 loop sequence-

5'-*GCG*NN$(N)_{19}$N*CTGTGAAGCCACAGATGGG*N$(N)_{19}$NN*TGC*-3' →into miR-30

-siRNA sense strand- -siRNA antisense strand-

5'-*GCG*X N$(N)_{19}$N*CTGTGAAGCCACAGATGGG*N$(N)_{19}$NN*TGC*-3' →create mismatch

-siRNA sense strand- -siRNA antisense strand-

5. Go to Integrated DNA Technologies, Inc. website (www.idtdna.com) and select SciTools option
6. Under SciTools, select for Oligo Analyzer to get analysis of designed oligo
    a. Copy/Paste sequences into software
    b. Select "Hairpin" option→Calculate
    c. Ensure that the minimal free energy structures obtained do not contain/form any extra secondary structures other than those of the miR-30 hairpin/loop
        i. It should give a total of 2 different structures (both with the hairpin/loop at a similar position as in [13].
7. Order oligos from IDT or any other reliable oligo-synthesis provider
    a. Forward oligo: add 6 T at end of sequence for termination signal → 75 bases total for expression under a U6 promoter

5'-*GCG*XNN(N)$_{17}$NN*CTGTGAAGCCACAGATGGG*NN(N)$_{17}$NNN*TGC*TTTTTT-3'

b. Reverse oligo: add "GATC" at 5' end & "CG" at 3' end of above complimentary strand →81 bases total

i. Sequences necessary for proper cloning of oligos into pSHAG vector [10]

5'GATCAAAAAA*GCA*NNN(N)$_{17}$NN*CCCATCTGTGGCTTCACAG*NN(N)$_{17}$NNX*CGC*CG-3'

c. Since oligos are relatively long, they must be ordered PAGE-purified to ensure proper and higher cloning efficiencies

3.2 Single knockdown

3.2.1 U6 promoter expression of an shRNA construct

Oligos containing TRPC4-shRNA sequences were cloned into the pSHAG vector as described in the cloning section of Chapter 2. Efficiency of these constructs was tested in the psiCHECK-2 system. This reporter system provides a quick and inexpensive method to test effectiveness of shRNA sequences at knocking down the reporter-mRNA sequence of the gene of interest. Effective TRPC4-shRNA sequences were then tested for TRPC4 knockdown experiments in the human myometrial cells. In order to understand the cause of the considerable variability experienced in the degree of TRPC4

knockdown (as described in more detail in Chapter 4) and in an attempt to increase TRPC4 knockdown levels, a number of parameters related to the shRNA process in myometrial cells were examined in more detail, as described in this section.

3.2.1.1 Addition of a CMV enhancer

Endogenous miRNA expression occurs from CMV promoters. Studies suggest that a CMV promoter may be necessary for the proper processing of the primary miRNA molecules, which are the precursors of miRNAs [15-17]. However, at the time I synthesized the first shRNA adenoviral constructs, the U6 promoter was being used almost exclusively for this purpose. It has been suggested that a random sequence of 100 bp should be placed between the U6 promoter and the transcriptional start site for the miRNA construct to induce the proper expression of the miRNA [17]. In order to test if a higher expression of the TRPC4 shRNA construct had an enhanced effect on TRPC4 knockdown, a CMV enhancer was placed upstream of the U6 promoter in the pSHAG vector (pSHIE). This technique was previously tested by another laboratory and shown to induce a greater knockdown of the protein of interest [18]. This plasmid was cotransfected along with psiTC4 into AD-293 cells. Fig. 3.2A shows that a slightly higher knockdown in TRPC4-reporter luminescence was observed with TC4sh1 expressed from pSHIE than from that expressed with regular pSHAG vector. However, the higher knockdown displayed by pSHIE-TC4sh1 (89% knockdown) was not significantly different from pSH-TC4sh1 (84% knockdown). These constructs were also transiently transfected into AD293 cells, RNA isolated 72 hr post-transfection and analyzed through RT-qPCR. Fig. 3.2B shows that the potential increase in shRNA

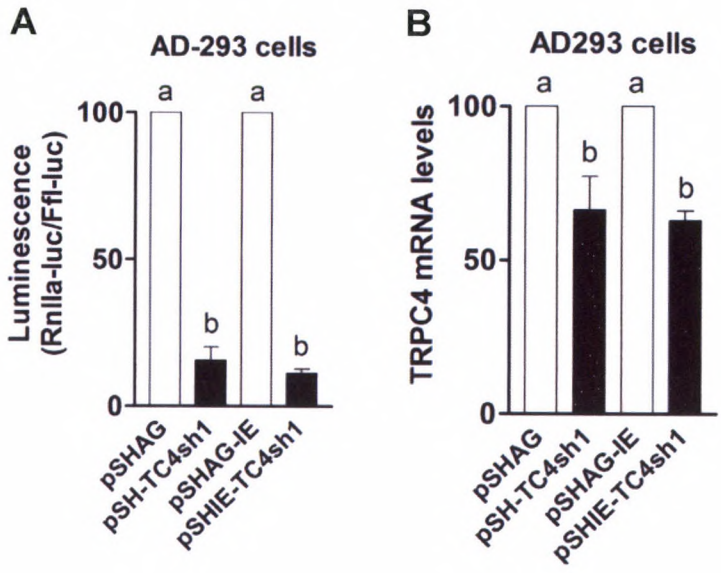

Fig.3.2. Addition of a CMV enhancer region to a U6 promoter does not significantly enhance TRPC4 knockdown by TC4sh1 expression. (A) AD-293 cells were cotransfected with psiTC4 and either pSH-TC4sh1 or pSHIE-TC4sh1. Luminescence from the Renilla TRPC4-reporter in these samples were compared to those cotransfected with control pSHAG or pSHAG-IE, respectively (n=5). (B) AD293 cells were transiently transfected with either pSH-TC4sh1 or pSHIE-TC4sh1 and their respective controls. mRNA was normalized to GUS in the same sample and expressed relative to the value in cells exposed to empty vector (n=4). In A and B, samples were isolated >72 h post-transfection. In all cases, data represent the mean ± S.E.M.; significant differences between groups ($p<0.05$), as analyzed by one-way ANOVA and Tukey's test, are indicated by different lowercase letters.

expression by the CMV enhancer induces no increase in TRPC4 mRNA knockdown levels (37%) than that obtained with pSH-TC4sh1 (34%).

3.2.2 Knockdown using pooled shRNA constructs

Evaluation of the effectiveness of multiple TRPC4-shRNA construct combinations was performed to determine if different combinations of TRPC4-shRNA constructs would result in an even stronger TRPC4 luciferase reporter knockdown using the psiCHECK-2 system (Fig. 3.3). Cotransfection of the TRPC4-shRNA constructs,

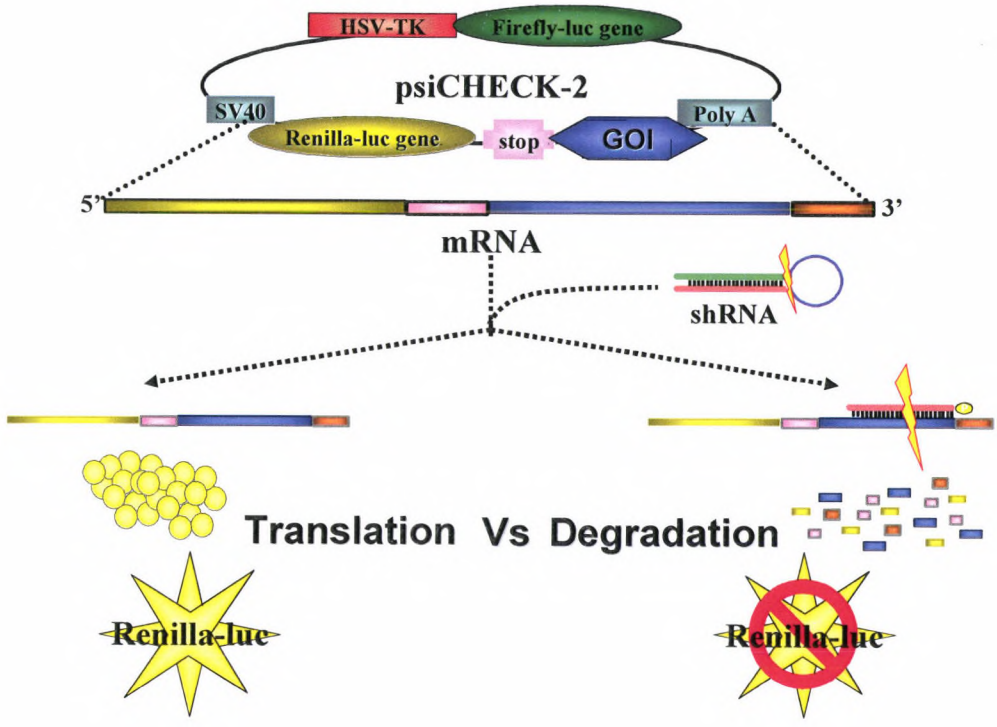

Fig. 3.3. Use of a Renilla luciferase reporter assay using the psiCHECK-2 to test the efficiency of shRNA constructs in targeting the mRNA sequence of their Gene of Interest (GOI). Expression of Firefly-luciferase takes place from a second promoter and aids in transfection efficiency monitoring. Figure adapted from Promega Corporation.

specified in Table 1, were performed in different combinations (i.e., shRNA#1+2, shRNA#1+4, shRNA#2+4, and shRNA #1+2+4) and were compared to single TRPC4-shRNA transfection experiments. These assays compared efficiencies from single-shRNA transfection versus multiple-shRNA transfection experiments for their efficiency to repress of TRPC4-mRNA expression levels. Interestingly, the results suggest that no one combination is able to induce a stronger TRPC4 mRNA knockdown than that induced by the strongest shRNA construct present in such combination (Fig. 3.4).

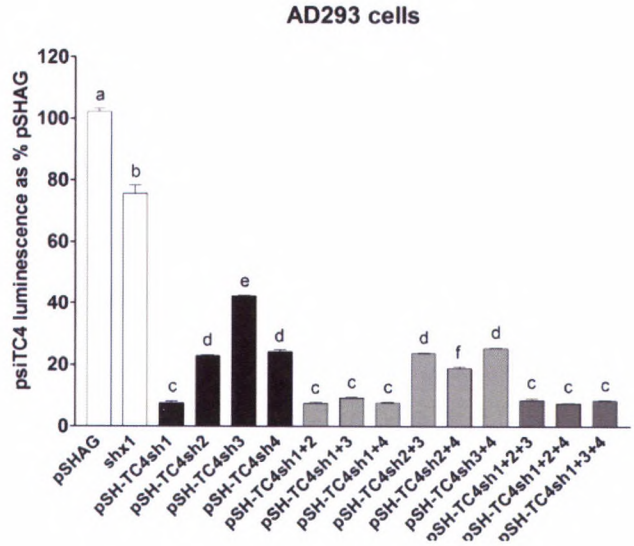

Fig. 3.4. Knockdown of TRPC4-luciferase reporter through use of pooled TRPC4-shRNA constructs versus single TRPC4-shRNAs. AD392 cells were transiently cotransfected with psiTC4 and different combinations of TRPC4-shRNAs (i.e., TRPC4sh1+2, TC4sh1+3, TC4sh1+4, TC4sh2+4, TC4sh1+2+4, and so forth) along with their single counterparts. In all cases, data represent the mean ± S.E.M. (n=5); significant differences between groups ($p<0.05$), as analyzed by one-way ANOVA and Tukey's test, are indicated by different lowercase letters.

3.3 Tandem shRNA expression

3.3.1 Multiple knockdowns with a single adenovirus

A modified pAdTrack-CMV vector was also constructed that contains a multiple cloning sequence in which sets of restriction sites define places for up to six shRNA inserts inserted between the CMV promoter and the sequence for the GFP protein, defined here as pAdT-CMR (Fig. 3.5). The GFP is expressed in cells, indicating infection, but fades with increasing number of shRNA constructs cloned upstream of the GFP transcription start site, presumably an indication of shRNA processing. This may actually be helpful to cell function. Additionally, a Renilla luciferase sequence was cloned into pAdT-MCS under the control of a second CMV promoter to allow independent monitoring of adenoviral infection. The resulting vector, named pAdT-CMR, was used to produce adenoviral constructs through homologous recombination with pAdEasy-1, as specified in the adenovirus construction section of Chapter 2. Adenoviral particles expressing either three copies of TC1sh2 (named TC1sh), TC4sh1 (named TC4sh) or Renilla-shRNA (named Rnllash) or single copies of TC1sh2 and TC4sh1 plus Renilla-shRNA in a single construct (named TC1+4sh) were used to infect human myometrial cells (Fig. 3.6). Additional adenoviral constructs were also made to study the effect of other TRPC knockdown combinations (i.e., TC1sh2+TC6sh1+Rnllash named TC1+6sh, TC4sh1+TC6sh1+Rnllash named TC4+6sh, TC1sh2+TC4sh1+TC6sh1 named TC1+4+6sh) and are ready to be tested (Fig. 3.6). The TRPC6-shRNA construct sequence is the same as that in the U6 vector construct used in Chung et al. [19]. These

Fig. 3.5. Construction of pAdT-CMR vector for tandem expression of shRNAs. A new multiple cloning site (MCS) was designed and inserted into the pAdTrack-CMV vector. The MCS enables the potential targeting of single or multiple proteins through tandem shRNA expression and infection with a single adenoviral vector. In the example, the TC1+4sh construct is shown. GFP expression in infected cells decreases with increasing number of shRNA constructs which serves as a marker of shRNA processing. Renilla-luciferase cDNA was also cloned within the vector's original multiple cloning site sequence for tracking of adenoviral expression. Thus, pAdT-CMR stands for CMV, MCS, Renilla-luciferase. Adenoviral particles are produced after the homologous recombination of pAdTCMV-MCS and pAdEasy-1.

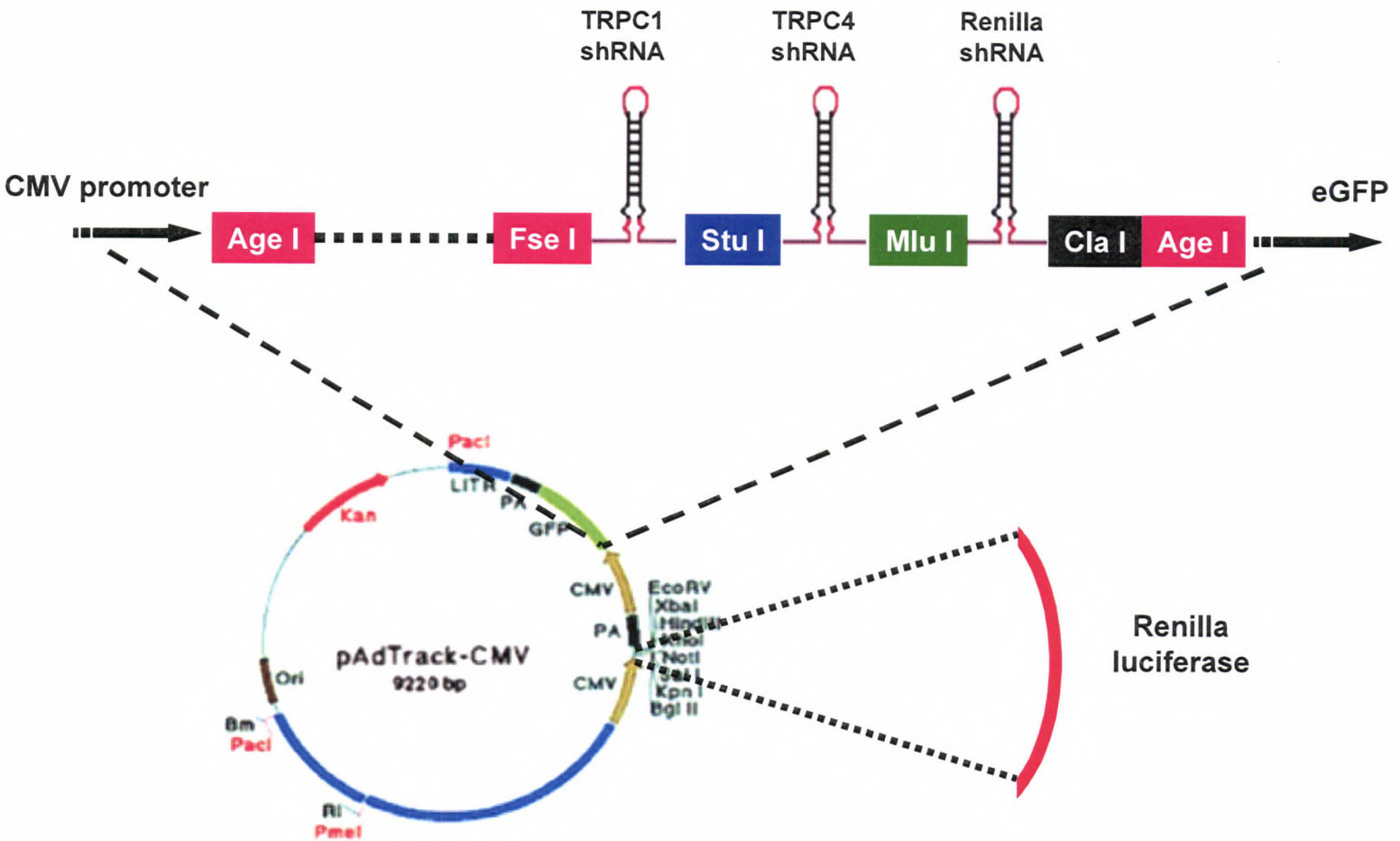
TRPC1
shRNA
TRPC4
shRNA
Renilla
shRNA
CMV promoter
eGFP
Age I
Fse I
Stu I
Mlu I
Cla I
Age I
Pacl
LITR
PA
GFP
Kan
CMV
EcoRV
XbaI
PA
NotI
SalI
KpnI
Bgl II
CMV
pAdTrack-CMV
9220 bp
Ori
Bm
PacI
RI
PmeI
Renilla
luciferase

constructs show valuable potential for knocking down many different proteins with a single adenoviral vector. For the purpose of this thesis work, however, the effect of the combined knockdown of TRPC1 plus TRPC4 through the use of the TC1+4sh construct was the only one studied.

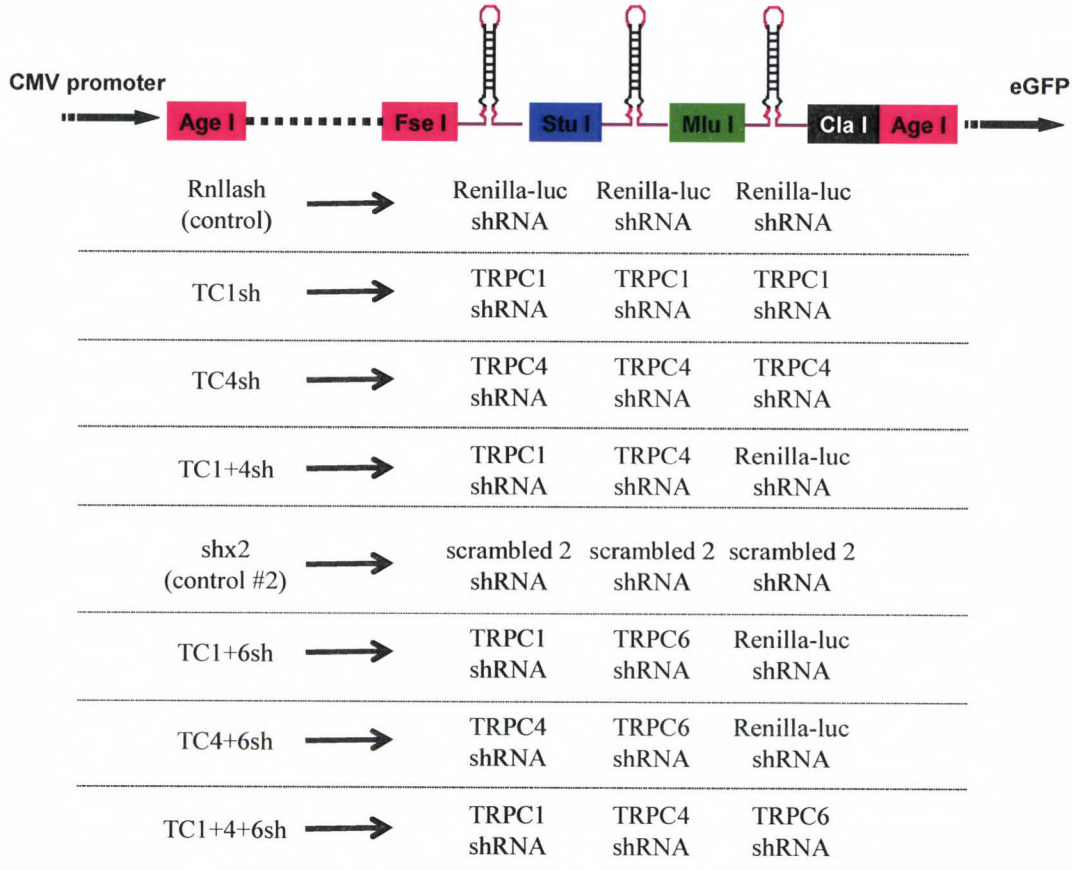

Fig. 3.6. Tandem shRNA constructs in pAdT-CMR vector. Rnllash, TC1sh, TC4sh and TC1+4sh constructs used in Chapter 5. Other constructs, shx2, TC1+6sh, TC4+6sh and TC1+4+6sh are ready to be tested and were not used for the present study.

3.4 Efficiency of adenoviral infection in PHM1 cells

To test the positive infection of PHM1 cells with adenoviral constructs, TRPC4 overexpression experiments were performed. An adenoviral vector was used to induce TRPC4 overexpression (TC4OE) at different time points. TRPC4 mRNA expression was determined at 24-96 hr post-infection by RT-qPCR. PHM1 cells infected with this vector displayed a >3 fold increase in TRPC4 mRNA level (Fig. 3.7). No changes in mRNA

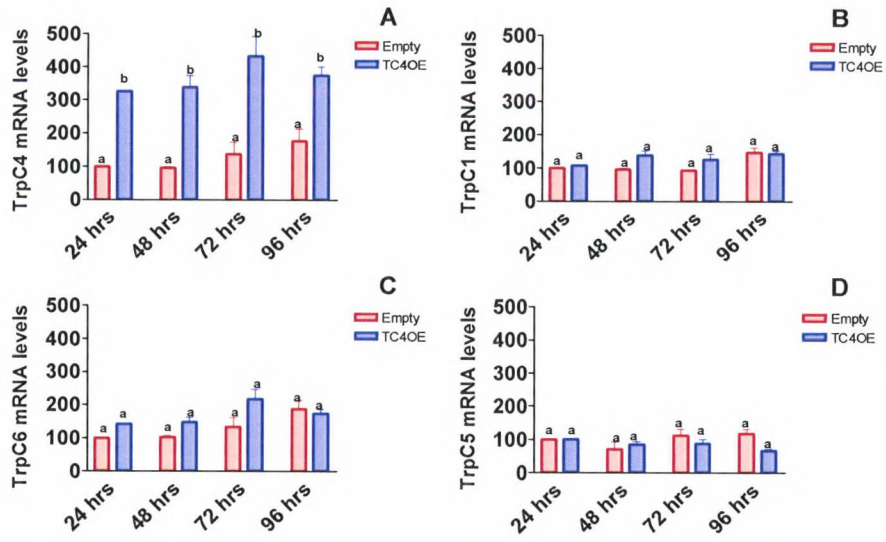

Fig. 3.7. TRPC4 overexpression in PHM1 cells. PHM1 cells were infected with an adenoviral vector for overexpression of TRPC4 (TC4OE). (A) A >3 fold increase in TRPC4 mRNA was observed over a period of 96 h post-infection when compared to cells infected with an empty vector. No significant changes in (B) TRPC1, (C) TRPC6 or (D) TRPC5 mRNA levels are observed. mRNA was normalized to GUS in the same sample and expressed relative to the value in cells exposed to empty vector. In all cases, data represent the mean ± S.E.M. (n=3); significant differences between groups ($p<0.05$), as analyzed by one-way ANOVA and Tukey's test, are indicated by different lowercase letters.

levels of TRPC1 and TRPC6, the two other most abundant TRPCs in the human myometrium, or in TRPC5 mRNA were detected after TRPC4 overexpression. Interestingly, infection of UtSMC cells with TC4OE displayed a ~40 fold increase in TRPC4 mRNA without any changes in TRPC1 or TRPC6 mRNA levels (Fig. 3.8).

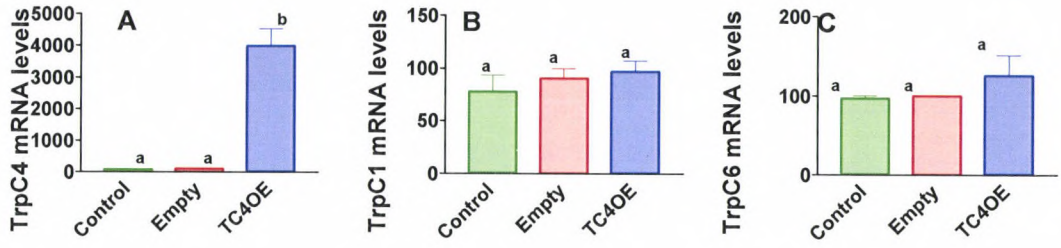

Fig. 3.8. Strong TRPC4 overexpression in UtSMC cells. UtSMC cells were infected with adenoviral vector TC4OE for expression of TRPC4. (A) TRPC4 mRNA levels displayed ~40 fold increase induced by TC4OE 72-96 h post-infection. No significant changes in (B) TRPC1 or (C) TRPC6 mRNA levels are observed. mRNA was normalized to GUS in the same sample and expressed relative to the value in cells exposed to empty vector. In all cases, data represent the mean ± S.E.M. (n=3); significant differences between groups ($p<0.05$), as analyzed by one-way ANOVA and Tukey's test, are indicated by different lowercase letters.

Calcium imaging with Fura-2 was used to measure intracellular calcium ($[Ca^{2+}]_i$) concentrations. Studies conducted to determine the effect of TRPC4 overexpression on calcium dynamics displayed no significant changes on oxytocin-, thapsigargin-, and OAG-stimulated calcium entry in UtSMC cells (Fig. 3.9).

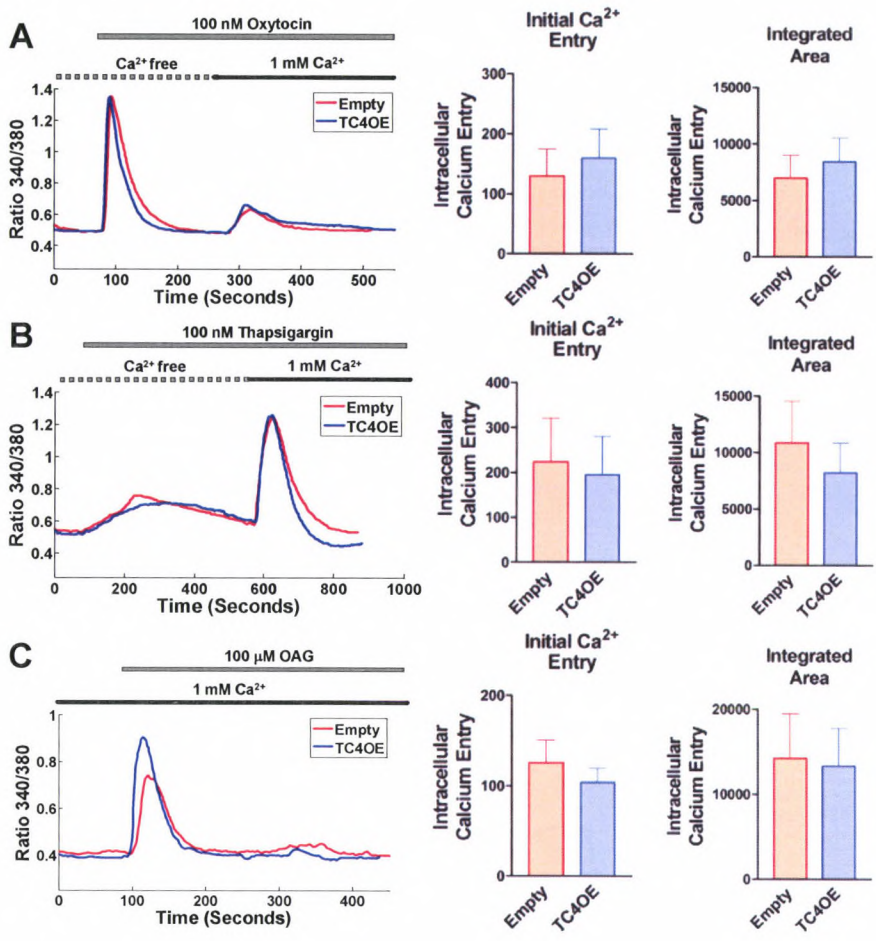

Fig. 3.9. Effects of TRPC4 overexpression on signal-regulated calcium entry. *Left.* SRCE induced by either (A) 100 nM oxytocin, (B) 100 nM thapsigargin or (C) 100 μM OAG in UtSMC cells infected with empty adenovirus (red lines) and cells infected with virus overexpressing TRPC4 (TC4OE, blue lines). *Right:* Mean changes in $[Ca^{2+}]_i$ resulting from addition of 1 mM extracellular Ca^{2+} (SRCE), calculated as area under the curve (integrated area) and peak height (initial calcium entry) (n=25-35 cells). Data are representative of 17, 5 and 6 independent experiments for oxytocin, TG and OAG, respectively.

References

1. Stevenson M. Dissecting HIV-1 through RNA interference. *Nat Rev Immunol* **2003**; 3: 851-858.

2. Dykxhoorn DM, Novina CD, Sharp PA. Killing the messenger: short RNAs that silence gene expression. *Nat Rev Mol Cell Biol* **2003**; 4: 457-467.

3. Dykxhoorn DM, Lieberman J. The silent revolution: RNA interference as basic biology, research tool, and therapeutic. *Annu Rev Med* **2005**; 56: 401-423.

4. Zhu X, Jiang M, Peyton M et al. trp, a novel mammalian gene family essential for agonist-activated capacitative Ca2+ entry. *Cell* **1996**; 85: 661-671.

5. Vandebrouck C, Martin D, Colson-Van SM, Debaix H, Gailly P. Involvement of TRPC in the abnormal calcium influx observed in dystrophic (mdx) mouse skeletal muscle fibers. *J Cell Biol* **2002**; 158: 1089-1096.

6. Fantozzi I, Zhang S, Platoshyn O, Remillard CV, Cowling RT, Yuan JX. Hypoxia increases AP-1 binding activity by enhancing capacitative Ca2+ entry in human pulmonary artery endothelial cells. *Am J Physiol Lung Cell Mol Physiol* **2003**; 285: L1233-L1245.

7. Philipp S, Trost C, Warnat J et al. TRP4 (CCE1) protein is part of native calcium release-activated Ca2+-like channels in adrenal cells. *J Biol Chem* **2000**; 275: 23965-23972.

8. Wu X, Babnigg G, Zagranichnaya T, Villereal ML. The role of endogenous human Trp4 in regulating carbachol-induced calcium oscillations in HEK-293 cells. *J Biol Chem* **2002**; 277**:** 13597-13608.

9. Brummelkamp TR, Bernards R, Agami R. A system for stable expression of short interfering RNAs in mammalian cells. *Science* **2002**; 296**:** 550-553.

10. Paddison PJ, Caudy AA, Bernstein E, Hannon GJ, Conklin DS. Short hairpin RNAs (shRNAs) induce sequence-specific silencing in mammalian cells. *Genes Dev* **2002**; 16**:** 948-958.

11. Reynolds A, Leake D, Boese Q, Scaringe S, Marshall WS, Khvorova A. Rational siRNA design for RNA interference. *Nat Biotechnol* **2004**; 22**:** 326-330.

12. Khvorova A, Reynolds A, Jayasena SD. Functional siRNAs and miRNAs exhibit strand bias. *Cell* **2003**; 115**:** 209-216.

13. Boden D, Pusch O, Silbermann R, Lee F, Tucker L, Ramratnam B. Enhanced gene silencing of HIV-1 specific siRNA using microRNA designed hairpins. *Nucleic Acids Res* **2004**; 32**:** 1154-1158.

14. Zeng Y, Cullen BR. Sequence requirements for micro RNA processing and function in human cells. *RNA* **2003**; 9**:** 112-123.

15. Zeng Y, Cullen BR. Efficient processing of primary microRNA hairpins by Drosha requires flanking nonstructured RNA sequences. *J Biol Chem* **2005**; 280**:** 27595-27603.

16. Chen CZ, Li L, Lodish HF, Bartel DP. MicroRNAs modulate hematopoietic lineage differentiation. *Science* **2004**; 303: 83-86.

17. Sun D, Melegari M, Sridhar S, Rogler CE, Zhu L. Multi-miRNA hairpin method that improves gene knockdown efficiency and provides linked multi-gene knockdown. *Biotechniques* **2006**; 41: 59-63.

18. Xia XG, Zhou H, Ding H, Affar eB, Shi Y, Xu Z. An enhanced U6 promoter for synthesis of short hairpin RNA. *Nucleic Acids Res* **2003**; 31: e100.

19. Chung D, Kim YS, Phillips JN et al. Attenuation of canonical transient receptor potential-like channel 6 expression specifically reduces the diacylglycerol-mediated increase in intracellular calcium in human myometrial cells. *Endocrinology* **2010**; 151: 406-416.

CHAPTER 4

Reduction in TRPC4 expression specifically attenuates G-protein coupled receptor-stimulated increases in intracellular calcium in human myometrial cells

4.1 Introduction

Ca^{2+} signaling is achieved as a result of increases in the concentration of intracellular free Ca^{2+} ($[Ca^{2+}]_i$). Increases in $[Ca^{2+}]_i$ correlate with increases in myosin light chain phosphorylation and with increases in tension [1]. Stimuli such as GPCR-activation, IP_3-R activation, inhibition of endoplasmic reticulum Ca^{2+}-ATPase (SERCA) pumps resulting in endoplasmic reticulum Ca^{2+} store depletion, and diacylglycerol itself (referred to in the present study as signal-regulated Ca^{2+} entry (SRCE)) have all been implicated in inducing TRPC activation directly or indirectly [2;3].

Human pregnant myometrial tissue, primary human myometrial cells and PHM1-41 cells all express TRPCs except TRPC 2 (a pseudogene in humans) [4-7]. TRPC4,

TRPC1 and TRPC6 mRNAs are present in higher relative abundance than TRPC3, TRPC5 and TRPC7 mRNAs [7]. TRPC1, 3, 4 and 6 proteins have been detected by immunoblot in human myometrial cells and tissue [4-7]. PHM1-41 immortalized human myometrial cells exhibit SRCE in response to oxytocin, thapsigargin and OAG [4;8-11], but the involvement of specific TRPCs in one or more of these responses has not been determined to date.

In this study the specific role of TRPC4 in myometrial SRCE was investigated using RNA interference (RNAi). Because we have found that PHM1-41 and primary human uterine smooth muscle (UtSMC) cells are difficult to transfect efficiently, we constructed an adenoviral vector expressing a TRPC4 short hairpin RNA (shRNA) construct to achieve specific TRPC4 knockdown. The data indicate that attenuation of TRPC4 expression specifically induces a decrease in GPCR-stimulated, but not in thapsigargin- or OAG-stimulated increases in $[Ca^{2+}]_i$ in myometrial cells.

4.2 Results

4.2.1 A functional RNA interference mechanism is present in human myometrial cells.

In order to study the function of endogenous TRPC4 in human myometrial cells, we designed four putative shRNA sequences that included a pre-microRNA backbone and tested them for their efficiency to decrease TRPC4 mRNA using the psiCHECK-2 system with a Renilla luciferase-TRPC4 fusion reporter vector (psiTC4). The sequences of these constructs are listed in Table 1. Figure 4.1A shows that the four TRPC4-shRNA (TC4sh1-4) constructs produced between 68 and 94% reduction in Renilla luciferase

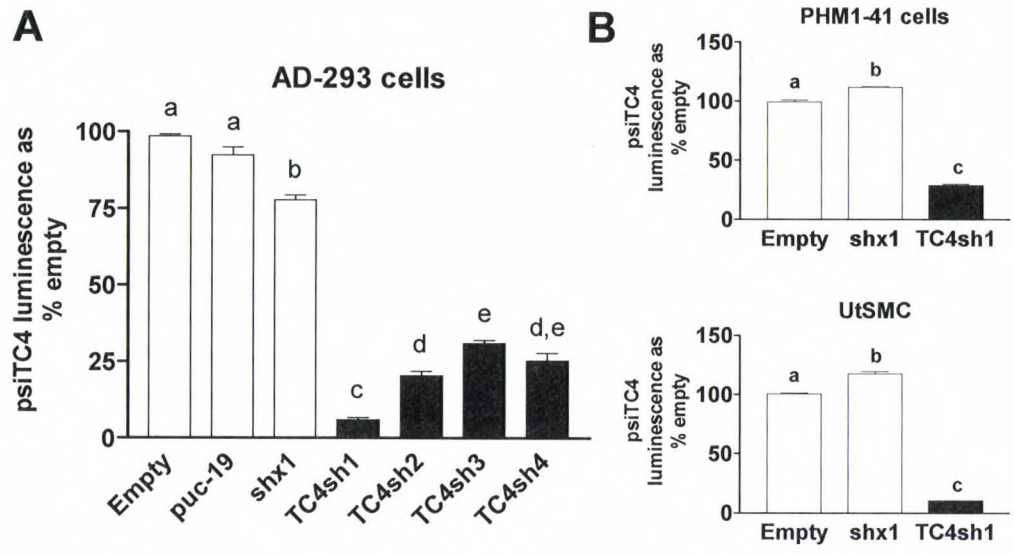

Fig. 4.1. TRPC4-reporter mRNA is suppressed by TRPC4-shRNA constructs in AD-293, PHM1-41 and UtSMC cells. (A) Significant suppression of luminescence from a Renilla luciferase-TRPC4 fusion reporter (psiTC4) following co-transfection of the reporter and plasmids expressing TRPC4 shRNAs (TC4sh1-4) in AD-293 cells as described in Methods. Controls include empty vector, puc-19 vector and scrambled shRNA (shx1). (B) psiTC4 was electroporated into PHM1-41 and UtSMC cells, together with TRPC4-shRNA#1 (TC4sh1) in pSHAG vector as described in Methods. Controls include empty vector (pSHAG) and pSHAG plasmid expressing a scrambled shRNA control sequence (shx1). In A and B samples were isolated >72 h post-electroporation. Data are expressed as % of luminescence exhibited by co-transfection of empty vector and represent mean ± S.E.M. (n=3). Background luminescence (~7%) was subtracted from all samples. Data were analyzed by one-way ANOVA and Tukey's test. Significant difference between groups ($p<0.05$) is indicated by different lowercase letters.

protein expression compared to empty vector, a pUC19 vector, and a construct expressing a scrambled TRPC4 shRNA sequence (shx1).

RNAi requires expression and function of many components necessary for the production and processing of the shRNA constructs. To determine the effectiveness of this mechanism in processing the TC4sh1 construct in myometrial cells, the psiCHECK-2 TRPC4 reporter vector was electroporated into PHM1-41 and UtSMC cells, along with a plasmid expressing the TC4sh1 construct. Electroporation efficiency was ~60% as determined by visual assessment of maxGFP expression from a separate plasmid. TRPC4 mRNA was effectively targeted by the TC4sh1 construct, achieving >70 and 90% reduction of the reporter in PHM1-41 and UtSMC cells, respectively (Fig. 4.1B). These data indicated that the RNAi mechanism was adequate in myometrial cells and that the TC4sh1 targeting sequence was effective.

4.2.2 TRPC4 knockdown in human myometrial cells is TRPC4-specific and attenuates oxytocin- stimulated increases in $[Ca^{2+}]_i$

The TC4sh1 construct was cloned downstream of a U6 promoter into an adenoviral vector expressing GFP under the control of a separate CMV promoter. In PHM1-41 cells infected with the adenovirus expressing TC4sh1, significant TRPC4 mRNA knockdown occurred 48-96 h post infection, with the greatest knockdown at 72-96 h. Fig. 4.2A shows that PHM1-41 cells infected with empty adenovirus displayed no changes in expression of any TRPC mRNA compared to noninfected cells. This demonstrates that viral infection itself did not alter TRPC expression. TRPC RT-qPCR amplicons show single products in agarose gels (Fig. 4.2B). In all cases, no product was observed if the reverse transcriptase was omitted from the mixture, indicating that there

Fig. 4.2. Adenovirus vector expressing TC4sh1 produced a specific TRPC4 mRNA knockdown in PHM1-41 cells. (A) PHM1-41 infection with adenovirus expressing TC4sh1 induced specific TRPC4 mRNA knockdown compared to effects of empty vector (E) or scrambled shRNA (shx1). Also shown are the TRPC mRNA levels in PHM1-41 cells not treated with adenovirus (UN). mRNA levels of other TRPCs are unchanged by exposure to any of these viral constructs. mRNA was normalized to GUS in the same sample and expressed relative to the value in cells exposed to empty vector. In all cases, data represent the mean ± S.E.M. (n=3); significant differences between groups ($p<0.05$), as analyzed by one-way ANOVA and Tukey's test, are indicated by different lowercase letters. (B) RT-qPCR products for TRPC1, TRPC4, TRPC6, and GUS (obtained from 100 ng RNA) as well as for TRPC3, TRPC5 and TRPC7 (obtained from 1 μg RNA) were run in 3% agarose gels. In all cases, single bands of the expected size were observed. No bands are observed in samples lacking reverse transcriptase (RT) in the reaction.

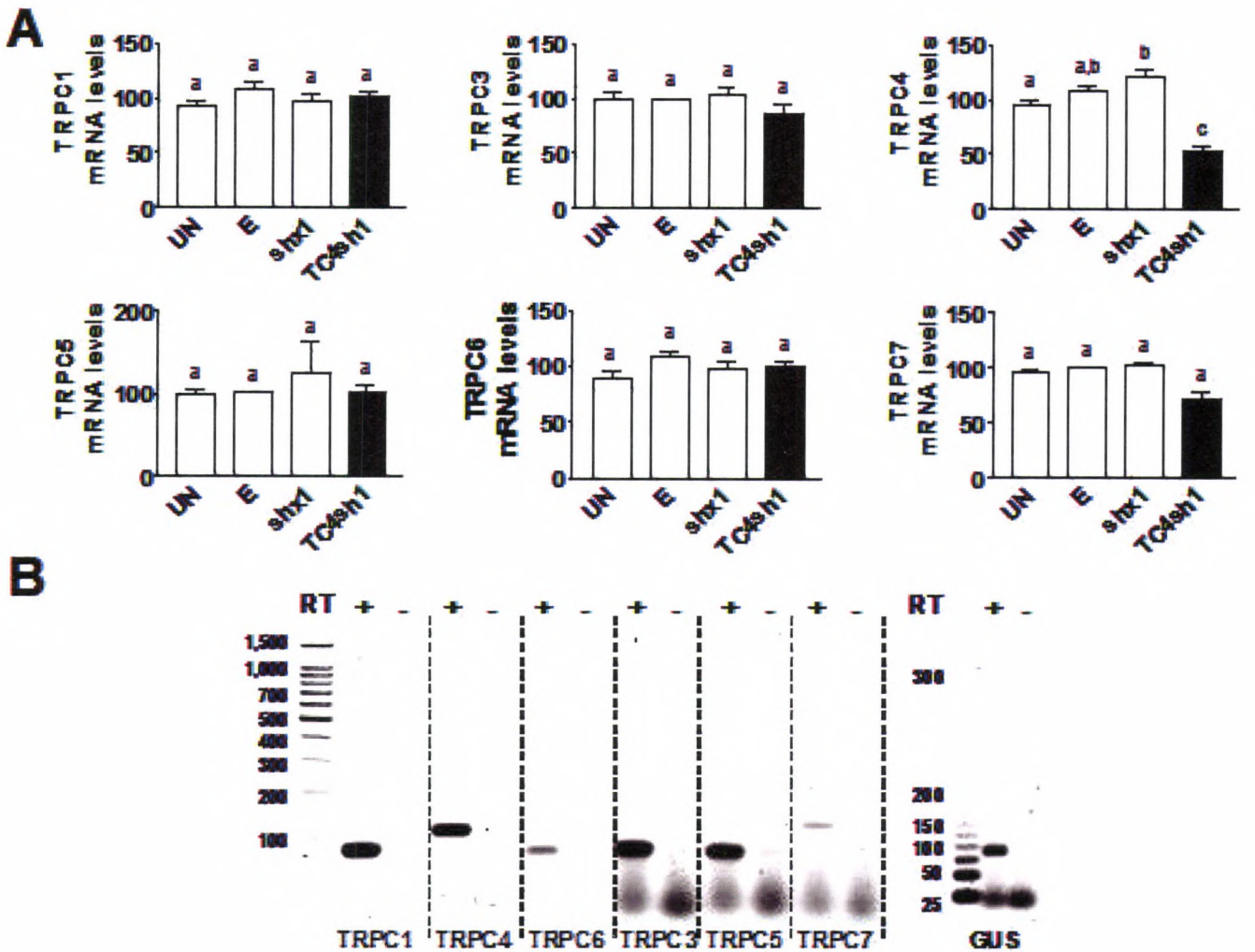
A
TRPC1 mRNA levels
TRPC3 mRNA levels
TRPC4 mRNA levels
TRPC5 mRNA levels
TRPC6 mRNA levels
TRPC7 mRNA levels
UN
E
shx1
TC4sh1
B
RT
TRPC1
TRPC4
TRPC6
TRPC3
TRPC5
TRPC7
GUS

was no significant amplification of DNA in these samples. The adenoviral construct expressing TC4sh1 produced specific knockdown in TRPC4 mRNA, with no effect on other TRPC mRNAs 72 h post infection as shown in the real time RT-qPCR data (Fig. 4.3). Under these conditions, there were also no apparent changes in the mRNAs for PMCA 1, PMCA 4 or SERCA 2 (Fig 4.4). The degree of TRPC4 knockdown was variable between experiments; we achieved a maximal knockdown of 73%, with a mean of 54 ± 3.28%. Fig. 4.5A and 4.5B show that TC4sh1 suppressed TRPC4 protein expression in both whole cell and purified plasma membrane extracts (by 40 % and 70% relative to empty vector, respectively). In contrast, the concentration of TRPC1 protein, the membrane expression of which has been reported to be enhanced by TRPC4 [12;13], was not significantly changed, relative to empty vector, in purified plasma membrane extracts.

The specificities of the TRPC4 and TRPC1 antibodies, as demonstrated by reduction in TRPC signal once the antibody was exposed to antigenic peptide, are shown in Fig 4.5C and Fig 4.5D, respectively. TRPC4 exhibited a band between 86 and 94 kDa in PHM1 cells using the TRPC4 antibody obtained from Alomone (and other suppliers). When transiently expressed in COSM6 cells, the TRPC4 overexpression (TRPC4 OE) vector produced a 100 kDa band detected with the HA tag that was reduced >70% when coexpressed with the TC4sh1 construct (Figure 4.5E). Differences in apparent size may represent differences in protein glycosylation in different cell types. Regardless, the suppression of expression of the HA-tagged protein by TC4sh1 further attests to its efficacy.

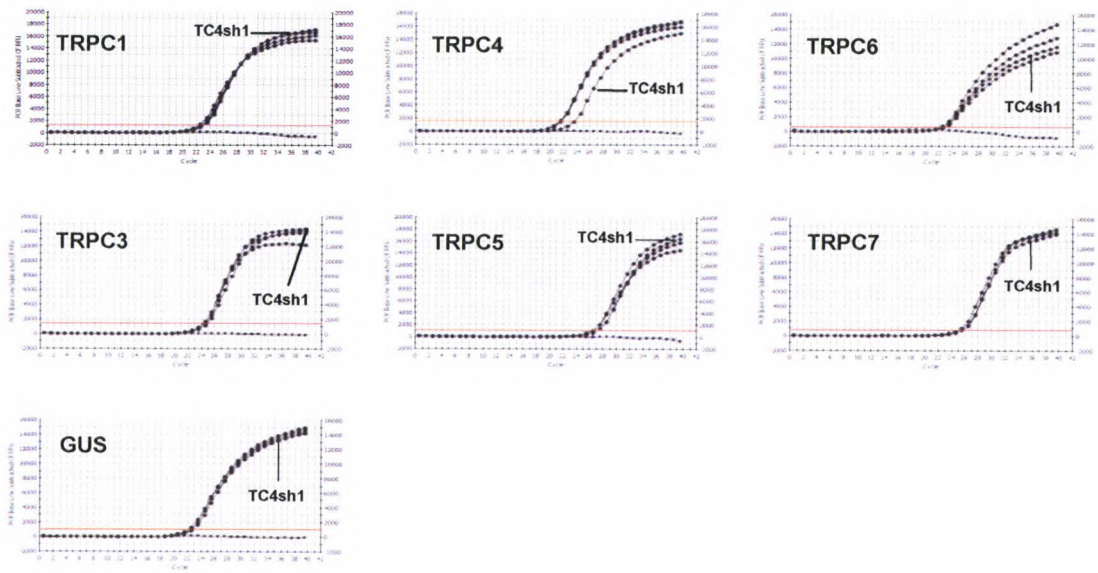

Fig. 4.3. Real-time fluorescence emission of SYBR Green during PCR amplification of the TRPCs cDNAs. TC4sh1 induced a specific TRPC4 knockdown of 70% in this individual experiment without affecting other TRPC mRNA expression. RNA was isolated from uninfected PHM1-41 cells and from cells infected with empty adenovirus, adenovirus expressing shx1 and adenovirus expressing TC4sh1. A control sample lacking reverse transcriptase in the reaction is also shown.

To assess effects of TRPC4 knockdown on increases in myometrial $[Ca^{2+}]_i$ in response to various stimuli, PHM1-41 cells were infected with adenoviral vectors carrying either empty vector or the TC4sh1 construct and tested for effects on SRCE, defined as a stimulus- and extracellular Ca^{2+}-dependent increase in $[Ca^{2+}]_i$. Noninfected PHM1-41 cells and cells infected with empty adenovirus behaved similarly with respect to the SRCE responses tested, indicating that viral infection per se had no effect on responsiveness (Fig. 4.6). The SRCE response is illustrated in the tracing in Fig. 4.7A

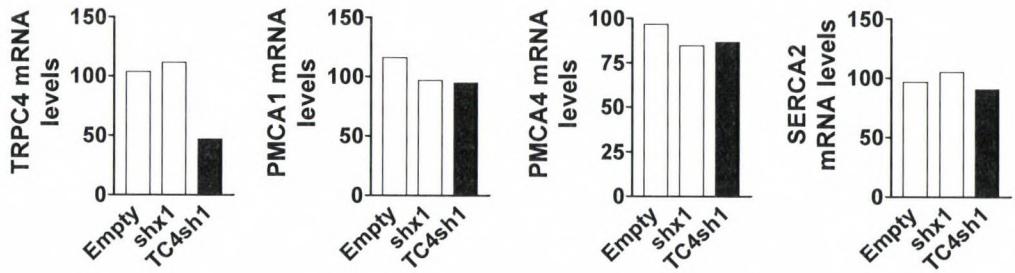

Fig. 4.4. TRPC4 knockdown does not affect mRNA expression of PMCA1, PMCA4 and SERCA2 (both a and b isoforms for each) in PHM1 cells. PHM1 cells were infected with the adenoviral constructs indicated. RNA was isolated >72 h post-infection. Data are expressed relative to empty vector (n=1).

(left panel). Cells were stimulated in Ca^{2+}-free buffer with oxytocin, a GPCR-activator resulting in IP_3 generation, eliciting a transient increase in $[Ca^{2+}]_i$. Once $[Ca^{2+}]_i$ returned to basal levels, 1 mM extracellular Ca^{2+} was added and SRCE was observed, as indicated by a second, extracellular Ca^{2+}-dependent increase in $[Ca^{2+}]_i$. No such increase was observed if the cells were not exposed to 1 mM extracellular Ca^{2+} or if Ca^{2+}-free buffer were added instead. TRPC4 knockdown did not significantly affect the initial $[Ca^{2+}]_i$ transient but resulted in >70% inhibition of oxytocin-stimulated SRCE (dotted line in the tracing in Fig. 4.7A). In this particular experiment, a 73% reduction in TRPC4 mRNA knockdown was achieved (Fig. 4.7A, middle panel). The summarized data for individual cells are presented in the right panel of Fig. 4.7A.

Both the degree of TRPC4 mRNA knockdown and the extent of the inhibition of the oxytocin SRCE response were variable between experiments for reasons that we have yet to ascertain. Fig. 4.7B summarizes the effect of TRPC4 on inhibition of oxytocin-

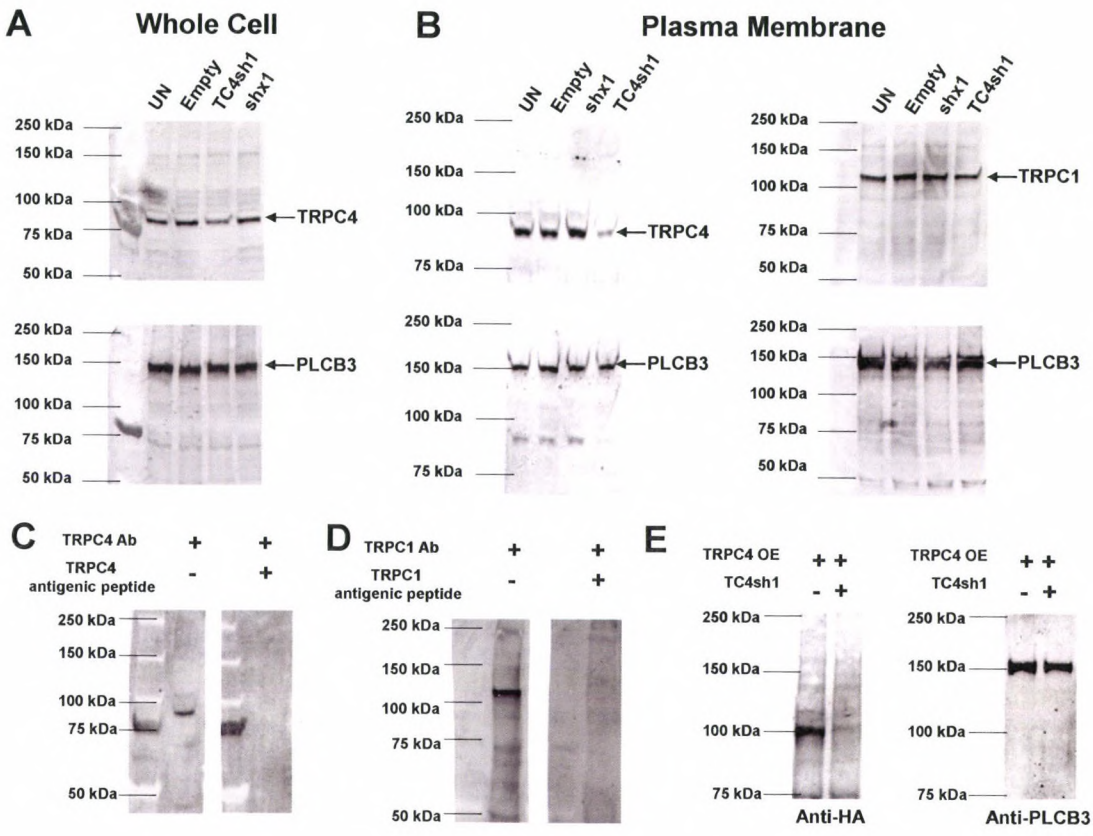

Fig 4.5. Adenovirus vector expressing TC4sh1 produced a specific TRPC4 protein knockdown in PHM1-41 cells. (A). whole cell extracts and (B) purified membrane extracts from uninfected (UN) cells and cells exposed to empty adenovirus (E), virus expressing a scrambled shRNA sequence (shx1), or virus expressing TC4sh1 for > 72 h. PLCB3 was used as normalization control. (C) TRPC4 antibody (Ab) specificity is shown by the absence of 92 kDa band when the antibody was preabsorbed with TRPC4 antigenic peptide. (D) Antibody preabsorption using TRPC1 antigenic peptide specifically blocks 116 KDa TRPC1 band detection by the TRPC1 antibody (Ab). (E) Expression of the TRPC4-HA tag protein overexpressed (TRPC4 OE) in COSM6 cells and suppression of this expression by cotransfection with the TC4sh1 construct.

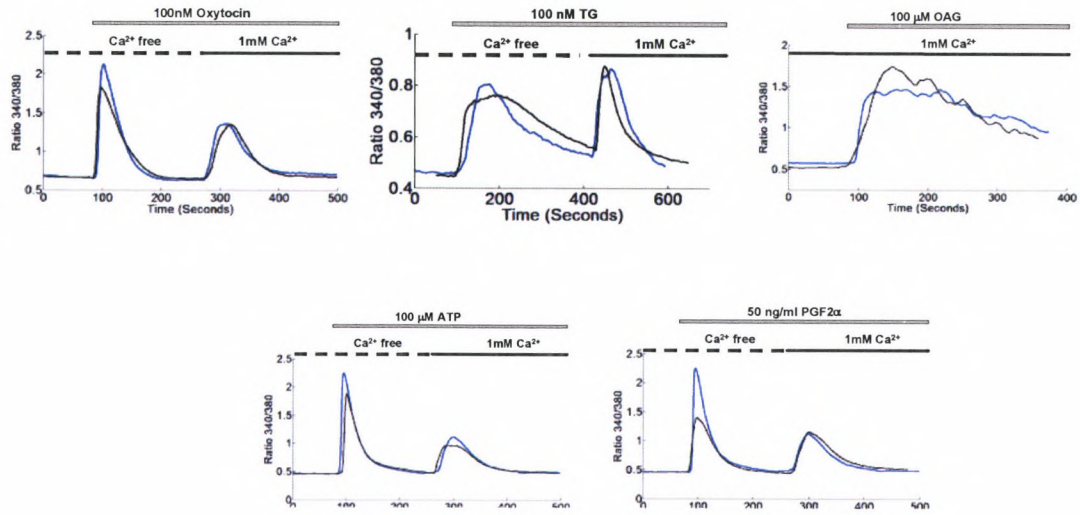

Fig. 4.6. Adenoviral infection of PHM1 cells does not affect SRCE mechanisms. PHM1 cells were uninfected (blue line) or infected with empty vector (black line) and SRCE mechanisms were tested >72 h post-infection. Tracings are from single experiments (20-45 cells), representative of 3-10 individual experiments.

stimulated SRCE in nine experiments (mean inhibition of 52 ± 3.61%). Importantly, the degree of inhibition of the oxytocin SRCE response correlated with the degree of TRPC4 knockdown (Fig. 4.7C) and the qualitative specificity of the response was always observed, regardless of the degree of knockdown. Furthermore, although considerably less efficient, we also used electroporation to introduce shRNA plasmids into UtSMC cells and observed a >45% decrease in TRPC4 mRNA and a >50% decrease in oxytocin-stimulated SRCE relative to empty vector in cells co-expressing GFP from a second plasmid (Fig. 4.8).

PHM1-41 cells are immortalized myometrial cells. Effects of oxytocin-stimulated increases in $[Ca^{2+}]_i$ were also observed in UtSMC cells. Fig. 4.9 shows >77% and >65%

Fig 4.7. Attenuation of oxytocin signal-regulated calcium entry (SRCE) induced by TRPC4 knockdown in PHM1-41 cells. (A) *Left.* SRCE induced by 100 nM oxytocin in PHM1-41 cells infected with either empty adenovirus (empty, solid line) or adenovirus expressing TC4sh1 (dotted line) for >72 h. *Middle.* TRPC4 mRNA levels, normalized relative to empty vector, in the experiment shown. *Right.* Mean ± S.E.M. (n= 20-40 cells) of changes in $[Ca^{2+}]_i$ resulting from addition of 1 mM extracellular Ca^{2+} (SRCE) in the experiment shown, calculated as area under the curve (integrated area) and by peak height (initial calcium entry). (B) Mean changes in $[Ca^{2+}]_i$ observed in 9 experiments. Data are presented as mean ± S.E.M. and were analyzed by t-test. In all cases, significant differences from empty vector ($p<0.05$) are indicated by an asterisk (*). (C) TRPC4 mRNA knockdown is strongly correlated with attenuation of the oxytocin-SRCE response (R= 0.88196, $\rho = <0.01$). Data samples are from PHM1-41 cells (circles) and UtSMC experiments (squares).

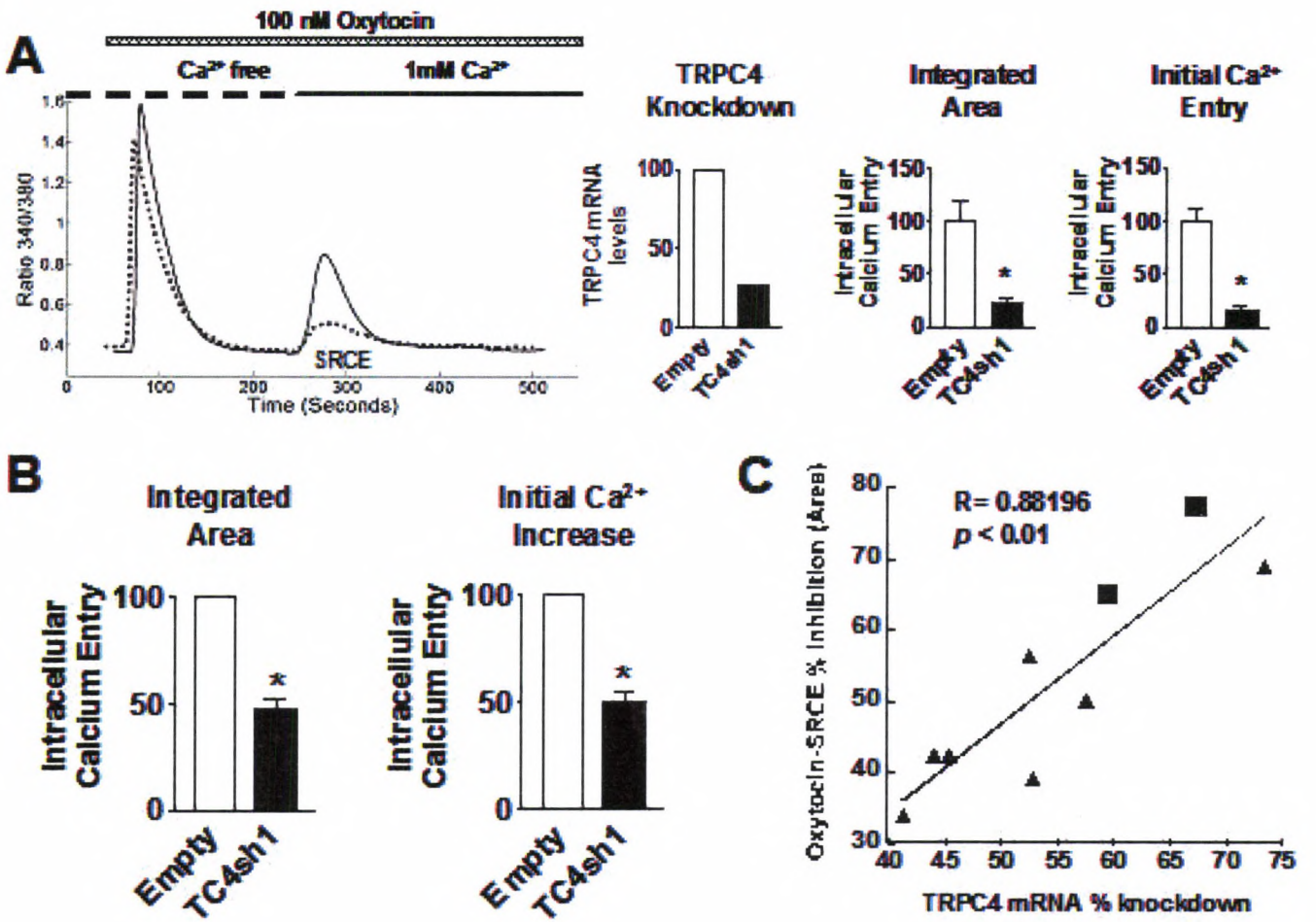
A
100 nM Oxytocin
Ca2+ free
1mM Ca2+
Ratio 340/380
SRCE
Time (Seconds)
TRPC4 Knockdown
TRPC4 mRNA levels
Empty
TC4sh1
Integrated Area
Intracellular Calcium Entry
Initial Ca2+ Entry
B
Integrated Area
Initial Ca2+ Increase
C
R= 0.88196
p < 0.01
Oxytocin-SRCE % Inhibition (Area)
TRPC4 mRNA % knockdown

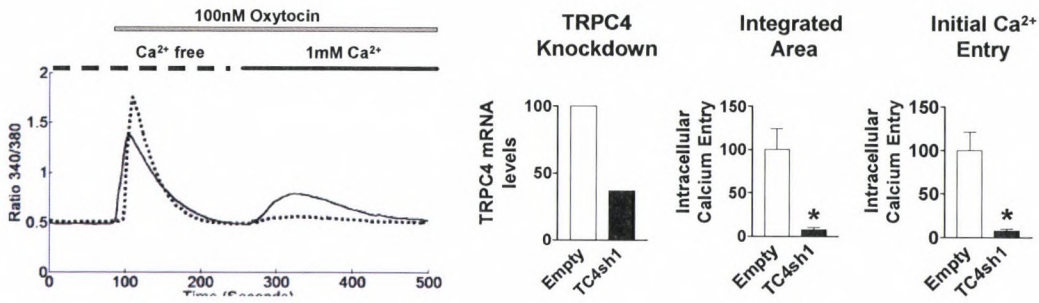

Fig. 4.8. TRPC4 knockdown through non-viral delivery of TC4sh1 produces a similar phenotype as that obtained using an adenoviral delivery method. UtSMC cells were electroporated using the Basic Smooth Muscle Cell Nucleofector kit with either an empty vector (solid line) or vector expressing the TC4sh1 (dotted line), selected on the basis of GFP fluorescence. *Left.* SRCE induced by 100 nM oxytocin in cells expressing either empty or TC4sh1. Middle. TRPC4 mRNA levels expressed relative to empty vector in the experiment shown. *Right* Intracellular calcium levels are represented by measuring area under the curve (integrated area) and by peak height (initial calcium increase). Samples were isolated >72hr post-electroporation (average of 15-20 cells/dish). In all cases, significant differences from empty vector ($p<0.05$) are indicated by an asterisk (*). Data are representative of 3 independent experiments.

inhibition of the $[Ca^{2+}]_i$ transient area and peak height, respectively, of the oxytocin-stimulated SRCE response in an experiment where > 67% mRNA knockdown was achieved.

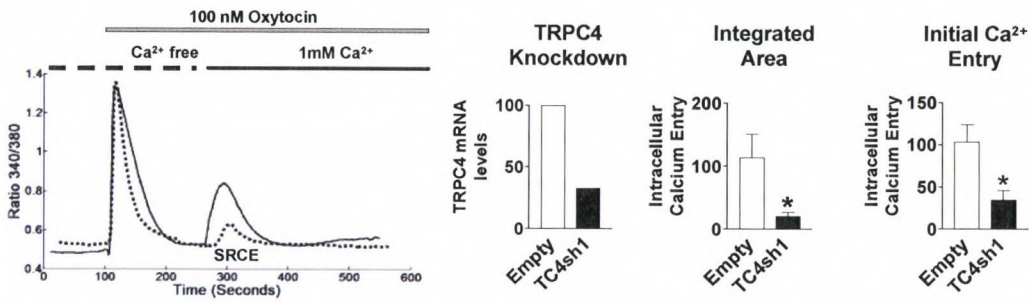

Fig. 4.9. Specific TRPC4 mRNA knockdown and inhibition of oxytocin-stimulated SRCE in UtSMC cells. *Left.* SRCE induced by 100 nM oxytocin in UtSMC cells infected for >72 h with empty vector (empty, solid lines) or adenovirus expressing TC4sh1 (dotted line). *Middle.* TRPC4 mRNA, normalized relative to empty vector, in the experiment shown. *Right.* Mean changes in $[Ca^{2+}]_i$ resulting from addition of 1 mM extracellular Ca^{2+} (SRCE) in the experiment shown, calculated as area under the curve (integrated area) and by peak height (initial calcium entry). Data are presented as mean ± S.E.M. (n= 15-25 cells) and were analyzed by t-test. In all cases, significant differences from empty vector ($p<0.05$) are indicated by an asterisk (*). Data are representative of 3 independent experiments.

4.2.3 TRPC4 knockdown attenuates SRCE stimulated by other G protein-coupled receptors

In order to determine if the effect of TRPC4 knockdown was specific to oxytocin signaling or pertained to other GPCR stimulants, we examined the effect of TRPC4 knockdown on SRCE elicited in response to stimulation of PHM1-41 cells with ATP and PGF2α. Significant suppression of SRCE induced by ATP (65% and 79% inhibition of

area and peak height, respectively) and PGF2α (86% and 79% inhibition of area and peak height, respectively) was observed in cells infected with adenovirus expressing TC4sh1, but not with empty vector (Fig. 4.10). In unrelated studies, we have determined that ATP effects on phospholipase C beta activation in PHM1-41 cells are inhibited by Reactive Blue-2, a P2Y-specific inhibitor, indicating that the action of ATP is GPCR-mediated (D. Murtazina, unpublished observations). These data support a link between TRPC4 knockdown and attenuation of GPCR-stimulated calcium entry in myometrial cells.

4.2.4 TRPC4 knockdown had no effect on thapsigargin- or diacylglycerol-stimulated extracellular calcium-dependent increases in $[Ca^{2+}]_i$ in human myometrial cells

Using the same experimental design as in Fig. 4.7, the effect of TRPC4 knockdown on store-operated SRCE elicited by exposure to thapsigargin, which induces Ca^{2+} store depletion by blocking the endoplasmic reticulum Ca^{2+}-ATPase, was determined. Thapsigargin treatment resulted in an increase in $[Ca^{2+}]_i$ in the absence of extracellular Ca^{2+} (Fig. 4.11A) Notably, in contrast to the effect of TRPC4 knockdown on oxytocin-stimulated SRCE, the thapsigargin-stimulated SRCE observed in response to the addition of extracellular Ca^{2+} was not affected by TRPC4 knockdown. Similarly, no significant changes were observed in the elevation of $[Ca^{2+}]_i$ elicited in the presence of extracellular $Ca^{2+}$by OAG, a cell permeable diacylglycerol (Fig 4.11B). In UtSMC, knockdown of TRPC4 also did not alter the thapsigargin response (Fig. 4.12).

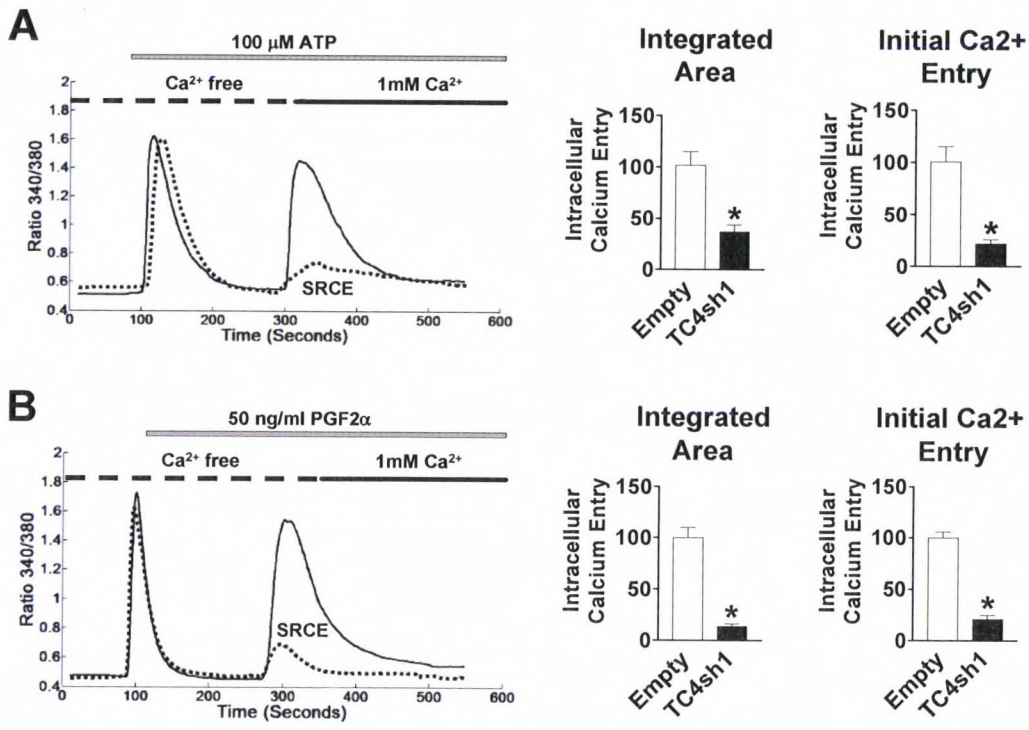

Fig. 4.10. TRPC4 knockdown induces attenuation of other GPCR-stimulated SRCE. *Top*: SRCE induced by 100 μM ATP (A) and 50 ng/ml PGF2α (B) in PHM1-41 cells infected with empty adenovirus (solid lines) and cells infected with virus expressing TC4sh1 (dotted lines). *Bottom:* Mean changes in $[Ca^{2+}]_i$ resulting from addition of 1 mM extracellular Ca^{2+} (SRCE) in the experiment shown, calculated as area under the curve (integrated area) and by peak height (initial calcium entry). Data are presented as mean ± S.E.M. (n=35-45 cells) and were analyzed by t-test. In all cases, significant differences from empty vector ($p<0.05$) are indicated by an asterisk (*). Data are representative of 4 independent experiments.

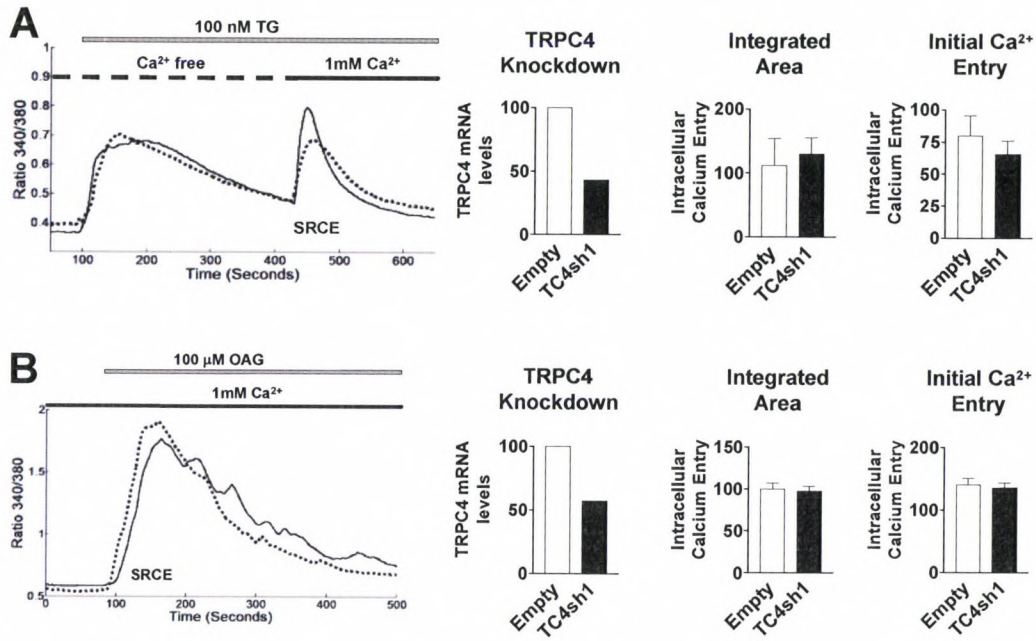

Fig.4.11. Lack of effect of TRPC4 knockdown on thapsigargin- and OAG-stimulated SRCE. *Left.* SRCE induced by either (A) 100 nM thapsigargin and (B) 100 µM OAG in PHM1-41 cells infected with empty adenovirus (solid lines) and cells infected with virus expressing TC4sh1 (dotted lines). *Middle.* TRCP4 mRNA levels expressed relative to empty vector in the experiment shown. *Right:* Mean changes in $[Ca^{2+}]_i$ resulting from addition of 1 mM extracellular Ca^{2+} (SRCE) in the experiment shown, calculated as area under the curve (integrated area) and peak height (initial calcium entry) (n=45-55 cells). Data are representative of 10 and 7 independent experiments for thapsigargin and OAG, respectively.

4.2.5 Activation of cation currents by oxytocin in PHM1-41 cells was attenuated by the expression of TC4sh1

Using cell-attached patch clamp electrophysiology, single channel activity was recorded in response to 100 nM oxytocin in PHM1-41 cells. In these experiments, potential contributions from L-type calcium channels were minimized by inclusion of 100 nM nifedipine in the bath solution. Furthermore, a significant contribution to OT-stimulated currents from BK_{Ca} channels activated by calcium entry, as previously reported [14], were essentially eliminated by inclusion of 20 mM TEA in the bath solution and 10 μM paxilline in the pipette solution. Fig. 4.13A shows a representative baseline recording with distinct single channel openings (Control). The administration of oxytocin increased both the frequency and duration of channel activity in cells infected with empty control vector (Fig 4.13A, Control + OT). Cells in which TRPC4 expression was suppressed by TC4sh1 showed significantly lower response to oxytocin (Fig 4.13B, TC4sh1 + OT). The change in total open probability (ΔNP_o) in response to oxytocin was significantly reduced in cells treated with TC4sh1 versus cells treated with empty vector (Fig. 4.13C). (These data were obtained by A. L. Gonzales).

4.3 Discussion

TRPC proteins have been implicated in calcium signaling dynamics in myometrial smooth muscle [4;10;15]. Previous studies have shown that, although human myometrium expresses most TPRC mRNAs, TRPC4 and TRPC1 mRNAs are expressed in high relative abundance, along with TRPC6 [7]. However, to date, no TRPC

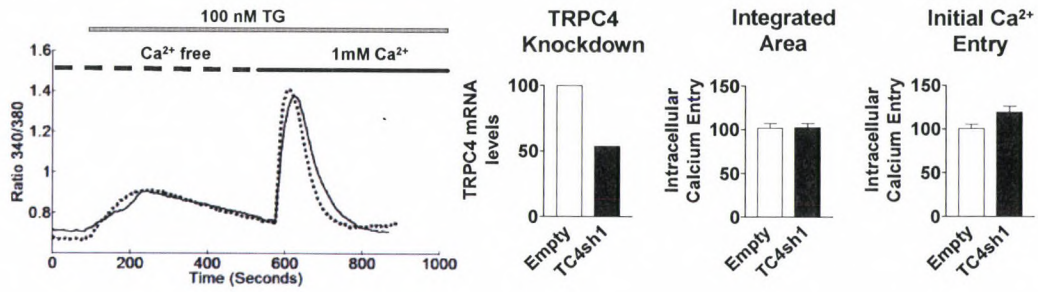

Fig. 4.12. TRPC4 knockdown induces no changes in thapsigargin-stimulated SRCE in UtSMC cells. UtSMC cells were infected with adenovirus carrying an empty vector (solid line) or adenovirus carrying TC4sh1 (dotted line). Cells were analyzed >72 h post-infection. *Left.* SRCE induced by 100 nM thapsigargain (TG) . *Middle.* TRPC4 mRNA levels expressed relative to empty vector in this experiment. *Right.* Intracellular calcium levels are represented by measuring area under the curve (integrated area) and by peak height (initial calcium entry). (average of 35-45 cells). Data are representative of 4 individual experiments.

knockdown studies had been conducted in this system. Since the TRPC profile can be dramatically different between systems and since profile is hypothesized to dictate the physiological function of the homo- and heterotetrameric TRPC channels that are formed, it is important to determine the role of specific TRPC proteins in affecting signal-stimulated myometrial calcium dynamics.

In an attempt to assess the role of endogenous TRPC4 in myometrial SRCE in response to various stimuli, we used RNA interference to diminish its expression. Since PHM1-41 and UtSMC cells are difficult to transfect by conventional methods (<40% efficiency) and are not easily selectable, we used a viral vector to express the shRNA

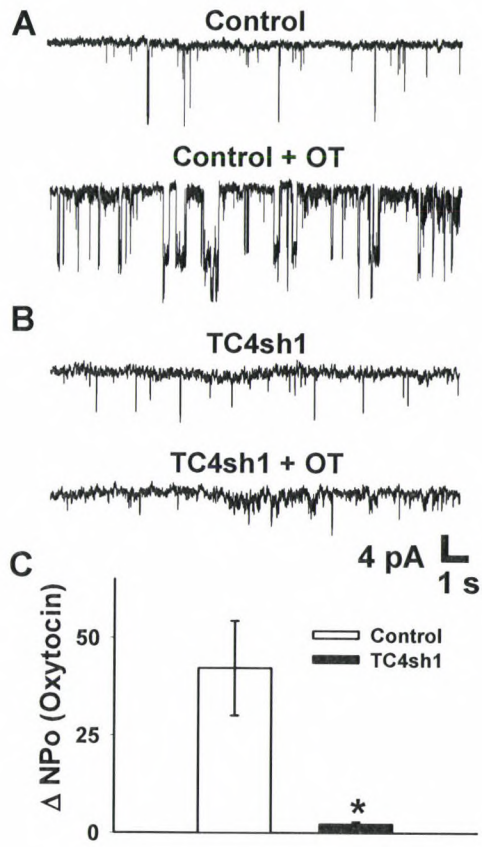

Fig. 4.13. Activation of cation currents by oxytocin in PHM1-41 cells was attenuated by the expression of TC4sh1. (A) Representative trace of single-channel cell-attached recordings from PHM1-41 cells infected with empty vector *(top)*, and in response to 100 nM oxytocin *(bottom)*. (B) Representative trace of single-channel cell-attached recordings from PHM1-41 cells infected with adenovirus expressing TC4sh1 for >72 h *(top)*, and in response to oxytocin (bottom). (C) Summary of the change in total open probability (ΔNP_o) in response to administration of oxytocin for control (n=5) and TC4sh1 (n=5) treated PHM1-41 cells. Data are presented as mean ± S.E.M. and were analyzed by t-test. The difference between the two groups was significant at ($p<0.05$) and is indicated by an asterisk (*).

constructs. Despite demonstrating that the shRNA construct was effective at targeting an exogenous TRPC4 reporter for degradation, we experienced a variable degree of endogenous TRPC4 knockdown using an adenoviral vector between experiments. Although adenoviral vectors usually achieve 90-95% infection efficiency with minimal cell toxicity, variability in the efficiency of knockdowns using viral shRNA constructs has been reported [16;17]. Additionally, smooth muscle cells display low adenovirus binding levels, potentially due either to the lack or low expression of Coxsackie Adenovirus Receptor (CAR) [18], which could contribute to variability.

The data indicate that TRPC4 mRNA and protein expression were specifically diminished in PHM1-41 and UtSMC by the adenoviral construct expressing TC4sh1, while concentrations of other TRPCs were unaffected. PHM1-41 and UtSMC cells, as well as rat myometrial cells, respond to oxytocin with increases in $[Ca^{2+}]_i$ that are partially dependent on extracellular Ca^{2+} and are not affected by voltage-operated channels (VOC) blockers such as nifedipine [10;19;20]. Reduction in TRPC4 expression preferentially attenuated GPCR-operated SRCE in PHM1-41 and UtSMC cells. This appears to be a relatively general mechanism, as oxytocin, PGF2α and ATP-mediated SRCE were also affected. Both oxytocin and PGF2α are important endogenous stimulators of uterine contractions and play important roles during labor [21]. In contrast, TRPC4 knockdown did not affect thapsigargin- or OAG-stimulated SRCE. The finding that suppression of a single endogenous TRPC in myometrial cells affected a specific type of SRCE response is further supported by our recent observation that suppression of expression of TRPC6 has very different effects [22].

We also observed an increase in ion channel activity after oxytocin stimulation in cell-attached patches on cells infected with empty adenoviral vector. This activity was observed in the presence of nifedipine, paxilline and TEA, suggesting that it was not due to nifedipine-sensitive L-type channels or BK_{Ca} channels. Importantly, oxytocin-stimulated channel activity was markedly inhibited by expression of TC4sh1. This observation adds further support to the contention that TRPC4 plays an important role in oxytocin-mediated SRCE.

The effects of endogenous TRPC4 knockdown in myometrial cells are similar in some respects but not others to effects noted in other studies. TRPC4 antisense as well as TRPC4 siRNA constructs inhibited both GPCR- and OAG-stimulated but not thapsigargin-stimulated Sr^{2+} or Ba^{2+} entry in HEK cells expressing endogenous TRPCs [23;24]. In contrast, no effect of TRPC4 knockdown on methacholine-mediated increases in $[Ca^{2+}]_i$ in HEK293 cells was noted [25]. HEK cells have a very different TRPC profile than myometrial cells, and endogenous channel composition may be quite different. The specific effect of TRPC4 knockdown on GPCR-stimulated SRCE suggests that tetrameric channels in myometrial cells that contain a significant proportion of TRPC4 may be affected by activation of the GPCRs tested, either as a result of direct interactions, signalplex organization or possibly as a result of co-localization in membrane subdomains. TRPC channels can assemble into signaling complexes containing proteins such as caveolin-1, $G_{\alpha q/11}$ and PLCB3 [26]. TRPC4 and TRPC5 also contain multiple binding motifs and domains (CaM, CIRB, protein 4.1-, PDZ, and auto-inhibitory) that may contribute to interaction with other proteins as well as to regulation of activity [27].

The most obvious interpretation for our data is that endogenous TRPC4 is primarily responsible for GPCR-stimulated SRCE response in myometrial cells. Alternatively, TRPC4 has been reported to enhance the localization of TRPC1 in the plasma membrane [12;13]. However, since no changes in plasma membrane expression of TRPC1 in response to a TRPC4 knockdown were detected, it is unlikely that TRPC4 knockdown disrupts GPCR-mediated SRCE indirectly by reducing TPRC1 concentration at the cell surface in myometrium. While we cannot totally rule out contributions by other TRPC channels expressed at significantly lower mRNA levels, it seems less likely that these TRPCs would significantly contribute to formation of heterotetrameric channels involved in the TRPC4-sensitive parameters measured here. Although TRPC4 knockdown did not affect PMCA or SERCA pump mRNA, the possibility that changes in expression or activity of these proteins may affect the dynamics of the $[Ca^{2+}]_i$ transients cannot be excluded.

The activation of the SRCE response by GPCRs in myometrial cells appears to be largely dependent on phospholipase C activation [9;10]. Capacitative or receptor- and store-operated Ca^{2+} entry have been postulated to involve IP_3-R activation, conformation coupling mechanisms, or signals generated by release of Ca^{2+} from intracellular stores [28]. Alternatively, phosphatidylinositol bisphosphate (PIP_2) may exert an inhibitory effect on TRPC4 and TRPC5 which is relieved by the GPCR-mediated degradation of PIP_2 by phospholipase C, resulting in channel activation [29].

Studies in $TRPC4^{-/-}$ mice implicate TRPC4 in agonist-induced Ca^{2+} entry [30]. Ca^{2+} entry induced by thrombin was significantly diminished in aortic and lung vascular endothelial cells isolated from $TRPC4^{-/-}$ mice, leading to impaired regulation of vascular

tone and permeability. Interestingly, the TPRC6 mRNA PCR product [31] appears to be more intense in TRPC4$^{-/-}$ compared to wild-type mice. Primary aorta endothelial cells isolated from TRPC4$^{-/-}$ mice exhibited diminished Ca^{2+} entry stimulated by SERCA inhibition [30].

In the present study, OAG-mediated SRCE, which we have previously shown to be protein kinase C-independent [11], was not significantly affected by TRPC4 knockdown. In contrast, TRPC4 knockdown attenuated OAG-stimulated Ba^{2+} entry in HEK-293 cells [24]. Other studies have shown a negative regulatory effect of diacylglycerol on overexpressed TRPC4 and TRPC5 activation mediated by protein kinase C in DT40 B-cells [32]. In myometrial cells, TRPC4 may not be a major contributor to the overall OAG response if OAG exerts an inhibitory effect. GPCR-mediated SRCE was never completely inhibited by TRPC4 knockdown, however, leaving open the possibility that a portion of the SRCE response to GPCRs might involve activation of other TRPCs as a result of localized GPCR-stimulated diacylglycerol production.

The data presented here support our hypothesis that specific signals can affect specific types of signal-regulated Ca^{2+} entry in the myometrium. This work increases our understanding of the regulation of Ca^{2+} dynamics in myometrial cells and points to a specific role for TRPC4 in GPCR-regulated myometrial Ca^{2+} dynamics.

References

1. Word RA, Tang DC, Kamm KE. Activation properties of myosin light chain kinase during contraction/relaxation cycles of tonic and phasic smooth muscles. *J Biol Chem* **1994**; 269**:** 21596-21602.

2. Parekh AB, Putney JW, Jr. Store-operated calcium channels. *Physiol Rev* **2005**; 85: 757-810.

3. Ramsey IS, Delling M, Clapham DE. An introduction to TRP channels. *Annu Rev Physiol* **2006**; 68: 619-647.

4. Yang M, Gupta A, Shlykov SG, Corrigan R, Tsujimoto S, Sanborn BM. Multiple Trp isoforms implicated in capacitative calcium entry are expressed in human pregnant myometrium and myometrial cells. *Biol Reprod* **2002**; 67: 988-994.

5. Dalrymple A, Slater DM, Beech D, Poston L, Tribe RM. Molecular identification and localization of Trp homologues, putative calcium channels, in pregnant human uterus. *Mol Hum Reprod* **2002**; 8: 946-951.

6. Dalrymple A, Slater DM, Poston L, Tribe RM. Physiological induction of transient receptor potential canonical proteins, calcium entry channels, in human myometrium: influence of pregnancy, labor, and interleukin-1 beta. *J Clin Endocrinol Metab* **2004**; 89: 1291-1300.

7. Ku CY, Babich L, Word RA et al. Expression of transient receptor channel proteins in human fundal myometrium in pregnancy. *J Soc Gynecol Investig* **2006**; 13: 217-225.

8. Monga M, Ku CY, Dodge K, Sanborn BM. Oxytocin-stimulated responses in a pregnant human immortalized myometrial cell line. *Biol Reprod* **1996**; 55: 427-432.

9. Monga M, Campbell DF, Sanborn BM. Oxytocin-stimulated capacitative calcium entry in human myometrial cells. *Am J Obstet Gynecol* **1999**; 181**:** 424-429.

10. Shlykov SG, Yang M, Alcorn JL, Sanborn BM. Capacitative cation entry in human myometrial cells and augmentation by hTrpC3 overexpression. *Biol Reprod* **2003**; 69**:** 647-655.

11. Shlykov SG, Sanborn BM. Stimulation of intracellular Ca2+ oscillations by diacylglycerol in human myometrial cells. *Cell Calcium* **2004**; 36**:** 157-164.

12. Hofmann T, Schaefer M, Schultz G, Gudermann T. Subunit composition of mammalian transient receptor potential channels in living cells. *Proc Natl Acad Sci U S A* **2002**; 99**:** 7461-7466.

13. Alfonso S, Benito O, Alicia S et al. Regulation of the cellular localization and function of human transient receptor potential channel 1 by other members of the TRPC family. *Cell Calcium* **2008**; 43**:** 375-387.

14. Zhou XB LSSFKMWT. Oxytocin receptors differentially signal via Gq and Gi proteins in pregnant and nonpregnant rat uterine myocytes: implications for myometrial contractility. *Molecular Endocrinology* **2007**; 21**:** 740-752.

15. Dalrymple A, Mahn K, Poston L, Songu-Mize E, Tribe RM. Mechanical stretch regulates TRPC expression and calcium entry in human myometrial smooth muscle cells. *Mol Hum Reprod* **2007**; 13**:** 171-179.

16. Arts GJ, Langemeijer E, Tissingh R et al. Adenoviral vectors expressing siRNAs for discovery and validation of gene function. *Genome Res* **2003**; 13**:** 2325-2332.

17. Jones RJ, Jourd'heuil D, Salerno JC, Smith SM, Singer HA. iNOS regulation by calcium/calmodulin-dependent protein kinase II in vascular smooth muscle. *Am J Physiol Heart Circ Physiol* **2007**; 292**:** H2634-H2642.

18. Wickham TJ, Segal DM, Roelvink PW et al. Targeted adenovirus gene transfer to endothelial and smooth muscle cells by using bispecific antibodies. *J Virol* **1996**; 70**:** 6831-6838.

19. Anwer K, Sanborn BM. Changes in intracellular free calcium in isolated myometrial cells: role of extracellular and intracellular calcium and possible involvement of guanine nucleotide-sensitive proteins. *Endocrinology* **1989**; 124**:** 17-23.

20. Burghardt RC, Barhoumi R, Sanborn BM, Andersen J. Oxytocin-induced Ca2+ responses in human myometrial cells. *Biol Reprod* **1999**; 60**:** 777-782.

21. Challis JRG, Matthews SG, Gibb W, Lye SJ. Endocrine and paracrine regulation of birth at term and preterm. *Endocr Rev* **2000**; 21**:** 514-550.

22. Chung D, Kim YS, Phillips JN et al. Attenuation of canonical transient receptor potential-like channel 6 expression specifically reduces the diacylglycerol-mediated increase in intracellular calcium in human myometrial cells. *Endocrinology* **2010**; 151**:** 406-416.

23. Wu X, Babnigg G, Zagranichnaya T, Villereal ML. The role of endogenous human Trp4 in regulating carbachol-induced calcium oscillations in HEK-293 cells. *J Biol Chem* **2002**; 277**:** 13597-13608.

24. Zagranichnaya TK, Wu X, Villereal ML. Endogenous TRPC1, TRPC3, and TRPC7 proteins combine to form native store-operated channels in HEK-293 cells. *J Biol Chem* **2005**; 280**:** 29559-29569.

25. Wedel B, Boyles RR, Putney JW, Jr., Bird GS. Role of the store-operated calcium entry proteins Stim1 and Orai1 in muscarinic cholinergic receptor-stimulated calcium oscillations in human embryonic kidney cells. *J Physiol* **2007**; 579**:** 679-689.

26. Ambudkar IS, Bandyopadhyay BC, Liu X, Lockwich TP, Paria B, Ong HL. Functional organization of TRPC-Ca2+ channels and regulation of calcium microdomains. *Cell Calcium* **2006**; 40**:** 495-504.

27. Plant TD, Schaefer M. Receptor-operated cation channels formed by TRPC4 and TRPC5. *Naunyn Schmiedebergs Arch Pharmacol* **2005**; 371**:** 266-276.

28. Putney JW, Jr. Recent breakthroughs in the molecular mechanism of capacitative calcium entry (with thoughts on how we got here). *Cell Calcium* **2007**; 42**:** 103-110.

29. Putney JW, Jr. Inositol lipids and TRPC channel activation. *Biochem Soc Symp* **2007**; 37-45.

30. Freichel M, Vennekens R, Olausson J et al. Functional role of TRPC proteins in native systems: implications from knockout and knock-down studies. *J Physiol* **2005**; 567**:** 59-66.

31. Tiruppathi C, Freichel M, Vogel SM et al. Impairment of store-operated Ca2+ entry in TRPC4(-/-) mice interferes with increase in lung microvascular permeability. *Circ Res* **2002**; 91**:** 70-76.

32. Venkatachalam K, Zheng F, Gill DL. Control of TRPC and store-operated channels by protein kinase C. *Novartis Found Symp* **2004**; 258**:** 172-185.

CHAPTER 5

TRPC1 and TRPC4 regulate intracellular calcium dynamics in a different manner than STIM1 in human myometrial cells

5.1 Introduction

The previous chapter analyzed the role of TRPC4, the most abundant TRPC in human myometrium, on SRCE through knockdown mechanisms using shRNA constructs. These studies implicated TRPC4 in G protein-coupled receptor-stimulated Ca^{2+} entry. This appeared to be a specific role for TRPC4 as other SRCE mechanisms studied, such as thapsigargin- and OAG-stimulated Ca^{2+} entry, displayed no changes after a TRPC4 knockdown.

TRPC1 is the second most abundant TRPC in the human myometrium. Studies involving TRPC1 overexpression have provided valuable yet contradictory data as to the role for TRPC1 in intracellular Ca^{2+} dynamics. Attenuation of TRPC1 expression/activity results in reduction of store-operated Ca^{2+} entry [1-7]. TRPC4 and

TRPC1 have been suggested to form heterotetramer channels possessing biological properties distinct from those observed in their homotetramer counterparts. [8]. Additional TRPC channel regulation can also be provided by the STIM1 and Orai1 proteins [9]. Studies have shown that knockdown of TRPC1 and TRPC4 can transform other TRPC channel activity from being STIM1-dependent to being STIM1-independent [10]. In a similar fashion, individual knockdown of TRPC1 and TRPC4 may result in changes on different Ca^{2+} entry mechanisms from the mechanisms affected by inducing the combined knockdown of TRPC1 plus TRPC4 in myometrial cells. This was achieved through the tandem expression of shRNAs targeting TRPC1, TRPC4, or TRPC1 plus TRPC4 using the pAdT-CMR adenoviral vector. This vector provided the ability to infect cells with a single adenovirus to obtain single or multiple TRPC knockdowns. The role of STIM1 in myometrial Ca^{2+} dynamics was also investigated by use of a STIM1ΔERM construct. This is a dominant negative form of STIM1 which is incapable of interacting with TRPCs [11].

The data obtained in this study suggest that both TRPC1 and TRPC4 are activated by similar G protein-coupled receptor-stimulated Ca^{2+} entry mechanisms and that no additive effects were observed by their combined knockdown. Additionally, thapsigargin- and OAG-stimulated Ca^{2+} entry are not affected by either the individual or combined knockdown of TRPC1 and TRPC4. In contrast, STIMΔERM appeared to induce an inhibitory effect on all three types of SRCE stimulation.

5.2 Results

5.2.1 Effective single and double knockdown of TRPC1 and TRPC4 through expression of single and tandem shRNAs

Study of endogenous TRPC1 and TRPC4 was achieved using TRPC1 and TRPC4 shRNA constructs. The TRPC4 shRNA sequence used in the present study (TC4sh) is the same as that specified in Chapter 4, except its ends have been changed for efficient cloning into the pAdT-CMR vector (Table 2). The sequences for the TRPC1 shRNA constructs are specified in Table 2. TRPC1 sequences were tested using the psiCHECK-2 system for their ability to suppress a Renilla luciferase TRPC1 fusion reporter vector (psiTC1), as previously described in Materials and Methods. In the pSHAG assay the TRPC1 shRNA constructs induced 76-92% knockdown in Renilla luciferase protein expression compared to empty vector, a scrambled TRPC4 shRNA (shx1) and a TRPC4 shRNA construct (TC4sh1) (Fig. 5.1).

Adenoviral particles were used to infect the specified human myometrial cells expressing either three copies of TC1sh, TC4sh or Rnllash as well as an adenovirus expressing a single copy of each TC1sh, TC4sh and Rnllash (creating the TC1+4sh) were used to infect UtSMC myometrial cells. Effectiveness of these CMR adenoviral constructs was tested along with constructs used in the study described in Chapter 4. TRPC4 mRNA knockdowns were measured and compared in UtSMC cells expressing a single TC4sh1 sequence under a U6 promoter (U6-TC4sh1), along with cells expressing one (CMV-TC4sh1X1), three (CMV-TC4sh1X3) or six (CMV-TC4sh1X6) copies of TC4sh1 sequence under a CMV promoter (Fig. 5.2). Figure 5.3 shows that expression of CMV-TC4sh1X3 and CMV-TC4sh1X6 constructs induced a greater TRPC4 mRNA

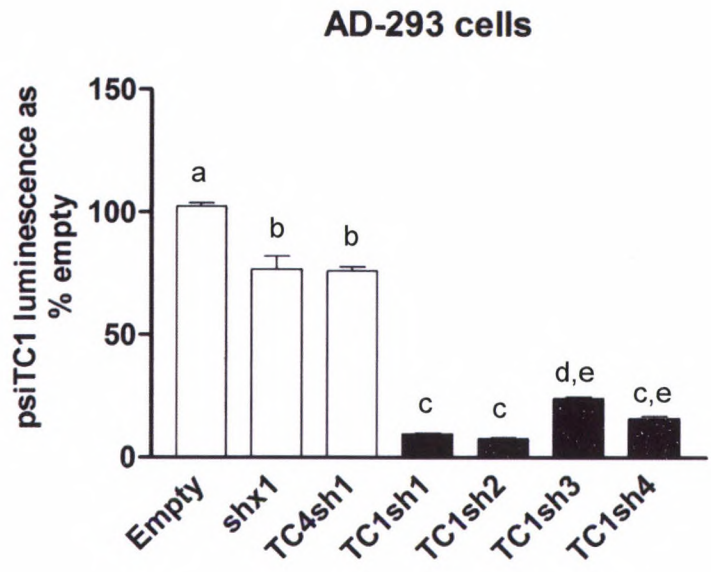

Fig. 5.1. TRPC1-reporter mRNA is suppressed by TRPC1-shRNA constructs in AD-293 cells. Significant suppression of luminescence from a Renilla luciferase-TRPC1 fusion reporter (psiTC1) following co-transfection of the reporter and plasmids expressing TRPC1 shRNAs (TC1sh1-4) in AD-293 cells as described in Methods. Controls include empty vector, scrambled shRNA (shx1) and TRPC4 shRNA (TC4sh1). Data are expressed as % of luminescence exhibited by co-transfection of empty vector and represent mean ± S.E.M. (n=3). Data were analyzed by one-way ANOVA and Tukey's test. Significant differences between groups ($p<0.05$) are indicated by different lowercase letters.

knockdown (76% and 92%, respectively) than that obtained with the expression of one copy of TC4sh1 under either the U6 or the CMV promoter (54% and 69%, respectively). mRNAs of other TRPCs displayed no changes in expression using this tandem shRNA expression system (Fig. 5.3). It is important to note that the strength offered by this

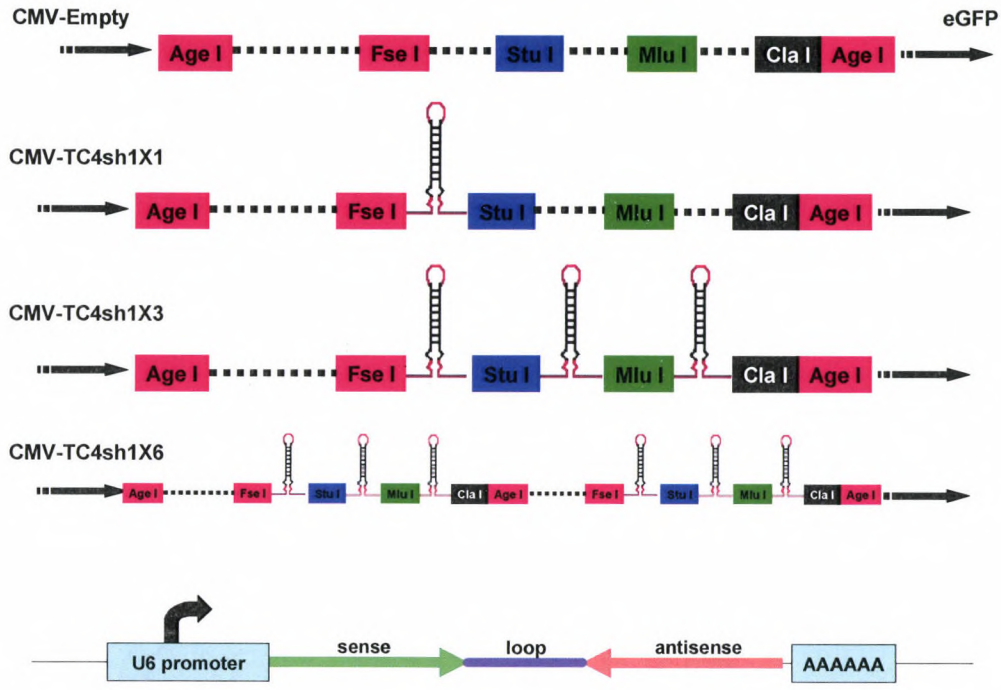

Fig. 5.2. Schematic representation of constructs used for comparing the effectiveness of the TRPC4-shRNA#1 construct expressed from different promoters in Figure 5.3. A single (CMV-TC4sh1X1), three (CMV-TC4sh1X3) or six (CMV-TC4sh1X6) copies of TC4sh1were expressed in tandem from a CMV promoter using the pAdT-MCS vector. Constructs were tested along a single copy of TC4sh1 expressed from a U6 promoter using the pSHAG vector for comparing the level of TRPC4 mRNA knockdown induced by each construct relative to that of U6-Empty vector.

tandem shRNA expression system is suggested to be due to the number of shRNA constructs processed by the RNAi machinery (i.e., one shRNA construct versus three shRNA constructs versus six shRNA constructs) and not due to the specific number of

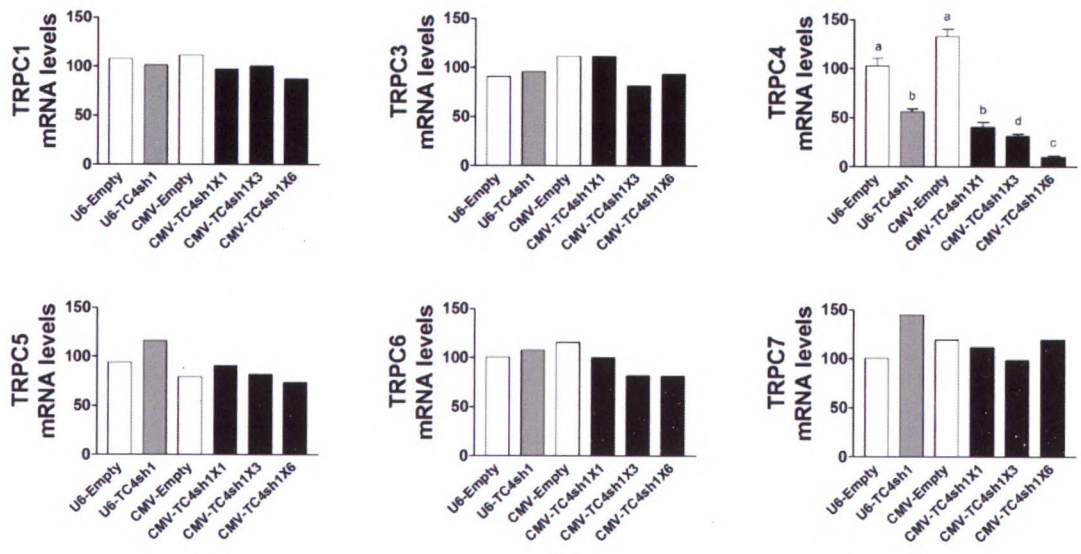

Fig. 5.3. Adenoviral expression of tandem TC4sh1 constructs produced a stronger and specific TRPC4 mRNA knockdown in UtSMC cells than that obtained from the single expression of TC4sh1. TC4sh1 was cloned into pAdT-MCS for expression of a one (CMV-TC4sh1X1), three (CMV-TC4sh1X3), or six (CMV-TC4sh1X6) shRNA constructs from a single adenoviral vector. TRPC4 mRNA knockdown was determined and compared to effects of empty pAdT-MCS vector (CMV-Empty). Knockdowns were also compared to previously used adenoviral vectors such as empty (U6-Empty) and TC4sh1 expressed under a U6 promoter (U6-TC4sh1). mRNA levels of other TRPCs were unchanged by exposure to any of these viral constructs. mRNA was normalized to GUS in the same sample and expressed relative to the value in cells exposed to U6-Empty vector. Data represent the mean ± S.E.M. (n=3 for TRPC4); significant differences between groups ($p<0.05$), as analyzed by one-way ANOVA and Tukey's test, are indicated by different lowercase letters. (n=2 for other TRPCs).

copies of the same shRNA targeting the same protein (i.e., having three copies of TC4sh1) (Fig. 5.4) [12].

Infection of UtSMC cells with adenoviral vectors expressing tandem TC1sh constructs induced a 57% TRPC1 mRNA knockdown without affecting TRPC4 mRNA levels when compared to cells infected with shRNA targeting Renilla luciferase (Rnllash) (Fig. 5.5, left). Similarly, tandem expression of TC4sh constructs induced a 75% TRPC4 mRNA knockdown while the TRPC1 mRNA levels were not strongly affected (Fig. 5.5 right). The TC1+4sh construct induced a double knockdown of TRPC1 plus TRPC4 (61% and 48%, respectively) (Fig. 5.5). Hence the use of these adenoviral vectors for the tandem expression of shRNA constructs proved effective at inducing single as well as double knockdowns of TRPC1 and TRPC4. Thus, this method allows for the knockdown of various mRNAs using a single adenovirus. This system is especially helpful when working with systems that prove difficult to transfect and/or infect such as the UtSMC and PHM1-41 cells used in the present study. Furthermore, knocking down multiple mRNAs with one virus eliminates the requirement for multiple infections of the same cells and associated ambiguities.

5.2.2 TRPC1 and TRPC4 share a role in G protein-coupled receptor-stimulated calcium entry

The role of TRPC4 in human myometrial cells on SRCE in response to various stimuli was analyzed in a previous study (Chapter 4). To ensure that the new viral system rendered similar results, TRPC4 knockdown studies were conducted in addition to examining the effects resulting from a TRPC1 knockdown on SRCE.

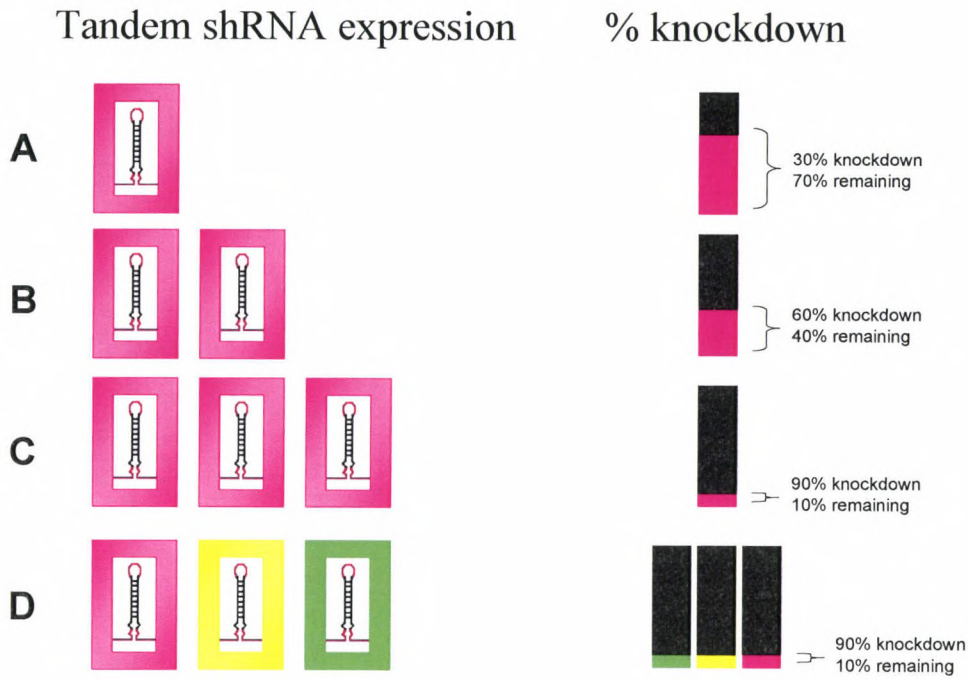

Fig. 5.4. Schematic representation of the effect obtained from the tandem expression of shRNA constructs. Increased "pink protein" knockdown levels are observed as the number of shRNAs expressed increases. That is, three shRNAs result in a better knockdown than two shRNAs (compare C and B). Two shRNAs result in a better knockdown than a single shRNA (compare B and A). Notice that the same level of knockdown for "protein pink" is achieved in C and D as long as the same number of shRNAs is expressed. That is, as long as a total of three shRNA constructs are expressed in each case, the specific number for the same pink-shRNA (three copies of pink-shRNA in C versus a single copy of pink-shRNA in D) becomes irrelevant. This is because the observed increase in effectiveness is provided by the tandem expression of the shRNA constructs which results in greater processivity, rather than by the increase in copy number for a specific shRNA.

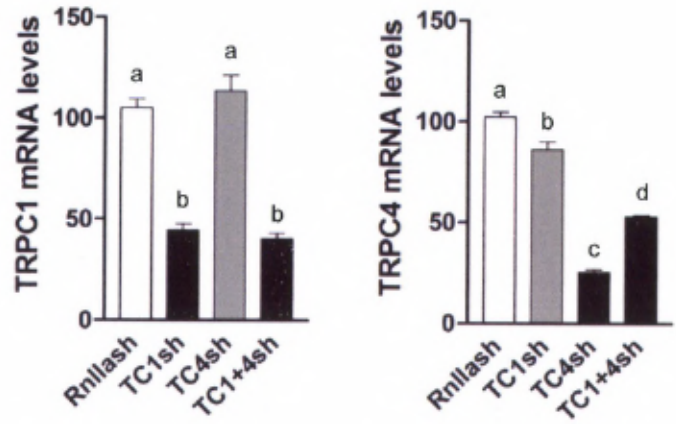

Fig. 5.5. Specific TRPC mRNA knockdowns produced by adenovirus vector expressing tandem TC1sh, TC4sh and TC1+4sh in UtSMC cells. *Left.* TRPC1 mRNA knockdown was obtained by tandem expression of TC1sh and TC1+4sh compared to effects of control shRNA (Rnllash) and TC4sh. *Right.* Tandem expression of TC4sh and TC1+4sh induced a TRPC4 mRNA knockdown when compared to Rnllash and TC1sh. mRNA was normalized to GUS in the same sample and expressed relative to the value in cells exposed to empty vector. In all cases, data represent the mean ± S.E.M. (n=4); significant differences between groups ($p<0.05$), as analyzed by one-way ANOVA and Tukey's test, are indicated by different lowercase letters.

UtSMC cells were infected with a single adenovirus expressing either Rnllash (control), TC1sh, or TC4sh constructs for the study of their single and specific knockdown effects on SRCE. Cells infected with the control shRNA (Rnllash) were stimulated in Ca^{2+}-free buffer with oxytocin, a GPCR-activator resulting in IP_3 generation, eliciting a transient increase in $[Ca^{2+}]_i$. Once $[Ca^{2+}]_i$ returned to basal levels, 1 mM extracellular Ca^{2+} was added and oxytocin-stimulated SRCE was observed, as

indicated by a second, extracellular Ca^{2+}-dependent increase in $[Ca^{2+}]_i$ (Fig. 5.6, blue line). In contrast, expression of TC1sh resulted in a significant decrease of oxytocin-stimulated SRCE (Fig. 5.6, green line). An overall inhibition of 41% and 56% of the $[Ca^{2+}]_i$ transient area and peak height, respectively, was produced by TC1sh (Fig. 5.6, green bars).

Similar to the results obtained in Chapter 4 with the U6-promoter virus, inhibition of oxytocin-stimulated SRCE was observed in cells expressing TC4sh through this new system (Fig. 5.6, red line). This construct induced a 38% and 45% inhibition of the $[Ca^{2+}]_i$ transient area and peak height, respectively (Fig. 5.6, red bars) These data suggest that TRPC1 and TRPC4 share a similar role, by aiding in regulation of calcium entry stimulated by G protein-coupled receptor activation. Similar experiments were also performed in PHM1-41 cells and comparable inhibitory effects of TRPC1 and TRPC4 knockdowns on oxytocin-stimulated SRCE inhibition were observed (Fig. 5.7).

5.2.3 Stimulation of calcium entry through thapsigargin or diacylglycerol does not involve TRPC1

The potential regulation of calcium entry by TRPC1 induced by store-depletion through treatment with thapsigargin, an endoplasmic-reticulum Ca^{2+}-ATPase blocker, was also analyzed. Stimulation of infected cells with thapsigargin in the absence of extracellular calcium displayed a slow and gradual increase in $[Ca^{2+}]_i$. Thapsigargin-stimulated SRCE was not affected by a TRPC1 knockdown (Fig. 5.8A, green line). As previously observed with the U6-construct, expression of TC4sh1 also had no significant effect on thapsigargin-stimulated calcium entry (Fig. 5.8A, red line). Additionally, elevation of $[Ca^{2+}]_i$ elicited in the presence of extracellular Ca^{2+} by OAG, a cell

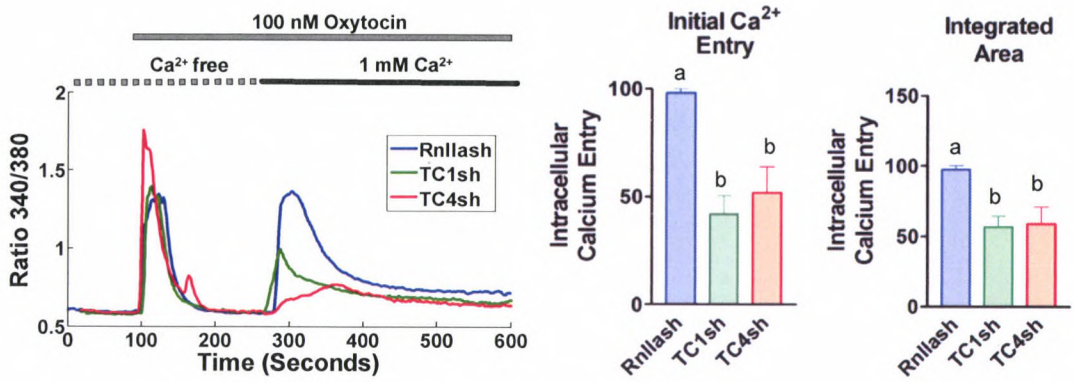

Fig 5.6. Oxytocin signal-regulated calcium entry (SRCE) is significantly attenuated by knockdown of TRPC1 and knockdown of TRPC4 in UtSMC cells. *Left.* SRCE induced by 100 nM oxytocin in UtSMC cells infected with either control adenovirus (Rnllash, blue line), adenovirus expressing TC1sh (green line) or adenovirus expressing TC4sh (red line) for >72 h (10-25 cells per experiment). *Right.* Mean ± S.E.M. of changes in $[Ca^{2+}]_i$ resulting from addition of 1 mM extracellular Ca^{2+} (SRCE), calculated as area under the curve (integrated area) and by peak height (initial calcium entry). Data are presented as mean ± S.E.M. (n=5); significant differences between groups ($p<0.05$), as analyzed by one-way ANOVA and Tukey's test, are indicated by different lowercase letters.

permeable diacylglycerol, displayed no significant changes with either TRPC1 or TRPC4 knockdown (Fig. 5.8B, green and red line, respectively). Similar responses were also found in PHM1-41 cells when treated with these adenoviral constructs (Fig. 5.9).

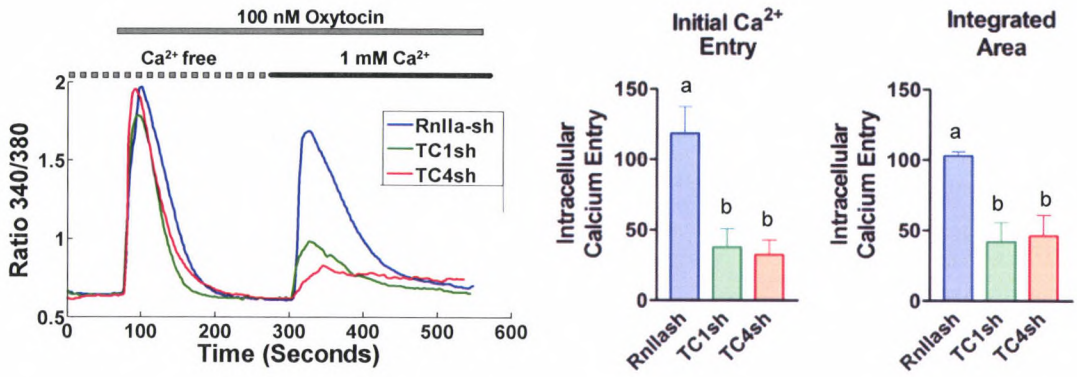

Fig. 5.7. Inhibition of oxytocin-stimulated SRCE in PHM1 cells by knockdown of either TRPC1 or TRPC4. *Left.* SRCE induced by 100 nM oxytocin in PHM1 cells infected for >72 h with control vector (RnIIash, blue line), adenovirus expressing TC1sh (green line), or adenovirus expressing TC4sh (red line) (n= 10-25 cells). *Right.* Mean changes in $[Ca^{2+}]_i$ resulting from addition of 1 mM extracellular Ca^{2+} (SRCE). TC1sh induced a 61% and 81% inhibition of the $[Ca^{2+}]_i$ transient area (integrated area) and peak height (initial calcium entry), respectively. TC4sh induced a 56% and 86% inhibition of the $[Ca^{2+}]_i$ transient area (integrated area) and peak height (initial calcium entry), respectively. Data are presented as mean ± S.E.M. (n=3); significant differences between groups ($p<0.05$), as analyzed by one-way ANOVA and Tukey's test, are indicated by different lowercase letters.

5.2.4 Dual knockdown of TRPC1 plus TRPC4 display no additive effects on SRCE mechanisms

In an effort to determine if combined TRPC1 plus TRPC4 knockdowns would produce an even stronger inhibition of calcium entry after oxytocin stimulation, UtSMC

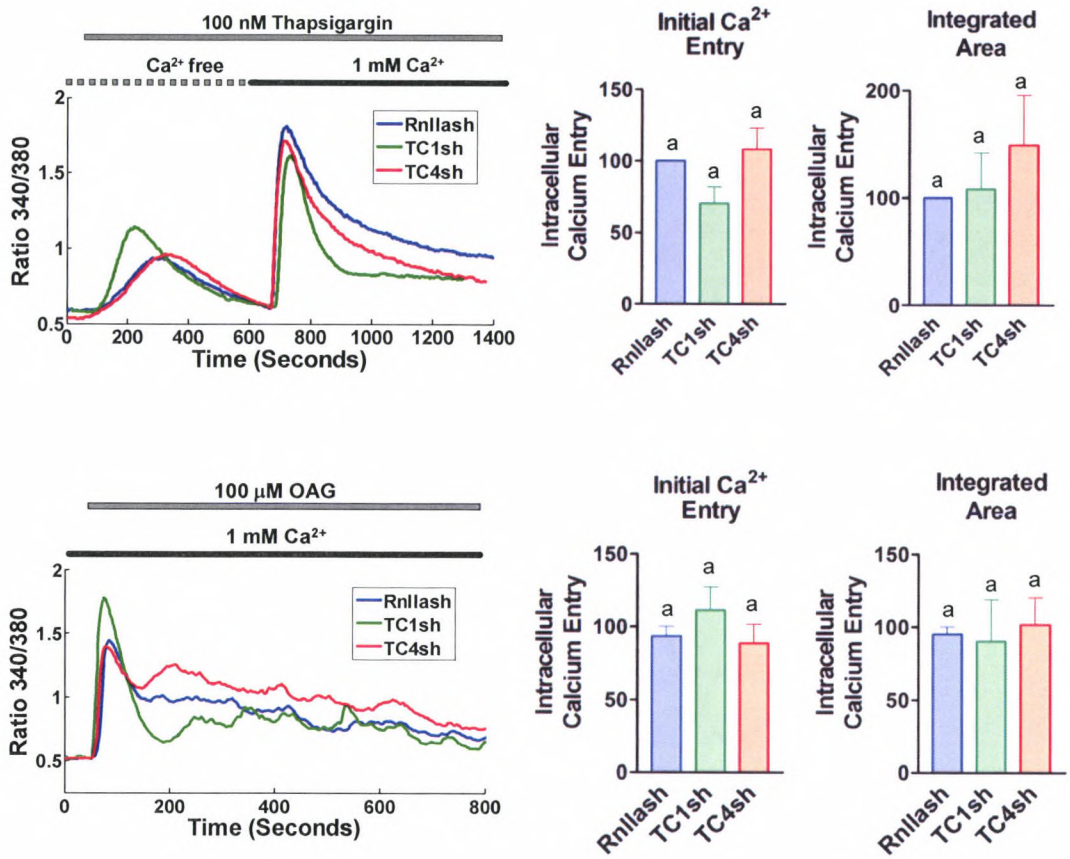

Fig. 5.8. Lack of effect of either TRPC1 or TRPC4 knockdown on thapsigargin- and OAG-stimulated SRCE in UtSMC cells. *Left.* SRCE induced by either (A) 100 nM thapsigargin and (B) 100 μM OAG in UtSMC cells infected with Rnllash adenovirus (blue lines) and cells infected with virus expressing TC1sh (green lines) or TC4sh (red lines). *Right:* Mean changes in $[Ca^{2+}]_i$ resulting from addition of 1 mM extracellular Ca^{2+} (SRCE), calculated as area under the curve (integrated area) and peak height (initial calcium entry) (n=20-35 cells). Data are presented as mean ± S.E.M. (n=5); significant differences between groups ($p<0.05$), as analyzed by one-way ANOVA and Tukey's test, are indicated by different lowercase letters.

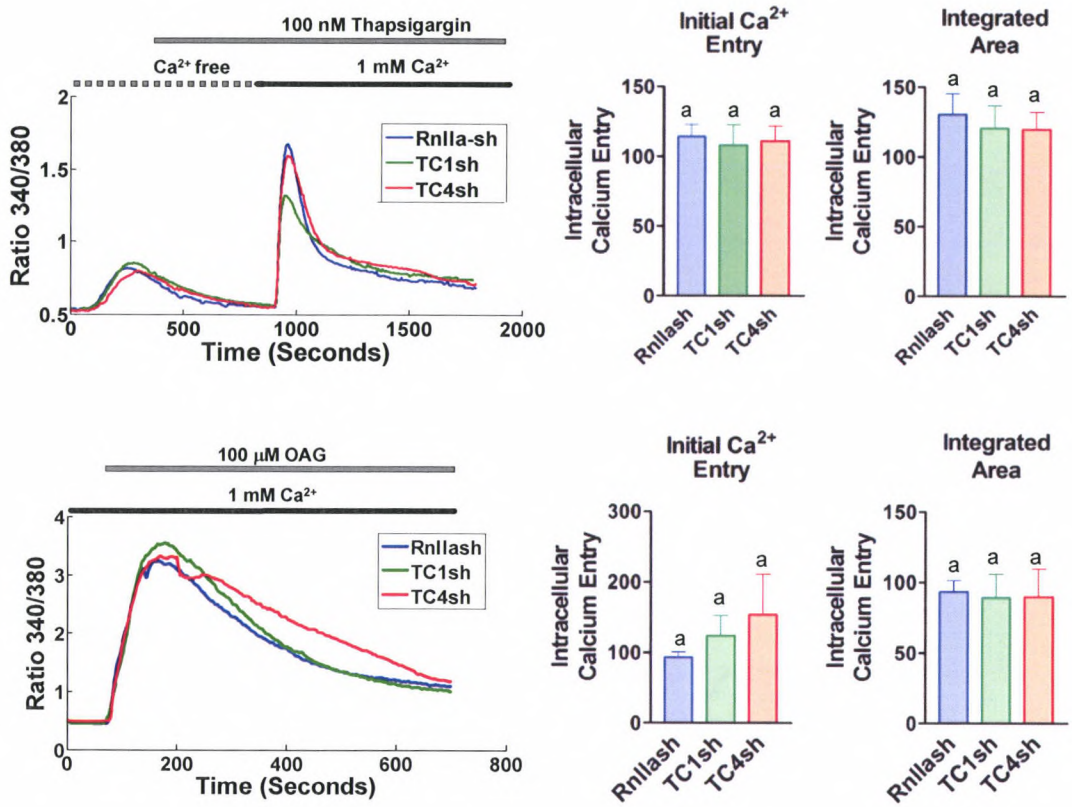

Fig.5.9. TRPC1 knockdown and TRPC4 knockdown induced no changes on thapsigargin- and OAG-stimulated SRCE in PHM1 cells. *Left.* SRCE induced by either (A) 100 nM thapsigargin and (B) 100 μM OAG in PHM1 cells infected with RnIIash adenovirus (blue lines) and cells infected with virus expressing TC1sh (green lines), or TC4sh1 (red lines). *Right:* Mean changes in $[Ca^{2+}]_i$ resulting from addition of 1 mM extracellular Ca^{2+} (SRCE), calculated as area under the curve (integrated area) and peak height (initial calcium entry) (n=20-35 cells). Data are presented as mean ± S.E.M. (n=10 for thapsigargin and n=5 for OAG); significant differences between groups ($p<0.05$), as analyzed by one-way ANOVA and Tukey's test, are indicated by different lowercase letters.

and PHM1 cells were infected with the virus expressing both TC1sh and TC4sh (TC1+4sh). Simultaneous knockdown of both TRPC1 and TRPC4 in the same cell induced a specific decrease on oxytocin-stimulated calcium entry (Fig. 5.10A). Interestingly, this inhibition was not significantly greater than that obtained after knockdown of either TRPC1 or TRPC4 alone. Furthermore, a TRPC1 plus TRPC4 knockdown showed no significant changes in thapsigargin-stimulated calcium entry (Fig. 5.10B) or OAG-stimulated calcium entry (Fig. 5.10C). Thus, TRPC1 and TRPC4 have a specific role in G protein-coupled receptor-stimulated SRCE in human myometrial cells. This role on SRCE seems to be dependent on the coexpression of TRPC1 and TRPC4 since their double knockdown shows no additive effects on oxytocin-stimulated SRCE from their single knockdown counterparts.

5.2.5 A dominant negative form of STIM1 affects G protein-coupled receptor-stimulated calcium entry through a potentially different mechanism than TRPC1 and TRPC4

Thapsigargin-stimulated SRCE was not affected by knockdown of TRPC1, TRPC4 or by TRPC6 [13]. In contrast, the STIM/Orai complex has been implicated in store depletion-operated calcium entry [9;14], which might be operable in myometrial cells. The laboratory has determined that both STIM1 and Orai1 mRNAs are expressed in PHM1 cells (Phillips and Sanborn, unpublished observations). To study the roles of STIM1 on SRCE in the human myometrium, a dominant negative form of STIM1, namely STIM1ΔERM, was used. Overexpression of STIM1ΔERM, cloned into an adenoviral vector under a CMV promoter, affected calcium dynamics following oxytocin stimulation. Similar to responses obtained from TRPC1 and/or TRPC4 knockdowns,

Fig. 5.10. Specific TRPC1, TRPC4 and TRPC1 plus TRPC4 knockdown induces a specific inhibition of oxytocin-stimulated SRCE in UtSMC (left) and PHM1 (middle) cells while displaying a lack of effect on thapsigargin- and OAG-stimulated SRCE. (A) SRCE induced by 100 nM oxytocin in cells infected for >72 h with a control shRNA targeting Renilla-luciferase (Rnllash, blue lines) or adenovirus expressing TC1sh (green lines), TC4sh (red lines), or TRPC1 plus TRPC4 shRNAs (TC1+4sh, pink lines). SRCE induced by either (B) 100 nM thapsigargin and (C) 100 μM OAG (n=10-35 cells). *Right:* Mean changes in $[Ca^{2+}]_i$ resulting from addition of 1 mM extracellular Ca^{2+} (SRCE) in both UtSMC and PHM1 cells, calculated as area under the curve (integrated area) and peak height (initial calcium entry). Data are presented as mean ± S.E.M. (n=6 for oxytocin; n=8 for thapsigargin; n=12 for OAG); significant differences between groups ($p<0.05$), as analyzed by one-way ANOVA and Tukey's test, are indicated by different lowercase letters.

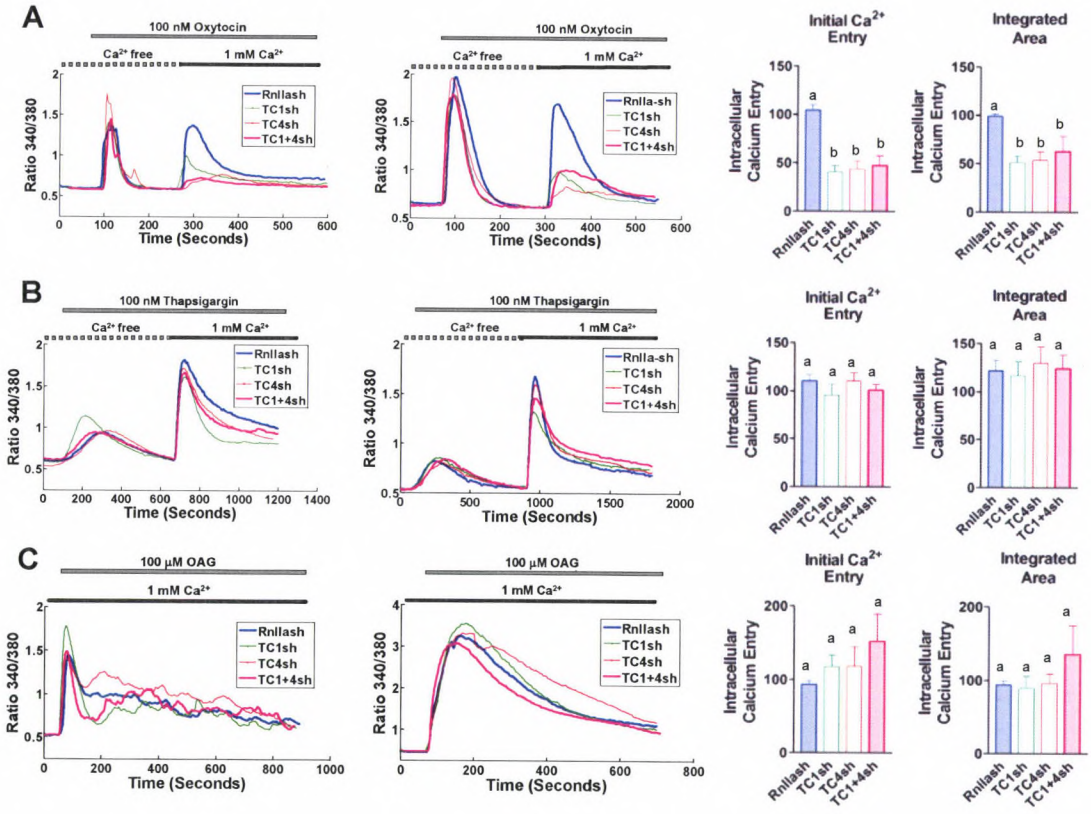
A
100 nM Oxytocin
Ca2+ free
1 mM Ca2+
Ratio 340/380
Time (Seconds)
RnIIash
TC1sh
TC4sh
TC1+4sh
RnIIa-sh
Initial Ca2+ Entry
Integrated Area
Intracellular Calcium Entry
B
100 nM Thapsigargin
C
100 µM OAG

STIM1ΔERM overexpression produced a significant decrease in SRCE elicited by oxytocin following extracellular Ca^{2+} administration (Fig. 5.11A). Effects observed were 70% and 61% inhibition of the $[Ca^{2+}]_i$ transient area and peak height, respectively when compared to those of control.

Further identification of potential additional roles for STIM1 on SRCE in the human myometrium was studied using thapsigargin to inhibit the endoplasmic reticulum Ca^{2+}-ATPase pump and deplete this store. Human myometrial cells expressing STIM1ΔERM stimulated with thapsigargin displayed an increase in $[Ca^{2+}]_i$ in the absence of extracellular Ca^{2+} (Fig. 5.11B). However, in contrast to the lack of effect of TRPC1 and TRPC4 on thapsigargin-stimulated calcium entry, a significant decrease in SRCE was observed after addition of extracellular Ca^{2+} in cells expressing the dominant negative STIM1 (Fig. 5.11B). STIM1ΔERM induced a 45% and 57% inhibition of the $[Ca^{2+}]_i$ transient area and peak height, respectively. These data suggest that STIM1 is involved in regulating intracellular Ca^{2+} dynamics after store-depletion through the action of thapsigargin.

Interestingly, stimulation of human myometrial cells expressing STIM1ΔERM with OAG in the presence of extracellular Ca^{2+} also induced an apparent inhibition in SRCE (Fig. 5.11C). A 32% and 57% inhibition of the $[Ca^{2+}]_i$ transient peak height and area are observed, respectively. Together, these data suggest that STIM1 may regulate $[Ca^{2+}]_i$ dynamics via pathways in addition to those involving TRPC1 and/or TRPC4.

Fig. 5.11. STIM1ΔERM significantly inhibits oxytocin and thapsigargin signal-regulated calcium entry (SRCE) while also inducing an apparent decrease in OAG-SRCE in UtSMC cells. *Left.* SRCE induced by (A) 100 nM oxytocin (B) 100 nM thapsigargin and (C) 100 μM OAG (n=10-15 cells). in UtSMC cells infected with either control adenovirus (Rnllash, solid line), adenovirus expressing STIMΔERM (dotted line) for >72 h (10-15 cells per experiment). *Right.* Mean ± S.E.M. of changes in $[Ca^{2+}]_i$ resulting from addition of 1 mM extracellular Ca^{2+} (SRCE), calculated as area under the curve (integrated area) and by peak height (initial calcium entry). Data are presented as mean ± S.E.M. (n=5 for oxytocin; n=7 for thapsigargin; n=2 for OAG) and were analyzed by t-test. In all cases, significant differences from Rnllash ($p<0.05$) are indicated by an asterisk (*).

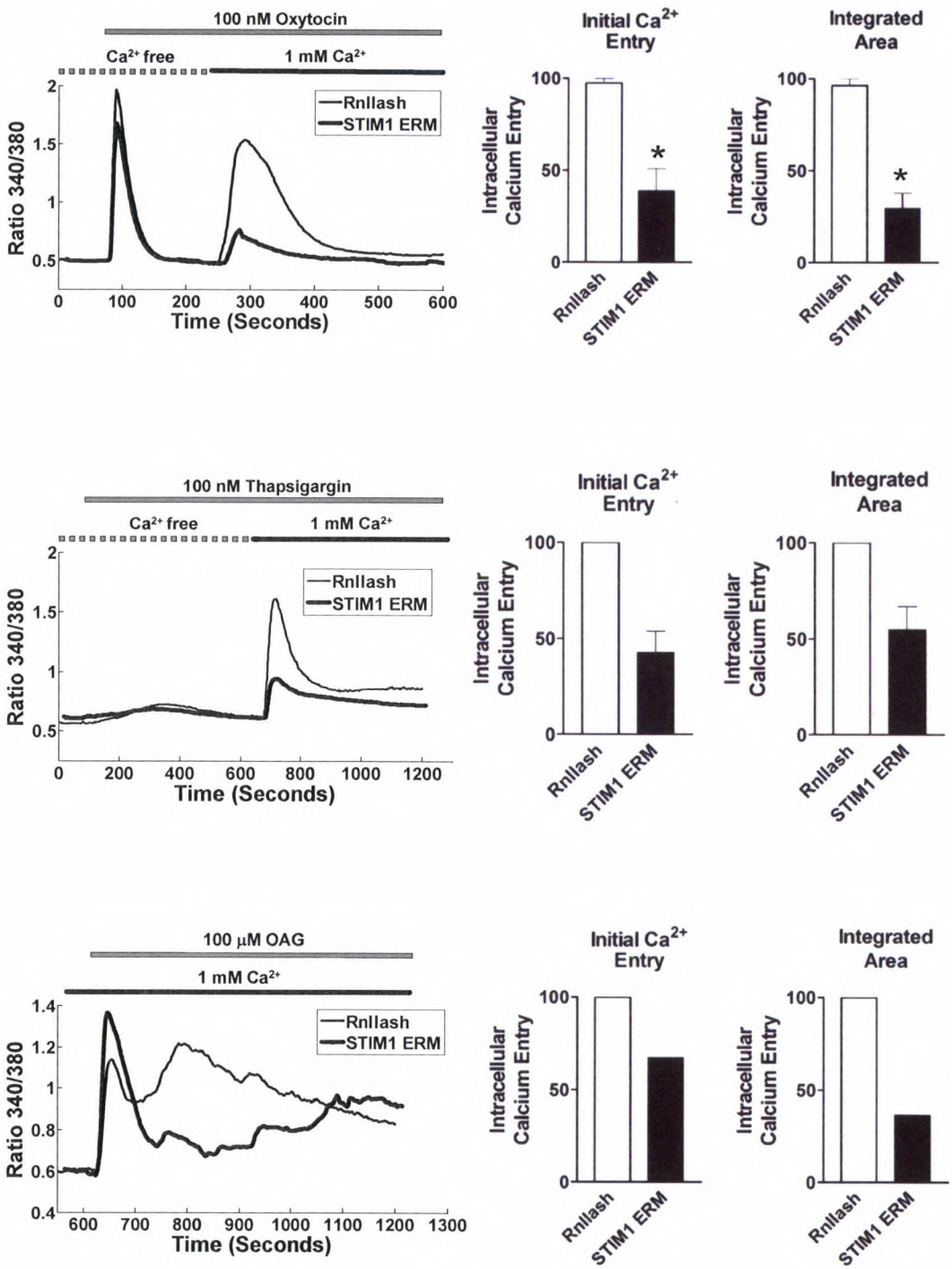
100 nM Oxytocin
Ca2+ free
1 mM Ca2+
RnIlash
STIM1 ERM
Ratio 340/380
Time (Seconds)
Initial Ca2+ Entry
Integrated Area
Intracellular Calcium Entry
100 nM Thapsigargin
100 μM OAG

5.3 Discussion

TRPC4 and TRPC1 are the two most abundant TRPC mRNAs in the human myometrium. Overexpression studies have been widely used for determination of the roles of TRPCs in intracellular Ca^{2+} dynamics. Potential risks arise from these types of studies, as the endogenous TRPC channels may be altered by the ectopic expression of a particular TRPC. Thus, our studies are centered on the effects that the individual TRPC1 and TRPC4 knockdowns had on SRCE mechanisms in human myometrial cells. Since these proteins are suggested to interact and form heterotetramers, the combined TRPC1 plus TRPC4 knockdown was also studied.

Based on a reporter assay screen, one shRNA was selected per respective TRPC protein to construct the TC1sh and TC4sh adenoviral expression vectors. Tandem expression of TRPC4-shRNA constructs under a CMV promoter proved effective at inducing stronger knockdowns than those observed by the single expression of the TRPC4-shRNA by either the U6 or CMV promoter. Additionally, levels of other TRPCs remained unchanged. Thus, adenoviral vectors Rnllash, TC1sh, TC4sh, and TC1+4sh, targeting knockdown of Renilla-luciferase (control), TRPC1, TRPC4 and TRPC1 plus TRPC4, respectively, allowed use of a single adenovirus for infection of myometrial cells to achieve knockdown of multiple TRPCs, thus maintaining cell viability to a maximum.

Expression of TC1sh, TC4sh and TC1+4sh constructs proved effective at inducing significant decreases in mRNAs for their respective TRPCs. Furthermore, TRPC4 mRNA levels were unaffected by the TRPC1 knockdown. In the same fashion, TRPC1 mRNA levels did not display strong changes after a TRPC4 knockdown.

Controversy exists on the specific role of TRPC1 and whether it is a multifunctional protein possessing cell-type specific roles (20). This controversy has arisen mostly as a result of data obtained in overexpression studies, thus not providing much insight into the actions of endogenous TRPC1-containing channels [15]. Analyses of endogenous TRPC1 via use of antisense DNA targeting TRPC1 reveal attenuation of store-operated Ca^{2+} entry in a variety of cell lines [1;3].

TRPC1 and TRPC4 predominate in myometrial cells. Due to the potential for TRPC1 to interact with TRPC4 in channel formation, several studies have looked at the effects resulting from the knockdown of either protein on intracellular Ca^{2+} dynamics. Some studies link TRPC1 and TRPC4 to activation via thapsigargin-stimulated Ca^{2+} entry [16]. For instance, antisense DNA targeted against TRPC1 and TRPC4 reduced these protein levels and inhibited basal channel currents that were enhanced by thapsigargin [2].

In human myometrial cells, specific TRPC1 knockdown induced a significant inhibition in the oxytocin-stimulated Ca^{2+} entry. In accordance with studies performed in Chapter 4, a similar oxytocin-stimulated SRCE inhibition was observed with reduction in TRPC4 mRNA. Another shared feature between TRPC1 and TRPC4 appears to be the lack of an effect on both thapsigargin- and OAG-stimulated SRCE. Thus, these data suggest that both TRPC1 and TRPC4 are specifically involved in G protein-coupled receptor-stimulated calcium entry. Interestingly, the combined knockdown of TRPC1 plus TRPC4 displayed was no more effective in inhibiting oxytocin-SRCE than responses obtained from single TRPC1 or TRPC4 knockdowns. Similarly, no changes in thapsigargin- or OAG-stimulated Ca^{2+} entry were observed between single or double

knockdowns of these TRPCs. Levels of other TRPCs resulting from these knockdowns could be analyzed to ensure that knockdown of TRPC1, TRPC4 or their combination do not induce changes in any other TRPC. Such an effect was observed in A7r5 vascular smooth muscle cells, where TRPC1 knockdown was accompanied by an increase in TRPC6 mRNA and protein levels as well as an increase in CPA-(a reversible SERCA-pump inhibitor) induced Ca^{2+} entry [17].

TRPC1 is suggested to form homo- or heterotetramers in different combinations with other TRPCs [8;15;18-22]. Since TRPC1 may be a key factor for heterotetramer formation, it may modify TRPC channels, giving them unique characteristics [1;23], which may be determined by the different signalplexes formed as a result of the subunit composition of a specific TRPC channel. Another protein involved in the regulation of TRPC channels is STIM1. This ER-Ca^{2+} sensor is suggested to modify TRPC channel activity in response to different stimuli.

The study of the effect of STIM1 on SRCE in the human myometrium was achieved through overexpression of the dominant negative STIM1, namely STIM1ΔERM. In contrast to the effects obtained by knockdown of TRPCs in the present study, STIM1ΔERM induced a significant inhibition in oxytocin-, thapsigargin-, and OAG-stimulated Ca^{2+} entry.

In agreement with our results, Abdullaev, et. al. [24] show that knockdown of either TRPC1 or TRPC4 in endothelial cells had no effects on thapsigargin-stimulated SRCE nor on I(CRAC). However, no studies were performed to test the roles of these TRPCs upon any other type of stimulation. Furthermore, knockdown of either STIM1 or Orai1 abolished thapsigargin-stimulated Ca^{2+} entry.

Other studies conducted in HEK293 cells suggested that STIM1/Orai signaling and TRPC signaling occur in different plasma membrane domains. TRPC channel activity was linked to mechanisms dependent on phospholipase C without involvement of STIM1 [25].

It is interesting to note that similar experiments in different systems of study render quite different results. For instance, contrary to the study found by Abdullaev, et. al.[24], shRNAs targeted for the single knockdown of TRPC1 or TRPC4 in mesangial cells induced a significant decrease in the thapsigargin-induced membrane currents to the same extent as that presented by the double knockdown of TRPC1 plus TRPC4 [26]. In this same study, RNAi silencing of STIM1 significantly reduced this same type of SRCE mechanism.

Other studies in our laboratory analyzed the role of another relatively abundant TRPC isoform, namely TRPC6, via RNAi. These studies suggest that TRPC6 is exclusively involved in OAG-mediated Ca^{2+} entry [13]. Due to the inhibitory effect induced by STIMΔERM on OAG-stimulated SRCE, it would be of interest to study the effect that the other TRPC knockdown combinations would have along with the study of STIM1. This would help elucidate if the responses obtained by STIM1ΔERM are due to the lack of STIM1 regulation on channels such as TRPC1, TRPC4 and TRPC6, or if the TRPC channels created work independently of STIM1. We cannot rule out the possibility that the inhibition in SRCE observed in these studies may be due to the overexpression of STIM1ΔERM, which even though it is a dominant negative form of STIM, it could still affect formation of endogenous TRPC channels.

A similar study to that proposed above was performed by Potier et. al. [27] which showed that in vascular smooth muscle cells, single knockdown of TRPC1, TRPC4 or TRPC6 as well as the combined knockdown of these TRPCs displayed no effects on thapsigargin-stimulated SRCE. However, knockdown of STIM1 significantly diminished the response to thapsigargin.

TRPC1 and TRPC4 channels have different properties in different systems, probably because the composition of endogenous channels is dependent upon the nature of isoforms expressed in a cell-specific pattern. For instance, study of TRPC4 plus TRPC1 double knockdown has previously been achieved in rat skeletal muscle [2], resulting in inhibition of thapsigargin-stimulated currents. These contradictory roles for TRPC1 and TRPC4 could be explained by the different TRPC profiles potentially found in each system. For example, as mentioned previously, human myometrial cells displayed a very different TRPC mRNA profile (TRPC4> TRPC1> TRPC6> TRPC3> TRPC5> TRPC7) to that found in rat myometrium (TRPC4>> TRPC6> TRPC1> TRPC5> TRPC7> TRPC2; no TRPC3 expressed) [28;29].

TRPC1 and TRPC4, the two most abundant TRPCs in the human myometrium, share a similar role in the regulation of $[Ca^{2+}]_i$ resulting from activation of G protein-coupled receptors. TRPC6, the next most abundant TRPC in the human myometrium, allows for regulation in $[Ca^{2+}]_i$ following OAG stimulation. The changes in $[Ca^{2+}]_i$ dynamics induced by STIM1ΔERM in response to all three types of stimulations tested may suggest that STIM1 could be required for TRPC1:TRPC4 heterotetramer channels to function in response to G protein-coupled receptor activation. In a similar fashion, since TRPC6 knockdown displays an inhibition in OAG-stimulated SRCE in human

myometrial cells [13], TRPC6 may also require an interaction with STIM1 for its activation in response to OAG stimulation. SRCE induced after store depletion by thapsigargin stimulation may occur through a required STIM1 interaction with Orai proteins. Together, these data suggest that the $[Ca^{2+}]_i$ dynamics resulting in response to different stimuli in the human myometrium may be finely tuned by the specific expression and potential interactions occurring among TRPCs and STIM1 proteins.

References

1. Beech DJ, Xu SZ, McHugh D, Flemming R. TRPC1 store-operated cationic channel subunit. *Cell Calcium* **2003**; 33: 433-440.

2. Vandebrouck C, Martin D, Colson-Van SM, Debaix H, Gailly P. Involvement of TRPC in the abnormal calcium influx observed in dystrophic (mdx) mouse skeletal muscle fibers. *J Cell Biol* **2002**; 158: 1089-1096.

3. Vaca L, Sampieri A. Calmodulin modulates the delay period between release of calcium from internal stores and activation of calcium influx via endogenous TRP1 channels. *J Biol Chem* **2002**; 277: 42178-42187.

4. Mori Y, Wakamori M, Miyakawa T et al. Transient receptor potential 1 regulates capacitative Ca(2+) entry and Ca(2+) release from endoplasmic reticulum in B lymphocytes. *J Exp Med* **2002**; 195: 673-681.

5. Xu SZ, Beech DJ. TrpC1 is a membrane-spanning subunit of store-operated Ca(2+) channels in native vascular smooth muscle cells. *Circ Res* **2001**; 88: 84-87.

6. Bergdahl A, Gomez MF, Dreja K et al. Cholesterol depletion impairs vascular reactivity to endothelin-1 by reducing store-operated Ca2+ entry dependent on TRPC1. *Circ Res* **2003**; 93: 839-847.

7. Sweeney M, Yu Y, Platoshyn O, Zhang S, McDaniel SS, Yuan JX. Inhibition of endogenous TRP1 decreases capacitative Ca2+ entry and attenuates pulmonary artery smooth muscle cell proliferation. *Am J Physiol Lung Cell Mol Physiol* **2002**; 283: L144-L155.

8. Strubing C, Krapivinsky G, Krapivinsky L, Clapham DE. TRPC1 and TRPC5 form a novel cation channel in mammalian brain. *Neuron* **2001**; 29: 645-655.

9. Lee KP, Yuan JP, Hong JH, So I, Worley PF, Muallem S. An endoplasmic reticulum/plasma membrane junction: STIM1/Orai1/TRPCs. *FEBS Lett* **2009**.

10. Yuan JP, Zeng W, Huang GN, Worley PF, Muallem S. STIM1 heteromultimerizes TRPC channels to determine their function as store-operated channels. *Nat Cell Biol* **2007**; 9: 636-645.

11. Huang GN, Zeng W, Kim JY et al. STIM1 carboxyl-terminus activates native SOC, I(crac) and TRPC1 channels. *Nat Cell Biol* **2006**; 8: 1003-1010.

12. Sun D, Melegari M, Sridhar S, Rogler CE, Zhu L. Multi-miRNA hairpin method that improves gene knockdown efficiency and provides linked multi-gene knockdown. *Biotechniques* **2006**; 41: 59-63.

13. Chung D, Kim YS, Phillips JN et al. Attenuation of canonical transient receptor potential-like channel 6 expression specifically reduces the diacylglycerol-mediated increase in intracellular calcium in human myometrial cells. *Endocrinology* **2010**; 151: 406-416.

14. Deng X, Wang Y, Zhou Y, Soboloff J, Gill DL. STIM and Orai: dynamic intermembrane coupling to control cellular calcium signals. *J Biol Chem* **2009**; 284: 22501-22505.

15. Ahmmed GU, Mehta D, Vogel S et al. Protein kinase Calpha phosphorylates the TRPC1 channel and regulates store-operated Ca2+ entry in endothelial cells. *J Biol Chem* **2004**; 279: 20941-20949.

16. Tu CL, Chang W, Bikle DD. Phospholipase cgamma1 is required for activation of store-operated channels in human keratinocytes. *J Invest Dermatol* **2005**; 124: 187-197.

17. Selli C, Erac Y, Kosova B, Tosun M. Post-transcriptional silencing of TRPC1 ion channel gene by RNA interference upregulates TRPC6 expression and store-operated Ca2+ entry in A7r5 vascular smooth muscle cells. *Vascul Pharmacol* **2009**; 51: 96-100.

18. Schilling WP, Goel M. Mammalian TRPC channel subunit assembly. *Novartis Found Symp* **2004**; 258: 18-30.

19. Liu X, Singh BB, Ambudkar IS. TRPC1 is required for functional store-operated Ca2+ channels. Role of acidic amino acid residues in the S5-S6 region. *J Biol Chem* **2003**; 278: 11337-11343.

20. Hofmann T, Schaefer M, Schultz G, Gudermann T. Subunit composition of mammalian transient receptor potential channels in living cells. *Proc Natl Acad Sci U S A* **2002**; 99: 7461-7466.

21. Lintschinger B, Balzer-Geldsetzer M, Baskaran T et al. Coassembly of Trp1 and Trp3 proteins generates diacylglycerol- and Ca2+-sensitive cation channels. *J Biol Chem* **2000**; 275: 27799-27805.

22. Zagranichnaya TK, Wu X, Villereal ML. Endogenous TRPC1, TRPC3, and TRPC7 proteins combine to form native store-operated channels in HEK-293 cells. *J Biol Chem* **2005**; 280: 29559-29569.

23. Burkhard P, Stetefeld J, Strelkov SV. Coiled coils: a highly versatile protein folding motif. *Trends Cell Biol* **2001**; 11: 82-88.

24. Abdullaev IF, Bisaillon JM, Potier M, Gonzalez JC, Motiani RK, Trebak M. Stim1 and Orai1 mediate CRAC currents and store-operated calcium entry important for endothelial cell proliferation. *Circ Res* **2008**; 103: 1289-1299.

25. Dehaven WI, Jones BF, Petranka JG et al. TRPC channels function independently of STIM1 and Orai1. *J Physiol* **2009**; 587: 2275-2298.

26. Sours-Brothers S, Ding M, Graham S, Ma R. Interaction between TRPC1/TRPC4 assembly and STIM1 contributes to store-operated Ca2+ entry in mesangial cells. *Exp Biol Med (Maywood)* **2009**; 234: 673-682.

27. Potier M, Gonzalez JC, Motiani RK et al. Evidence for STIM/Orai1-mediated calcium influx in PDGF-induced smooth muscle migration. *FASEB J* **2009**; 23: 2425-2437.

28. Babich LG, Ku CY, Young HW, Huang H, Blackburn MR, Sanborn BM. Expression of capacitative calcium TrpC proteins in rat myometrium during pregnancy. *Biol Reprod* **2004**; 70: 919-924.

29. Ku CY, Babich L, Word RA et al. Expression of transient receptor channel proteins in human fundal myometrium in pregnancy. *J Soc Gynecol Investig* **2006**; 13: 217-225.

CHAPTER 6

Conclusions and Future Directions

Myometrial smooth muscle contractions are achieved by increases in $[Ca^{2+}]_i$. The canonical type of transient receptor potential (TRPC) channels have been identified as potential candidates involved on signal-regulated Ca^{2+} entry (SRCE) mechanisms in human myometrial cells. The human myometrium expresses TRPC4 and TRPC1 mRNAs in greatest abundance. In response to stretch, human pregnant myometrial cells exhibit an increase in TRPC3 and TRPC4 mRNA, TRPC3 protein expression, and cyclopiazonic acid-induced store depletion [1]. Interleukin-1β specifically upregulated TRPC3 protein expression in myometrial cells without influencing TRPC3 mRNA and had no effect of TRPC4 mRNA or protein [2].

Significant increases in myometrial TRPC6 and TRPC7 mRNAs and TRPC3, TRPC4 and TRPC6 proteins have been reported in human myometrial term at labor compared to term not in labor samples [2]. In another study, a specific decrease in TRPC4 mRNA, but not protein was observed with the onset of labor in human fundal myometrium, with no changes in TRPC1, TRPC3 and

TRPC6 mRNA or protein [3]. The basis for the discrepancies between these studies and for the lack of correlation between changes in TRPC mRNA and protein are still unknown.

The main objective of this project was to determine the role of TRPC1 and TRPC4 on SRCE mechanisms after stimulation of G protein-coupled receptors via uterine contractants such as oxytocin, inhibition of the SERCA-pump via thapsigargin, and OAG, a cell-permeable form of diacylglycerol. Since TRPC overexpression risks alteration of endogenous TRPC channels, shRNA constructs were designed that significantly decreased TRPC1 and TRPC4 mRNA levels. Additionally, since myometrial cells used for these studies have proven difficult to transfect, adenoviral vectors were produced for the expression of each shRNA. These shRNA constructs were expressed from either a U6 promoter or through their tandem expression under a CMV promoter. This tandem expression was especially helpful for the induction of a combined TRPC1 plus TRPC4 knockdown in myometrial cells. TRPC1- and TRPC4-shRNAs induced a specific and significant knockdown in their respective TRPC mRNAs. TRPC4 protein levels were also significantly reduced after TRPC4 knockdown when shRNAs were expressed under a U6 promoter. TRPC1 protein is reduced using the tandem TRPC1 shRNA system (D. Murtazina, unpublished results). Protein levels obtained after TRPC4 and TRPC1 plus TRPC4 knockdown still remain to be determined. The TRPC4 antibodies currently in the market are of poor quality.

Calcium imaging experiments revealed that TRPC1 and TRPC4 are specifically involved in G protein-coupled receptor-stimulated SRCE, as neither TRPC1 nor TRPC4 knockdown showed changes in thapsigargin- or OAG-stimulated Ca^{2+} entry.

Interestingly, the combined TRPC1 plus TRPC4 knockdown displayed similar regulation of $[Ca^{2+}]_i$ dynamics as those obtained by the single TRPC1 or TRPC4 knockdown.

Since TRPC1 and TRPC4 are the most abundant TRPCs in the myometrium, there is a significant possibility that some endogenous TRPC heterotetramers include these two proteins. Due to the similar responses obtained after a TRPC1 or TRPC4 knockdown, it is possible that these TRPCs require each other for heterotetramer formation and function. This idea might explain the weak increase in oxytocin-SRCE observed after TRPC4 overexpression in human myometrial cells. Future experiments analyzing TRPC1 overexpression may show a similar lack of increase in $[Ca^{2+}]_i$ after G protein-coupled receptor stimulation as those observed with a TRPC4 overexpression system. No significant changes would be expected from TRPC1 overexpression, as some studies suggest that TRPC1 may require TRPC4 for TRPC1's translocation to the plasma membrane [4;5]. On the other hand, overexpression of both TRPC1 plus TRPC4 could potentially result in a significant increase in $[Ca^{2+}]_i$ after G protein-coupled receptor stimulation due to the ability of these proteins to come together in the right stoichiometry to forming functional channels in the human myometrium.

In the present study, OAG-mediated SRCE, which we have previously shown to be protein kinase C-independent [6], was not significantly affected by TRPC1 or TRPC4 knockdown. In contrast, TRPC4 knockdown attenuated OAG-stimulated Ba^{2+} entry in HEK-293 cells [7]. Other studies have shown a negative regulatory effect of diacylglycerol on overexpressed TRPC4 and TRPC5 activation mediated by protein kinase C in DT40 B-cells [8]. In myometrial cells, TRPC4 may not be a major contributor to the overall OAG response if OAG exerts an inhibitory effect.

Other studies in our laboratory identified TRPC6 as an important player in OAG-mediated SRCE but not GPCR- or store depletion-mediated SRCE [9]. OAG-mediated SRCE is sensitive to VOC inhibition by nifedipine and requires extracellular Na^+, suggesting that TRPC6 carried predominantly Na^+ and increased intracellular Ca^{2+} as a result of membrane depolarization and activation of VOC channels [9]. Interestingly, neither GPCR- nor store depletion-mediated SRCE were sensitive to nifedipine or removal of extracellular Na^+ in human myometrial cells. Further TRPC knockdown studies could be performed using the tandem shRNA constructs expressing different combinations of TRPC1, TRPC4 and TRPC6 shRNAs. These combined knockdown studies could help identify the relationships and/or interdependence existing among these TRPCs for the control of intracellular Ca^{2+} dynamics.

Since STIM1 has been suggested as a potential direct regulator of TRPC1 and TRPC4 channel activity, a STIMΔERM construct was used. This dominant negative form of STIM1 is unable to interact with TRPC proteins. Overexpression of STIM1ΔERM induced significant decreases in oxytocin-, thapsigargin- and OAG-stimulated Ca^{2+} entry. This observation suggests that STIM1 may require interaction with TRPCs for regulation of Ca^{2+} influx in response to at least some of the SRCE stimulants studied. However, the possibility that STIM1ΔERM overexpression affected the native channel assembly cannot be discarded. STIM1 and Orai1, predominantly endoplasmic reticulum and plasma membrane proteins, respectively, have been implicated in the Ca^{2+} entry response to endoplasmic reticulum store depletion resulting from Ca^{2+}-ATPase inhibition (Fig. 6.1) [10;11]. Stimulation of SRCE or Ca^{2+} currents by

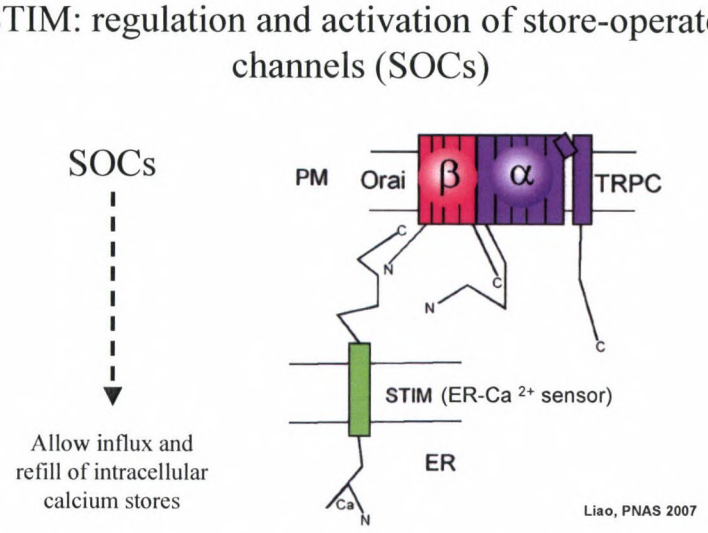

Fig. 6.1. STIM1 proteins act as Ca^{2+} sensors in the ER membrane. STIM1 regulates and activates store-operated channels (SOCs) which are important to allow the influx and refill of intracellular calcium stores. STIM1 is suggested to interact with Orai proteins and/or TRPC proteins to regulate the function of these channels as potential SOCs.

some, but not all, GPCRs has been reported to be attenuated by STIM1 knockdown or by STIM1 dominant negative expression [11;12]. Overexpression studies indicate that TRPC1, 4, and 5 can physically interact with STIM1 whereas TRPC3, 6, and 7 do not do so [13;14]. Other studies implicate Orai1 as a binding partner of TRPC3 and TRPC6 channels [15]. In this case, the STIM/Orai interaction stimulated by decreases in Ca^{2+} stores has been postulated to decrease the Orai/TPRC interaction and promote TRPC activation. The involvement of STIM was studied in Chapter 5. However, the role of Orai in GPCR-stimulated SRCE in myometrium remains to be explored, but the lack of an effect of TRPC1 and/or TRPC4 knockdown on thapsigargin-stimulated SRCE

suggests that any potential TRPC1 and/or TRPC4 interaction with STIM1 would not contribute markedly to this effect.

Evidence for a separate Ca^{2+} entry pathway involving intracellular phospholipase A2 activation by a calcium influx factor (CIF) generated in response to release of Ca^{2+} from intracellular stores has been reported [16]. Although the current studies do not directly address this pathway, the lack of effect of TRPC1 and TRPC4 knockdown on thapsigargin-mediated SRCE suggests that this mechanism is not a major component of the GPCR response in myometrial cells.

One possible mechanism for the regulation of TRPC1 and TRPC4 in the human myometrial cells might involve the formation of TRPC1-TRPC4 heterotetramers as a requirement for the formation of a functional channel. A signalplex could then be formed by STIM1 binding to TRPC1, aiding in its regulation (Fig. 6.2). On the other hand, β-catenin has been identified as a regulator of TRPC4-mediated Ca^{2+}-signaling [17]. β-catenin has been shown to promote TRPC4 plasma membrane targeting and a cell adhesion-dependent increase in agonist-induced Ca^{2+} signaling [17]. Regulation of β-catenin occurs via glycogen synthase kinase-3 beta (GSK-3β), a kinase involved in several cellular pathways such as cell division, cell adhesion and gene expression among many others [18]. Interestingly, GSK-3β interaction protein (GSKIP) has recently been identified as an A-kinase anchoring protein (AKAP) [19]. GSKIP directly interacts with PKA and GSK-3β, providing a mechanism for the integration of PKA-mediated inactivation of GSK-3β.

This potential pathway could be involved in a contraction-relaxation mechanism in which a relaxant such as the hormone relaxin activates $G_{\alpha s}$ pathways, thus inducing the

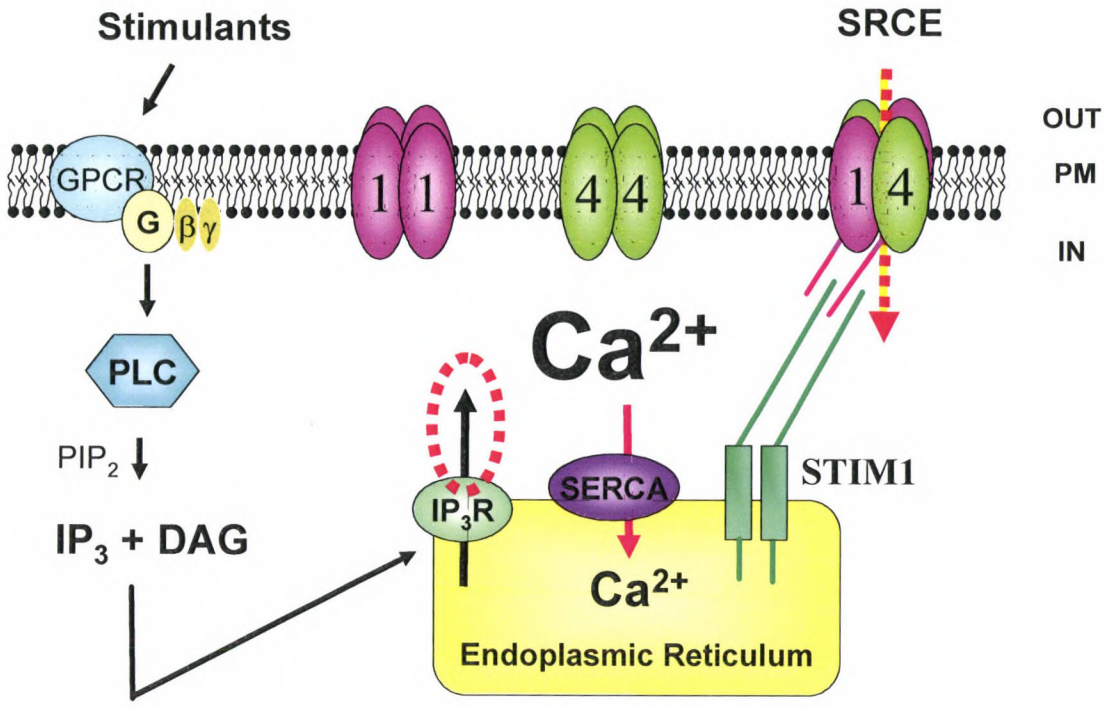

Fig. 6.2. Potential mechanism for the regulation of TRPC1 and TRPC4 in human myometrial cells. TRPC1 and TRPC4 protein expression allow formation of TRPC1:TRPC4 heterotetramers. This assembly of the TRPC1 and TRPC4 proteins serves as a requirement for the formation of a functional channel. A signalplex could then be formed by STIM1 binding to TRPC1. This interaction may aid in the regulation of TRPC1:TRPC4 heterotetramer channels in response to G protein-coupled receptor activation to induce SRCE in human myometrium.

production of cAMP. Increases in cAMP production result in the activation of PKA which allows for the activation or stimulation of relaxant pathways [20]. As the activation effects by PKA take place, PKA is able to bind to GSKIP. GSK-3β, also bound to GSKIP, is phosphorylated and inactivated by PKA [19]. This inactivation

prevents GSK-3β from phosphorylating and inactivating β -catenin [21]. This allows β -catenin to target TRPC4 to the plasma membrane and thus form functional heterotetramers along with TRPC1. The TRPC1-TRPC4 heterotetramer allows Ca^{2+} influx, inducing increase in $[Ca^{2+}]_i$ in response to a G protein-coupled receptor stimulus, which in turn activates the contractile machinery. TRPC1 ensures binding with STIM1, allowing for proper refilling of the intracellular Ca^{2+} stores which are vital for continued contractile activity (Fig. 6.3).

The present studies provide insights that may be helpful in dealing with the problem of preterm births. Premature birth is currently one of the greatest health problems worldwide contributing to about 75% of all perinatal deaths [22]. Furthermore, the rate of premature births in the U.S.A. has increased by a rate of approximately 20% from 1990 to 2005 (Fig. 6.4). The reported annual societal economic cost of preterm births in the U.S.A. in 2005 was of at least $26.2 billion [23]. Understanding the mechanisms governing the control of the contraction-relaxation mechanisms occurring in the human myometrium will aid in targeting effective treatment options for preterm labor.

The genomic and non-genomic actions of progesterone are thought to promote myometrial relaxation, making progesterone largely responsible for the maintenance of pregnancy [24;25]. In lower mammals, the onset of labor has been closely associated with mechanisms resulting in progesterone withdrawal along with a rise in estradiol levels. However, levels of both progesterone and estradiol remain stable in primates[25]. Efforts to determine the pathways involved in the transformation of the myometrium from a quiescent tissue to a highly contractile and excitable state involves array-based

Fig. 6.3. Potential pathway for regulation of the contraction-relaxation mechanism in the human myometrium. (Left) A relaxant hormone induces $G_{\alpha s}$ activation leading to the production of cAMP which in turn results in the stimulation of relaxant pathways through activation of PKA. PKA binds GSKIP. GSK-3β, also bound to GSKIP, is phosphorylated and inactivated by PKA preventing GSK-3β from phosphorylating and inactivating β-catenin. β-catenin then targets TRPC4 to the plasma membrane to form functional heterotetramers along with TRPC1. The TRPC1-TRPC4 heterotetramer allows Ca^{2+} influx, inducing increase in $[Ca^{2+}]_i$ in response to a G protein-coupled receptor stimulus, which in turn activates the contractile machinery. TRPC1 ensures binding with STIM1, allowing for proper refilling of the intracellular Ca^{2+} stores which are vital for continued contractile activity. (Right) Absence of a relaxation stimulus leads to GSK-3β activation and further β-catenin degradation. Lack of β-catenin regulation prevents TRPC4 from translocating to the plasma membrane allowing formation of nonfunctional TRPC1 homotetramers to form in the plasma membrane preventing SRCE, in response to a contractant signal activating G protein-coupled receptors, to occur. This system could potentially ensure a fine-tuning mechanism of the contraction-relaxation pathway.

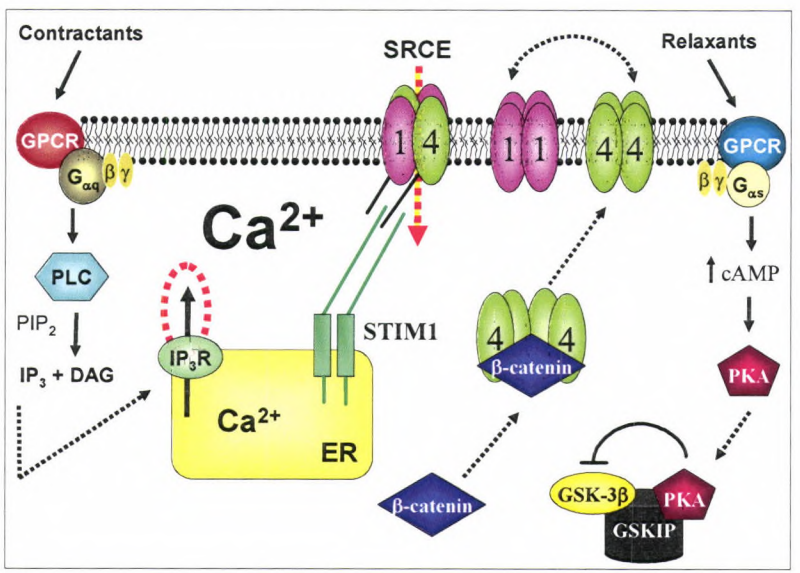
Contractants
SRCE
Relaxants
GPCR
$G_{\alpha q}$ β γ
PLC
PIP_2
IP_3 + DAG
Ca^{2+}
IP_3R
Ca^{2+}
ER
STIM1
1 4
1 1
4 4
β-catenin
β-catenin
GSK-3β
PKA
GSKIP
GPCR
β γ $G_{\alpha s}$
↑ cAMP
PKA

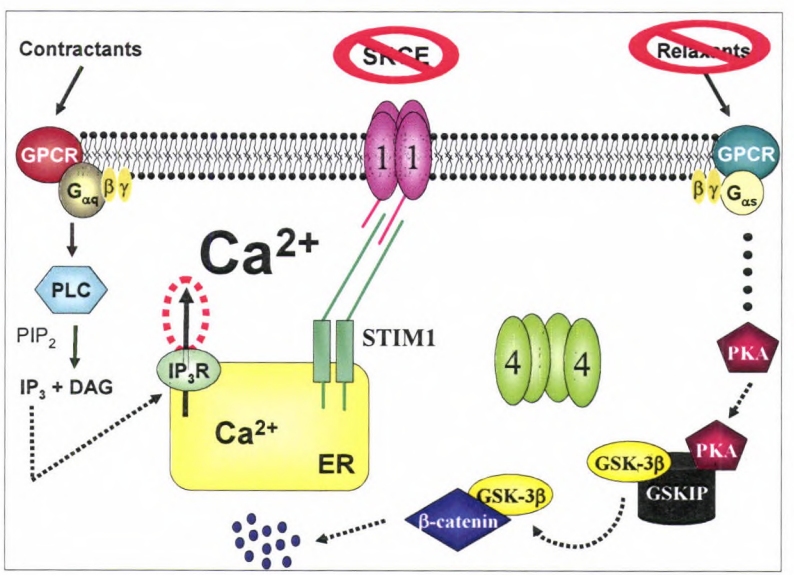
Contractants
GPCR
$G_{\alpha q}$ β γ
PLC
PIP_2
IP_3 + DAG
Ca^{2+}
IP_3R
Ca^{2+}
ER
STIM1
1 1
4 4
β-catenin
GSK-3β
PKA
GSKIP
GPCR
β γ $G_{\alpha s}$
PKA

studies. These studies suggest that activation of an inflammatory response has a causal relationship to the induction of a functional progesterone withdrawal [25]. Common agents used for the treatment of preterm labor involve selective β2-adrenoceptor agonists to induce activation of protein kinase-A (PKA) through cAMP production. Atosiban, a competitive inhibitor of the oxytocin receptor, prevents increases in $[Ca^{2+}]_i$ in a reversible manner, making it a good candidate for treatment of preterm labor [26]. Calcium channel antagonists, such as the L-type channel blockers nifedipine and verapamil, have also been considered for the prevention of preterm labor [27;28]. However, as with many other agents, adverse side effects to both the mother and fetus have to be considered as many other contractant signals activated by these channels are still required.

Stretch signals activate the contraction-relaxation pathways inducing phasic contractions of the myometrium [29]. Fine tuning of the contractile pathway involves activation of different SRCE mechanisms, such as GPCR-activation to allow Ca^{2+} entry from the extracellular space as well as the refilling of the intracellular Ca^{2+} stores for the proper continuation of contractions [30]. The lack of effect of nifedipine on SRCE in response to oxytocin stimulation as well as that induced by store depletion suggests that other channels, rather than voltage-operated channels, may be involved [29]. The TRPC knockdown studies presented here show a relevant link of these TRPC channels with the regulation of $[Ca^{2+}]_i$ dynamics in human myometrial cells and thus the potential regulation of myometrial contractions during labor.

This work increases our understanding of the regulation of Ca^{2+} dynamics in myometrial cells and points to a specific role for TRPC1 and TRPC4 in GPCR-regulated myometrial Ca^{2+} dynamics. The data suggest that this contribution, in addition to the

important role in Ca^{2+} homeostasis played by voltage-operated channels and the influences of Ca^{2+} pumps, exchangers and potassium channels, provide the myometrium with the ability to respond in specific and precise ways to influences in its environment, both during pregnancy and at the time of parturition.

Premature births in USA increased 20% between 1990 and 2005

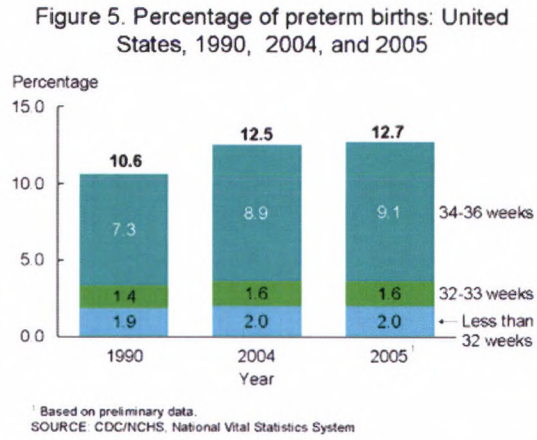

In 2005, premature birth cost the US $26.2 billion (Inst. Med., 2006)

Fig. 6.4. The incidence of premature births increased by around 20% from 1990 to 2005 in the United States. Several emotional and physical hurdles can arise due to premature births to both mother and baby. Additionally, premature births carry a high economic cost. In 2005 alone, premature births had a reported societal economic annual cost of $26.2 billion in the United States.

References

1. Dalrymple A, Mahn K, Poston L, Songu-Mize E, Tribe RM. Mechanical stretch regulates TRPC expression and calcium entry in human myometrial smooth muscle cells. *Mol Hum Reprod* **2007**; 13**:** 171-179.

2. Dalrymple A, Slater DM, Poston L, Tribe RM. Physiological induction of transient receptor potential canonical proteins, calcium entry channels, in human myometrium: influence of pregnancy, labor, and interleukin-1 beta. *J Clin Endocrinol Metab* **2004**; 89**:** 1291-1300.

3. Ku CY, Babich L, Word RA et al. Expression of transient receptor channel proteins in human fundal myometrium in pregnancy. *J Soc Gynecol Investig* **2006**; 13**:** 217-225.

4. Hofmann T, Schaefer M, Schultz G, Gudermann T. Subunit composition of mammalian transient receptor potential channels in living cells. *Proc Natl Acad Sci U S A* **2002**; 99**:** 7461-7466.

5. Alfonso S, Benito O, Alicia S et al. Regulation of the cellular localization and function of human transient receptor potential channel 1 by other members of the TRPC family. *Cell Calcium* **2008**; 43**:** 375-387.

6. Shlykov SG, Sanborn BM. Stimulation of intracellular Ca2+ oscillations by diacylglycerol in human myometrial cells. *Cell Calcium* **2004**; 36**:** 157-164.

7. Zagranichnaya TK, Wu X, Villereal ML. Endogenous TRPC1, TRPC3, and TRPC7 proteins combine to form native store-operated channels in HEK-293 cells. *J Biol Chem* **2005**; 280**:** 29559-29569.

8. Venkatachalam K, Zheng F, Gill DL. Control of TRPC and store-operated channels by protein kinase C. *Novartis Found Symp* **2004**; 258**:** 172-185.

9. Chung D, Kim YS, Phillips JN et al. Attenuation of canonical transient receptor potential-like channel 6 expression specifically reduces the diacylglycerol-mediated increase in intracellular calcium in human myometrial cells. *Endocrinology* **2010**; 151**:** 406-416.

10. Smyth JT, Dehaven WI, Jones BF et al. Emerging perspectives in store-operated Ca2+ entry: roles of Orai, Stim and TRP. *Biochim Biophys Acta* **2006**; 1763**:** 1147-1160.

11. Yuan JP, Zeng W, Huang GN, Worley PF, Muallem S. STIM1 heteromultimerizes TRPC channels to determine their function as store-operated channels. *Nat Cell Biol* **2007**; 9**:** 636-645.

12. Wedel B, Boyles RR, Putney JW, Jr., Bird GS. Role of the store-operated calcium entry proteins Stim1 and Orai1 in muscarinic cholinergic receptor-stimulated calcium oscillations in human embryonic kidney cells. *J Physiol* **2007**; 579**:** 679-689.

13. Huang GN, Zeng W, Kim JY et al. STIM1 carboxyl-terminus activates native SOC, I(crac) and TRPC1 channels. *Nat Cell Biol* **2006**; 8**:** 1003-1010.

14. Worley PF, Zeng W, Huang GN et al. TRPC channels as STIM1-regulated store-operated channels. *Cell Calcium* **2007**; 42**:** 205-211.

15. Liao Y, Erxleben C, Yildirim E, Abramowitz J, Armstrong DL, Birnbaumer L. Orai proteins interact with TRPC channels and confer responsiveness to store depletion. *Proc Natl Acad Sci U S A* **2007**; 104**:** 4682-4687.

16. Bolotina VM, Csutora P. CIF and other mysteries of the store-operated Ca2+-entry pathway. *Trends Biochem Sci* **2005**; 30**:** 378-387.

17. Graziani A, Poteser M, Heupel WM et al. Cell-cell contact formation governs Ca2+ signaling by TRPC4 in the vascular endothelium: evidence for a regulatory TRPC4-beta-catenin interaction. *J Biol Chem* **2010**; 285**:** 4213-4223.

18. Xu C, Kim NG, Gumbiner BM. Regulation of protein stability by GSK3 mediated phosphorylation. *Cell Cycle* **2009**; 8**:** 4032-4039.

19. Hundsrucker C, Skroblin P, Christian F et al. Glycogen synthase kinase 3beta interaction protein functions as an A-kinase anchoring protein. *J Biol Chem* **2010**; 285**:** 5507-5521.

20. Zhong M, Murtazina DA, Phillips J, Ku CY, Sanborn BM. Multiple signals regulate phospholipase CBeta3 in human myometrial cells. *Biol Reprod* **2008**; 78**:** 1007-1017.

21. Frame S, Cohen P. GSK3 takes centre stage more than 20 years after its discovery. *Biochem J* **2001**; 359**:** 1-16.

22. Lopez BA. Overview. Preterm labour: mechanisms and management. *BMC Pregnancy Childbirth* **2007**; 7 Suppl 1**:** S2.

23. Mathews TJ, MacDorman MF. Infant mortality statistics from the 2005 period linked birth/infant death data set. *Natl Vital Stat Rep* **2008**; 57**:** 1-32.

24. Madsen G, Zakar T, Ku CY, Sanborn BM, Smith R, Mesiano S. Prostaglandins differentially modulate progesterone receptor-A and -B expression in human myometrial cells: evidence for prostaglandin-induced functional progesterone withdrawal. *J Clin Endocrinol Metab* **2004**; 89**:** 1010-1013.

25. Mesiano S, Welsh TN. Steroid hormone control of myometrial contractility and parturition. *Semin Cell Dev Biol* **2007**; 18**:** 321-331.

26. Creasy RK. Preterm inhibition of myometrial contractility: clinical considerations. In: Garfield RE (Ed.). *Uterine Contractility*. Serono Symposia, USA, 1990: pp. 371-379.

27. Sanborn BM, Anwer K. Hormonal Regulation of myometrial intracellular calcium. In: Garfield RE (Ed.). *Uterine Contractility*. Serono Symposia, USA, 1990: pp. 69-82.

28. Sanborn BM. Hormones and calcium: mechanisms controlling uterine smooth muscle contractile activity. The Litchfield Lecture. *Exp Physiol* **2001**; 86**:** 223-237.

29. Sanborn BM. Hormonal signaling and signal pathway crosstalk in the control of myometrial calcium dynamics. *Semin Cell Dev Biol* **2007**; 18**:** 305-314.

30. Mironneau J. Ion channels and excitation-contraction coupling in myometrium. In: Garfield RE (Ed.). 100 Longwater Circle, Norwell, Massachusetts 02061, Serono, 1990: pp. 9-19.